3A1 Incompressible Flow

BOUNDARY LAYER THEORY[1]

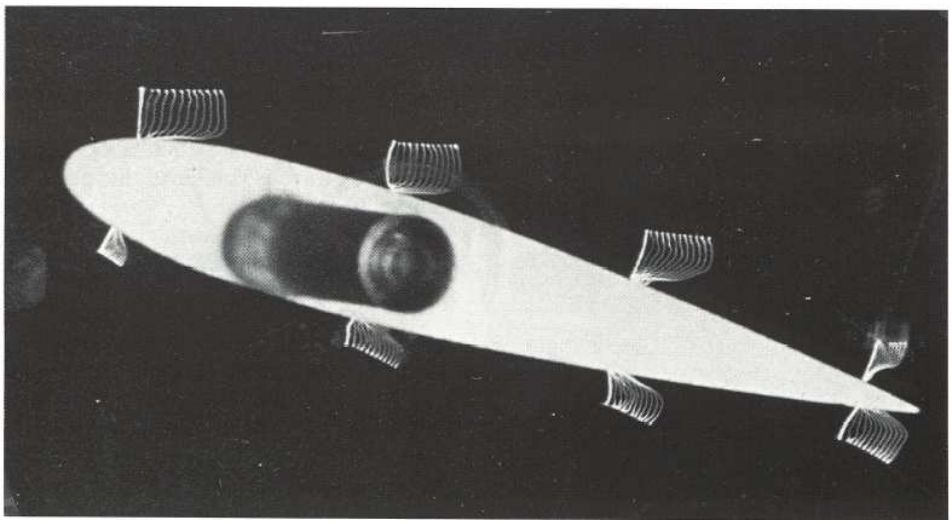

Velocity distribution around an aerofoild. Air velocity 20 m/s, chord length 150 mm , Re=150000. Sparking tracing method.

(Before 1905,) theoretical hydrodynamics was the study of phenomena which could be proved, but not observed, while hydraulics was the study of phenomena which could be observed but not proved.

—— James Lighthill

In 1904, a German engineer, Ludwig Prandtl (1875–1953), published perhaps the most important paper[2] ever written on fluid mechanics.

—— Frank M. White

The (boundary layer) concept makes it possible to think intelligently about almost any problem in real fluid flow.

—— Leslie Howarth

[1] Full information at "www2.eng.cam.ac.uk/~jl305/3A1/3A1.html". For all enquires, please email jl305@cam.ac.uk.

[2] 'On the motion of fluids of very small viscosity', presented at the Third International Congress of Mathematics, Heidelberg.

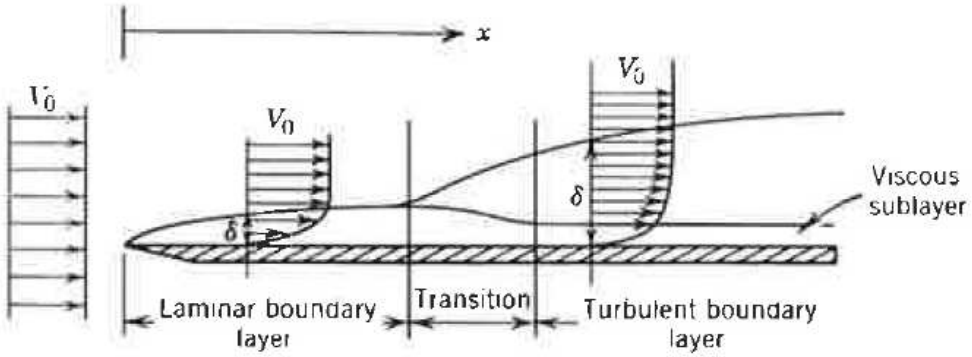

Figure 1: Flow past a flat plate (Ref. [1]).

In an inviscid fluid, there is no frictional effects between moving fluid layers or between the fluid layers and bounding walls. Analyses made on the basis of inviscid flow over streamlined bodies produces two results that are contrary to observation. First, the inviscid fluid slips smoothly by the body; real fluid does not (Fig. 1). Second, the calculated drag on the body is negligible, while the observed drag is not.

Separation of moving fluid from boundary surfaces is another important difference between the inviscid and real fluids. The mathematical theory of the inviscid fluid yields no information about the expectation of separation even in simple cases where intuition alone would predict separation with complete certainty. Examples are shown in Fig. 2 for a sharp projection on a wall and a flat plate normal to a rectilinear flow. For the inviscid fluid the flowfields will be found symmetrical upstream and downstream from such obstructions, the fluid rapidly accelerating towards the obstruction and decelerating in the same pattern downstream from it. However, the engineer would reason that the inertia of the moving fluid would prevent its following the sharp corners of such obstructions and that consequently separation of fluid from boundary surface is to be expected there, resulting in asymmetric flowfields featured by eddies and wakes downstream from the obstructions.

In a real fluid, viscosity introduces resistance to motion by causing shear or friction forces between fluid particles and between these and boundary walls. The derivation of the Euler equations can be altered to include the shear stresses in a real fluid in addition to the normal stress or pressure already included there. The result is a set of nonlinear, second-order partial differential equations, called the Navier-Stokes equations. Unfortunately, few useful analytic solutions to these equations have been found. Therefore, the engineer must be resort to experimental results, semi-empirical methods, and numerical simulations to solve problems. This requires a good basic understanding of a variety of physical phenomena, which are

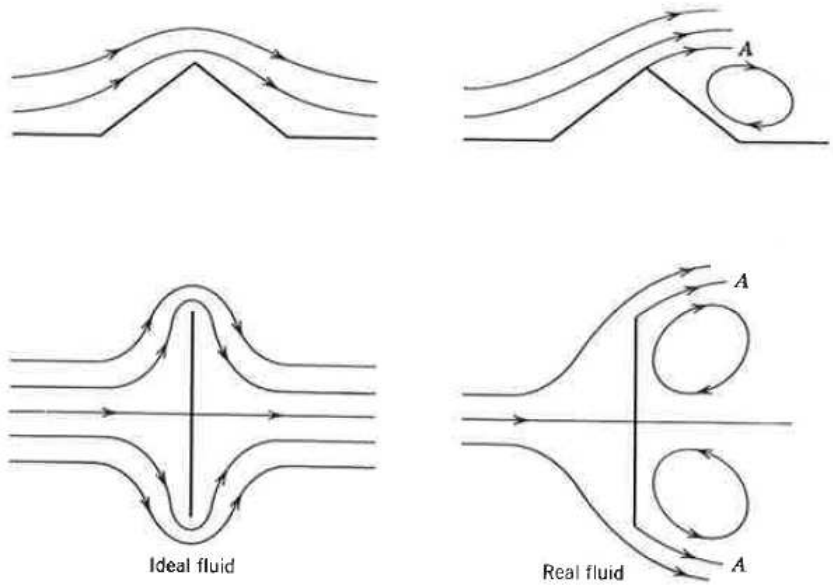

Figure 2: Flows past obstructions with sharp corners (Ref. [1]).

described in this part of the course.

In many flows of fluids with small viscosity (e.g., air and water) past streamlined shapes, the frictional aspects of the flow are confined to a thin boundary layer. Outside the boundary layer the fluid motion is accurately described by inviscid fluid theory (Euler and Bernoulli equations). This main inviscid flow acts as an "outer" flow which establishes both the velocity at the edge of the "inner" flow or boundary layer and the pressure distribution along the body. An engineering approach to solution of such a flow problem is to solve first the "outer" problem of inviscid fluid motion about the body, ignoring viscous effects entirely. Then, using the "outer" solution values of velocity and pressure at the surface of the body as approximate values for the edge of the boundary layer, the "inner" viscous flow problem is solved. Experiments have demonstrated that this is often an effective and accurate process. For streamlined shapes, this procedure gives, from the "outer" solution, the pressure distribution (including an accurate estimate of the lift force, if any) and, from the "inner" solution, an estimate of the friction force or drag on the shape. The boundary layer concept was first introduced by a German scientist, Ludwig Prandtl (1875-1953) in 1904. It found wide application in numerous problems of fluid dynamics and has provided a powerful tool for analysis of problem of fluid resistance; it has probably contributed more to the progress in modern fluid mechanics than any other single idea.

For example, consider flow past a thin aerofoil at small angle of incident, $\alpha < 5^{\circ}$, as

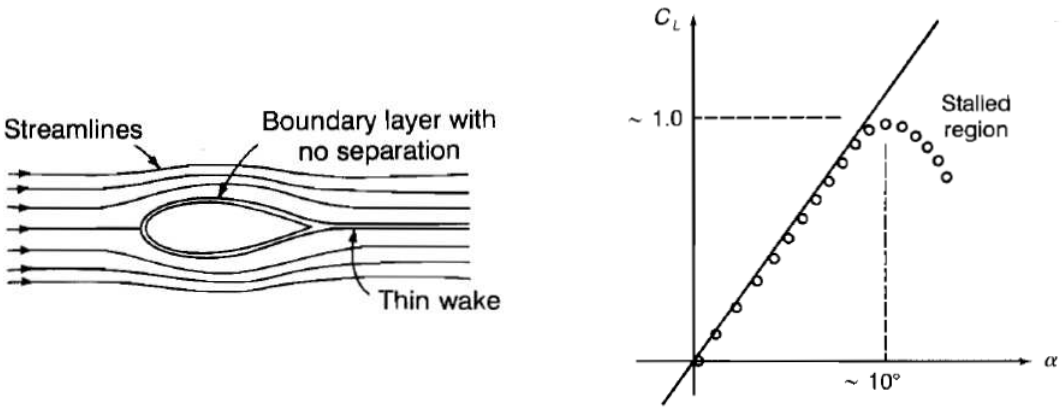

(a) (b)

Figure 3: Flow past a thin aerofoil: (a) low incidence angle, no separation; Typical comparison of theory and experiment for lift coefficient on a symmetric aerofoil (Ref. [5]).

sketched in Fig. 3(a). In practical applications, the Reynolds number is large. In these circumstances the flow creates a thin boundary layer near the aerofoil surface and a thin wake downstream. The pressure across the thin boundary layer is almost constant; the measured surface pressure distribution on the foil can be predicted by inviscid-flow theory. The wall shear stress can be computed with the boundary layer theory. According to inviscid theory, the dimensionless lift coefficient C_L is given by

$$C_L \approx 2\pi \sin\alpha \ .$$

Fig. 3(b) compares typical theoretical and experimental lift curves for a symmetric aerofoil. The agreement is excellent before the flow stalls (boundary separation).

Even though standard boundary-layer theory analysis is not applicable to (1) low Reynolds numbers or (2) flow separation, it is a very important subject, especially for understanding viscous flows. Chapter 13 of [1], Chapter 9 of [2], Chapter 7 of [3] and Chapter 8 of [4] provide a good elementary introduction to the subject (level lower than this course). Chapters 4-6 of [5] are a reasonable survey of the traditional approach (level slightly higher than this course). For further study, there are monographs entirely devoted to boundary-layer theory [6–8], plus the classical monograph by Rosenhead [9].

Fluid mechanics has always been a "visual" subject—much can be learned by viewing various aspects of fluid flow. You are strongly encouraged to study the many beautiful photographs and videos of the flows found in refs. [10–12].

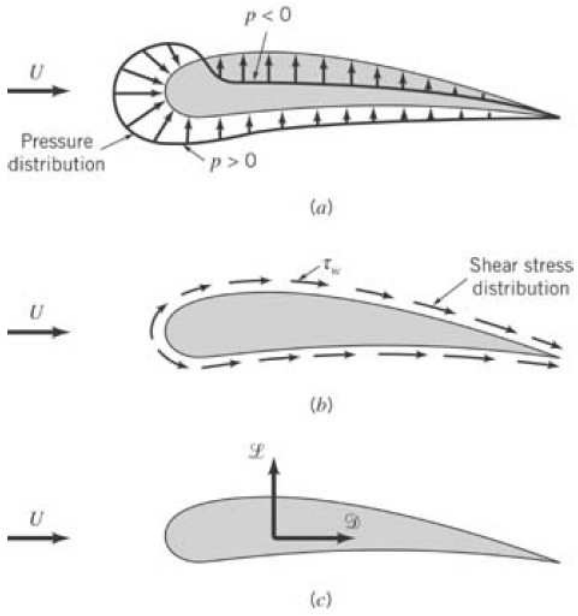

Figure 4: forces from surrounding fluid on a two-dimensional object: (a) pressure force, (b) viscous force, and (c) resultant force (lift and drag) (Ref. [2]).

Before we plunge into this important and fascinating subject, let us review some basic concepts, observations and facts on fluid mechanics.

1 Some Basic Concepts and Facts

1.1 Lift and Drag

When a body moves through a fluid, an interaction between the body and the fluid occurs; this effect can be given in terms of the forces at the fluid-body interface. These forces can be described in terms of the stress—wall shear stresses on the body, τ_w, due to viscous effects and normal stresses due to the pressure, p. Typical shear stress and pressure distributions are shown in Fig. 4(a) and Fig. 4(b). Both τ_w and p vary in magnitude and direction along the surface.

It is often useful to know the detailed distribution of shear stress and pressure over the surface of the body. Many times, however, only the integrated or resultant effects of these distributions are needed. The resultant force in the direction of the upstream velocity is termed the drag, $\mathcal{D}$, and the resultant force normal to the upstream velocity is termed the lift, $\mathcal{L}$, as indicated in Fig. 4 (c). For some three-dimensional bodies there may also be a side force that is perpendicular to the plane containing $\mathcal{D}$ and $\mathcal{L}$.

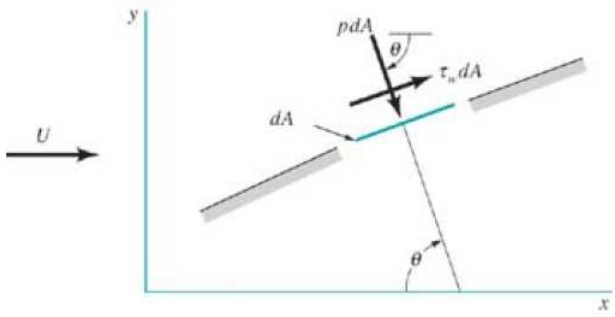

Figure 5: Pressure and shear forces on a small element of the surface of a body (Ref. [2]).

The resultant of the shear stress and pressure distributions can be obtained by integrating the effect of these two quantities on the body surface as indicated in Fig. 5. The x and y components of the fluid force on the small area element dA are

$$dF_x = (pdA)\cos\theta + (\tau_w dA)\sin\theta$$

and

$$dF_y = -(pdA)\sin\theta + (\tau_w dA)\cos\theta$$

where θ is the angle between the surface normal direction and the upstream flow direction. Thus, the net x and$y$ components of the force on the object are

$$\mathcal{D} = \int dF_x = \int p\cos\theta dA + \int \tau_w \sin\theta dA \tag{1.1}$$

and

$$\mathcal{L} = \int dF_y = -\int p\sin\theta dA + \int \tau_w \cos\theta dA \tag{1.2}$$

To carry out the integrations and determine the lift and drag, we must know the body shape (i.e., θ as a function of location along the body) and the distributions of τ_w and p along the surface. These distributions are often extremely difficult to obtain, either experimentally or theoretically. The pressure distribution can be obtained experimentally by use of a series of static pressure taps along the body surface. On the other hand, it is usually quite difficult to measure the wall shear stress distribution.

We introduce the following useful definitions. Friction drag, $\mathcal{D}_f$, is that part of drag that is due directly to the shear stress, τ_w, on the object. Pressure drag, $\mathcal{D}_p$, is that part of drag

that is due directly to the pressure, p. It is often referred to as form drag because of its dependency on the shape or form of the object. The dimensionless lift coefficient C_L and drag coefficient C_D are defined as

$$C_L = \frac{\mathcal{L}}{\frac{1}{2}\rho U^2 A} \tag{1.3}$$

and

$$C_D = \frac{\mathcal{D}}{\frac{1}{2}\rho U^2 A} \tag{1.4}$$

where A is a characteristic area of the object. Typically, A is taken to be frontal area—the projected area by a person looking toward the object from a direction parallel to the upstream velocity, U. In other situations A is taken to be the planform area—the projected area seen by an observer looking toward the object from a direction normal to the upstream velocity (i.e. from "above" it). Obviously, which area is used in the definition of the lift and drag coefficients must be clearly stated.

1.2 Governing Equations and Boundary Conditions

The Navier-Stokes equations are generally accepted to be sufficient to fully describe the flow of any Newtonian fluid. In most of the following analysis we will restrict ourselves to two-dimensional flows. In this case the Navier-Stokes equations may be written as

$$\rho\left(\frac{\partial u}{\partial t} + u\frac{\partial u}{\partial x} + v\frac{\partial u}{\partial y}\right) = -\frac{\partial p}{\partial x} + \mu\left(\frac{\partial^2 u}{\partial x^2} + \frac{\partial^2 u}{\partial y^2}\right)$$

$$\begin{aligned} \rho\left(\frac{\partial v}{\partial t} + u\frac{\partial v}{\partial x} + v\frac{\partial v}{\partial y}\right) &= -\frac{\partial p}{\partial y} + \mu\left(\frac{\partial^2 v}{\partial x^2} + \frac{\partial^2 v}{\partial y^2}\right) \\ \frac{\partial u}{\partial x} + \frac{\partial v}{\partial y} &= 0 \end{aligned} \tag{1.5}$$

It is often convenient to rewrite these equations in a more compact form using the vector notation:

$$\begin{aligned} \rho\left(\frac{\partial \mathbf{u}}{\partial t} + (\mathbf{u}.\nabla)\mathbf{u}\right) &= -\nabla p + \mu\nabla^2\mathbf{u}\ , \\ \nabla.\mathbf{u} &= 0\ . \end{aligned} \tag{1.6}$$

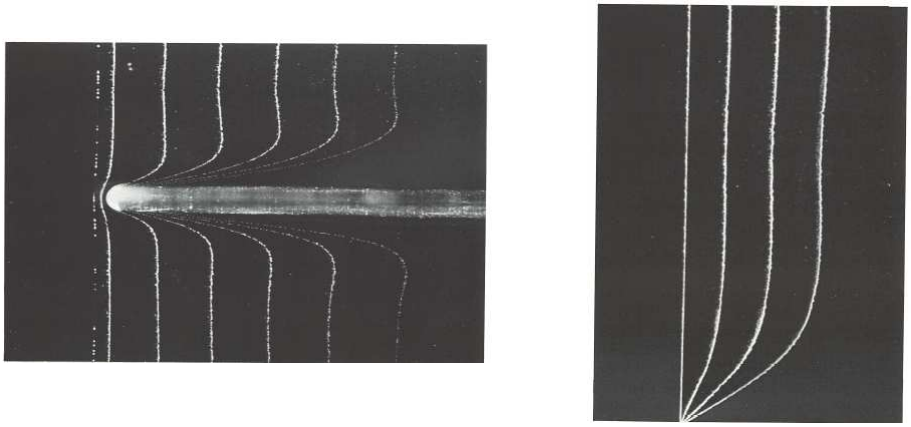

(a) (b)

Figure 6: (a) Photograph of velocity profiles for the laminar flow over a flat plate (0.01% salt water, free stream velocity 0.6 cm/s, thickness of the plate 0.5 mm). (b) Velocity profiles for the laminar flow over a flat plate (distance from the leading edge 200 mm, $Re = 1.2 \times 10^2$). (hydrogen bubble method, Ref. [11])

The correct boundary condition on a solid wall is the no-slip condition, the velocity u is zero relative to the wall:

$$\mathbf{u}_{\text{fluid}} \equiv \mathbf{u}_{\text{wall}}. \tag{1.7}$$

Fig. 6 illustrates the no-slip condition for water past from left to right over a fixed thin plate. There is clearly no slip at the wall, where the water takes on the zero velocity of the fixed plate. The velocity profile is made visible by the discharge of a line of hydrogen bubbles from the wire shown stretched across the flow.

The Navier-Stokes equations are extremely difficult to solve. There are several dozen known particular solutions, all are limited to simple geometries and most are unidirectional flows, where the difficult nonlinear convective terms were neglected. When faced with a difficult mathematical problem, it is natural to seek rigorous or at least reasonable simplifications. The values of the kinematic viscosity for air and water (the most important fluids in engineering applications) are so small that the Reynolds number is very large for most practical flows (roughly from 10^3 to 10^8). Under such circumstances, it certainly seems safe to neglect all viscous terms. This leads to Eulers inviscid flow equations:

$$\rho\left(\frac{\partial \mathbf{u}}{\partial t} + (\mathbf{u}.\nabla)\mathbf{u}\right) = -\nabla p \ . \tag{1.8}$$

By neglecting viscosity we have lost the second-order derivative of $\mathbf{u}$ in Eqn. (1.8); therefore we must relax one boundary condition on velocity. The only mathematically sensible condition to drop is the no-slip condition at the wall. We let the flow slip parallel to the wall but do not allow it to flow into the wall. The proper inviscid condition is that the normal velocities must match at any solid surface:

$$(u_n)_{\text{fluid}} = (u_n)_{\text{wall}} \ .$$

There is no condition whatever on the tangential velocity component at the wall in inviscid flow.

Digression: an elementary differential equation with a 'boundary layer' Consider the following equation for a function $u(y)$:

$$\epsilon u'' + u' = 1; \quad u(0) = 0, \quad u(1) = 2 \ , \tag{1.9}$$

where ϵ denotes a small positive constant. The exact solution is easily shown to be

$$u = y + \frac{1 - e^{-y/\epsilon}}{1 - e^{-1/\epsilon}} \ . \tag{1.10}$$

Some exact profiles are plotted in the Fig. 7(a) for various (small) values of ϵ. There is a "boundary layer", whose thickness is proportional to ϵ, rising from no slip at the wall to merge with a linear "outer stream".

Consider the case that ϵ is small. If we neglect the term $\epsilon u''$ entirely, on this basis, we obtained a first order equation

$$u' = 1, \quad \text{i.e.} \quad u = y + c \ ,$$

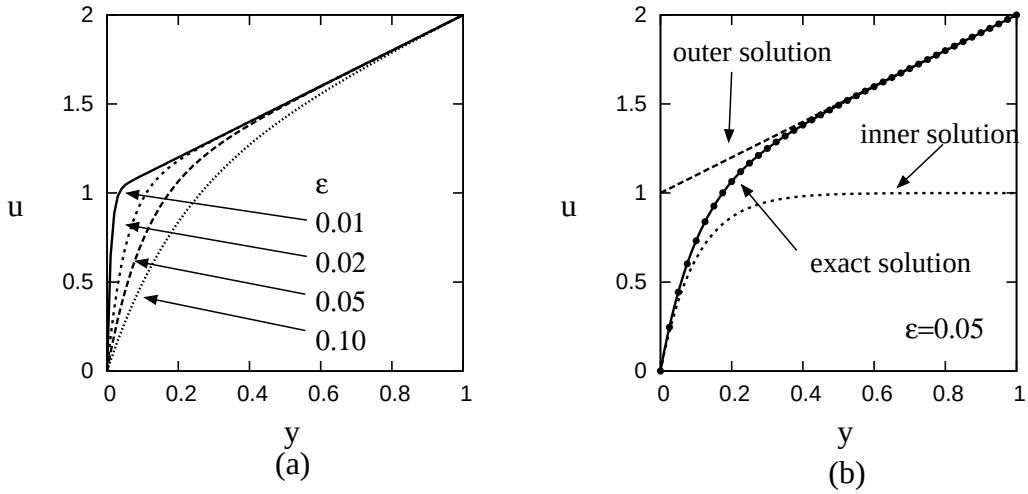

Figure 7: Exact and approximate solutions.

and on making this satisfy the condition $u(1) = 2$ we obtain an 'outer' solution

$$u(y) = y + 1 \ .$$

This solution is plotted together with the exact solution in the Fig. 7(b) for $\epsilon = 0.05$. The first order solution is an excellent approximation in the outer region, but is very different from the exact one near $y = 0$, no matter how small ϵ is. In the 'inner' region, the smaller ϵ is, the larger the derivative u''. It is not legitimate to neglect their product $\epsilon u''$. This procedure thus far is comparable with treating a high Reynolds number flow as being entirely inviscid; the small parameter ϵ multiplies the highest derivative in the equation, and by ignoring that term we lower the order of the system and are unable to satisfy all the boundary conditions. Here an 'inner' solution, or boundary layer, is needed near $y = 0$, in order to satisfy the boundary condition there. This matter will be explored later.

1.3 Comparison between Inviscid Theory and Experiment

Water and air are the most important fluids in engineering applications. Their viscosity is very small, practical flows are often of very high Reynolds number. It would appear reasonable to expect very good agreement between experiment and the inviscid theory. Perhaps the most glorious achievement of inviscid theory is the lift on an airfoil. Good agreement on the pressure distribution is obtained for a streamline body in a flow parallel to its axis. For example, Fig. 8(a) shows that good agreement exists here over almost the whole length of

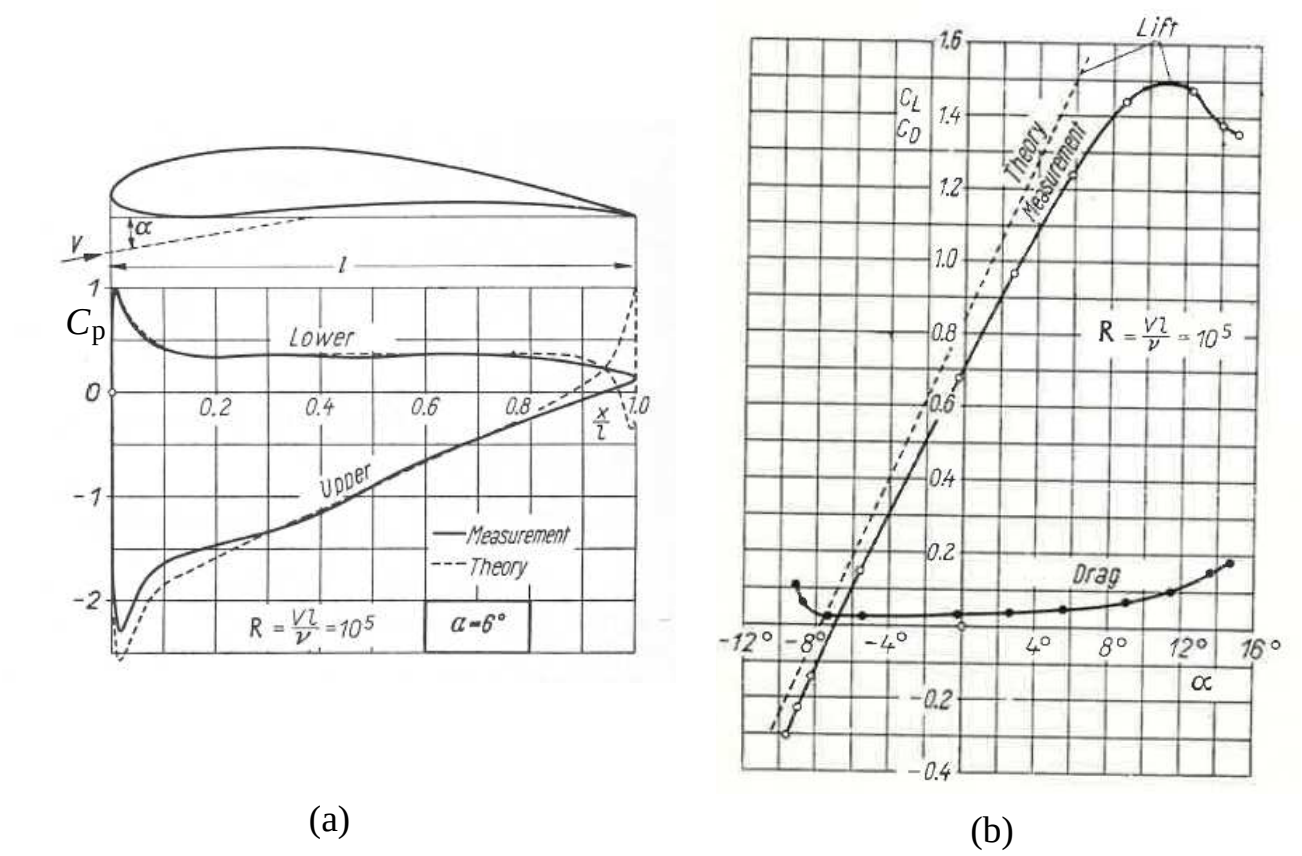

Figure 8: (a) Comparison between the theoretical and measured pressure distribution for Joukowski aerofoil at equal lifts, (b) lift and drag coefficients of a Joukowski aerofoil (Ref. [7]).

a Joukowsky aerofoil, with the exception of a small region near the trailing end. Although, generally speaking, the inviscid theory does not lead to useful results as far as drag calculations are concerned, the lift coefficient can be calculated from it very successfully. Fig. 8(b) represents the relation between the lift coefficient and angle of incidence, as measured by A. Betz in the case of Joukowski aerofoil of infinite span and provides a comparison with the theory. In the range of incidence angle $\alpha = -10^\circ$ to 10° the agreement is seen to be good and the small differences can be explained by the influence of the friction.

For a blunt-body flow, however, even at very high Reynolds number, the inviscid theory fails dramatically. A very common geometry in fluids engineering is cross-flow of a stream past a circular cylinder. The streamlines of the inviscid theory is plotted in Fig. 9(a), while the flow visualization of a real flow is shown in Fig. 9(b). The real streamlines are not symmetrical. The inviscid theory is completely unable to explain the existence of backward moving fluid at the rear of the cylinder, the "deadwater" region.

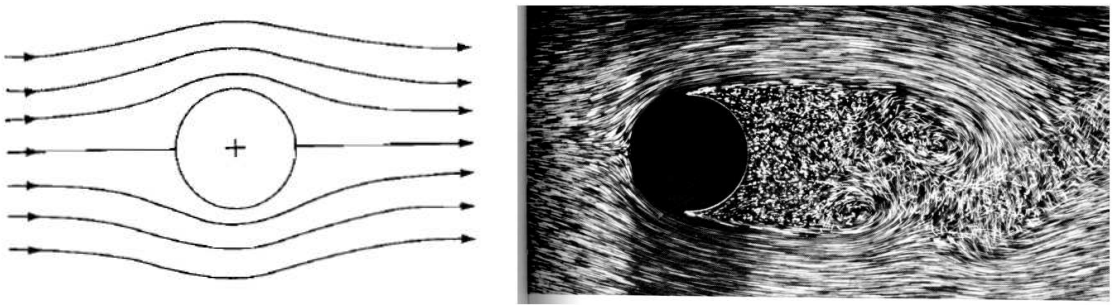

(a) (b)

Figure 9: (a) Inviscid fluid past a cylinder; (b) actual picture of the flow (Ref. [5]).

The pressure distribution from the inviscid theory is

$$C_p = \frac{p_s - p_\infty}{\frac{1}{2}\rho U_\infty^2} = 1 - 4\sin^2\theta$$

The distribution is shown in Fig. 10(c). The above equation illustrates a characteristic of inviscid flow without a "deadwater" region: There are no parameters such as Reynolds number and the pressure coefficient is independent of the fluid's physical properties. Also, the symmetry of $C_p(\theta)$ in Fig. 10(c) indicates that the integrated surface pressure force in the streamwise direction —the cylinder *drag*—is zero. This is an example of the d'Alembert paradox for inviscid flow past immersed bodies.

The experimental facts differ considerably from this inviscid symmetrical picture and depend strongly upon Reynolds numbers. Fig. 10(c) shows measured C_p for two Reynolds numbers. At the leading edge, both measured pressure distributions agree, to a certain extent, with that of the theory. At the trailing edge, the discrepancy between theory and measurement becomes large because of the flow separation. Note that the pressure is close to constant in the "dead water" region. For the laminar flow (Fig. 10(a)), separation occurs at $\theta = 82°$, which certainly could not have been predicted from inviscid theory. The broad wake and very low pressure in the separated laminar region cause the large drag: $C_D = 1.2$. The turbulent boundary layer in Fig. 10(b) is more resistant, and separation is delayed until $\theta = 120°$, with a resulting smaller wake, higher pressure on the rear, and 75 percent less drag, $C_D = 0.3$.

1.4 Characteristics of Turbulent Flows

"Turbulence" is not easy to define, but it is nearly ubiquitous. Tobacco smoke, industrial smoke, milk mixed into tea, all reveal turbulent motion. Osborne Reynolds (1842–1912) pub-

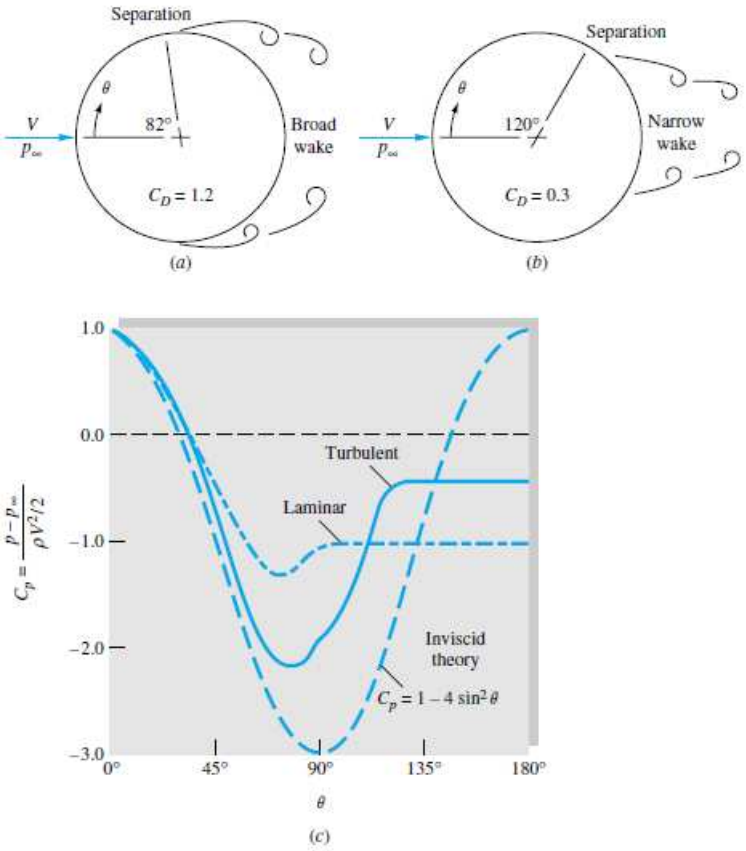

Figure 10: Flow past a circular cylinder: (a) laminar separation; (b) turbulent separation; (c) theoretical and actual surface-pressure distributions. (Ref. [3]).

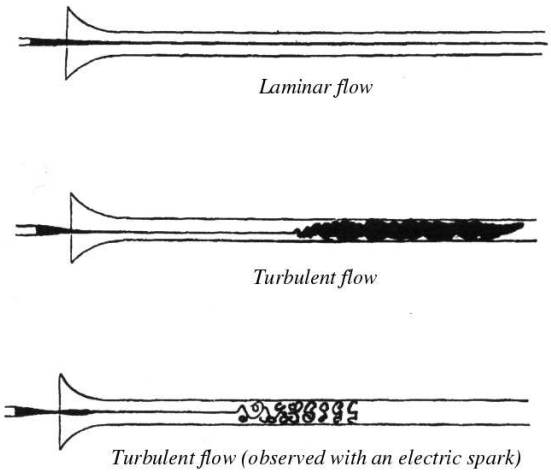

Figure 11: Reynolds' sketches of pipe-flow transition: (a) low-speed, laminar flow; (b) high-speed, turbulent flow; (c) spark photograph of condition (b). Ref. [3].

lished the classic pipe experiment in 1883 which showed the importance of the dimensionless Reynolds number named after him. By introducing a dye streak into a pipe flow, Reynolds could observe transition and turbulence. His sketches of the flow behavior are shown in Fig. 11.

Turbulent flows have common characteristics, one of the clearest of which is disorder. Fig. 12 shows a sheet of tiny bubbles advected by a flow along a flat plate. Compared to the laminar (steady, smooth and ordered) flow in Fig. 6, the flow here is turbulent (fluctuating, agitated and disordered). The instantaneous shape of the turbulent fluid suggests that the boundary layer consists of large vortical bulges rolling downstream on the wall. The outer edge of the boundary layer, which clearly divides the turbulent and non-turbulent regions, has a complex corrugated shape. The fluid decelerated near the wall is periodically lifting away towards the outer layers in an event of some violence, while high-speed fluid rushes in towards the wall to replace it.

The disorder is so central that no matter how carefully one reproduces the boundary conditions, the flow is never reproduced in detail (difficult hence interesting). On the other hand, averages, such as the mean speed of flow or correlation functions, are well defined and "stable" (there is hope).

There are disordered fluid motions—for example some fields of water or acoustic waves—which we prefer to exclude from the definition of turbulence, since they do very little mixing and mixing is an essential feature of turbulence. Turbulence performs efficient mixing and transport, not only of mass, but also of momentum (see Fig. 12 and Fig. 13) and heat,

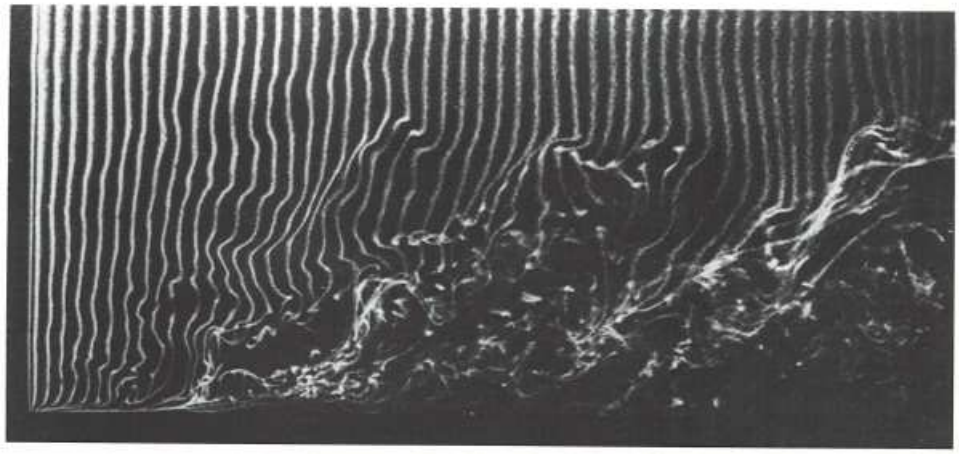

Figure 12: Turbulent boundary layer along a flat plate (water, free stream velocity 24.0 cm/s, $Re_\theta = 990$, hydrogen bubble method). Ref. [11].

hence affects enormously the surface friction and heat transfer, etc (which is why we care). The disorder is necessary but not sufficient for its description. A further characteristic of turbulence is the presence of vorticity, distributed continuously but irregularly in all three dimensions. This distinguishes turbulence from various kinds of wave motions and excludes two-dimensional flows. Something like turbulent motion can occur in two-dimensions; large-scale weather systems have this character. However, in strictly two-dimensional flows vorticity behaves as a scalar, and there is no vorticity production by vortex line stretching. Thus the characteristics of two-dimensional flows are quite different from those of three-dimensional turbulent flows.

2 Characterising the boundary layer

In IB you did an experiment in the small blue wind-tunnels in the hydraulics lab (it was a very long time ago). In that experiment you measured the streamwise velocity near the surface of a flat plate mounted in the wind-tunnel for two different cases: one in which the boundary layer was laminar and one in which it was turbulent. The latter case was made turbulent by the addition of a *trip* to the nose of the plate (essentially just a thin rod attached to the surface perpendicular to the oncoming flow). Some results are shown in Fig. 13. There are some obvious features of these results.

- The velocity drops from the *free-stream* value as the plate is approached down to zero at the plate (of course you can never measure the speed right at the plate but you can

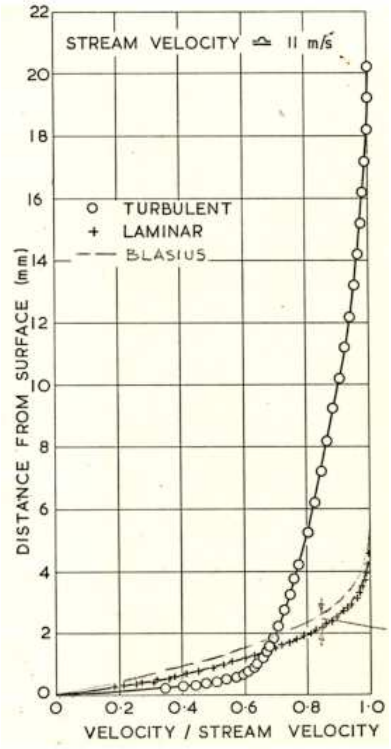

Figure 13: IB Lab results

safely extrapolate the trend down to zero).

- The region where the velocity is changing is fairly thin relative to the length of the plate.
- The laminar and turbulent velocity profiles are significantly different - the turbulent one has much larger gradients near the wall and extends further into the flow (is thicker).

The curve labelled "BLASIUS" refers to an exact solution for the laminar boundary layer that we will derive later in this part of the course.

Now before we go on to look at the boundary layer equations and solutions we might first look at how we can characterise, and parameterise the measured profiles.

2.1 The skin-friction

Probably the most important boundary layer parameter for an engineer is the drag it exerts on the wall. This is readily calculated using concepts from IB thermofluids. The shear stress in a Newtonian fluid is given by

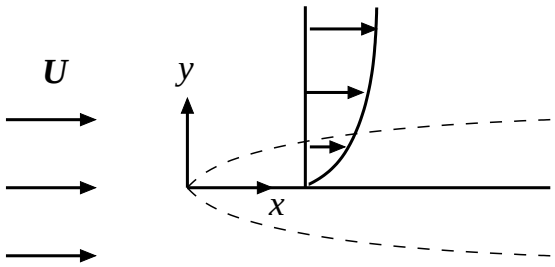

Figure 14: Flow past a flat plate and growth of the boundary thickness.

$$\tau = \mu \left(\frac{\partial u}{\partial y} + \frac{\partial v}{\partial x} \right). \tag{2.11}$$

Now if we want to know the shear-stress acting on the wall (or, equivalently, that the wall exerts on the fluid) then we consider the value of the shear stress at the wall,

$$\tau_w = \mu \frac{\partial u}{\partial y}\bigg|_{y=0}. \tag{2.12}$$

From this we can also come up with a non-dimensional skin-friction coefficient

$$C_f'/2 = \tau_w/(\rho U^2) \tag{2.13}$$

where the dash is there for historical reasons and just means the *local* skin friction coefficient at some point along the plate as opposed to the overall skin friction coefficient C_f for the whole plate (i.e. integrated over the whole plate length). If you look at Fig. 13 you can see that the turbulent boundary layer has a much larger shear-stress at the wall than the laminar one (look at the gradient at $y = 0$).

2.2 How thick is the boundary layer?

Since in some of the potential flow analysis we assume the solutions are valid outside the boundary layer then we might need to know the thickness of the boundary layer. Consider a uniform flow past a flat plate with a leading edge, as in Fig. 14. There is no flow component convecting vorticity towards the plate to counter the diffusion of vorticity from it, so the boundary layer becomes progressively thicker with downstream distance x. (In less formal

terms, the layers of fluid closest to the plate are the first to be slowed down as they pass the leading edge, and they in turn gradually slow down the layers of fluid which are further away).

We may estimate the boundary layer thickness δ by a simple argument based on the related problem in which the flat plate is instead suddenly pulled to the left, with speed U, through fluid which was previously at rest. We infer that at time t after the plate is moved vorticity will have diffused a distance of order $(\nu t)^{\frac{1}{2}}$. But by this time the leading edge of the plate will have moved a distance $x = Ut$ to the left. It follows that at distance x downstream from the leading edge there will be significant vorticity a distance of order

$$\delta \sim \left(\frac{\nu x}{U}\right)^{\frac{1}{2}}, \quad \frac{\delta}{x} \sim \sqrt{\frac{\nu}{xU}} = \frac{1}{\sqrt{Re_x}}, \quad \text{or} \quad \delta\sqrt{\frac{U}{\nu x}} = O(1) \tag{2.14}$$

from the plate, but not beyond. Here $Re_x = xU/\nu$ is the local Reynolds number. This crude estimate for the growth of the boundary condition with downstream distance x in the figure is indeed confirmed by the appropriate solution of the boundary layer equations. For a plate of finite length L the thickness (2.14) is small compared with L at all points of the plate if $Re = UL/\nu \gg 1$.

The effect of viscosity on the mean velocity drops off but it is hard to say where it becomes negligible. One crude measure of thickness sometimes used in experiments is the "99% thickness", see Fig. 15(a). This is the distance from the wall at which the velocity reaches 99% of its far-field or free-stream value. Whilst this value is useful it is also a bit arbitrary (why not the 98% thickness?) and it is also tricky to measure accurately since the velocity at this point changes very slowly with distance from the wall.

Another way to characterise the boundary layer is to compare the real flow with the flow we would have in the inviscid case , see Fig. 15(b) and (c). In this situation there would be slip at the wall and hence no profile. In comparison with this ideal flow we see that the mass flux is reduced (the velocities are less) and the momentum flux is also reduced (for the same reason). Further we could say that the kinetic energy flux is also reduced (we could extend this to other quantities). So we might say that in the boundary layer we have a mass flow deficit, a momentum deficit and an energy deficit (when compared with the inviscid flow). The amount of these deficits is related to the thickness of the boundary in some way. We have already discussed displacement thickness (related to the mass flow deficit) in the first part of the course but we will re-cap here.

Mass flux - displacement thickness. If we want the inviscid flow to have the same mass flux as the real flow then we need to remove a layer of fluid from the inviscid flow near the

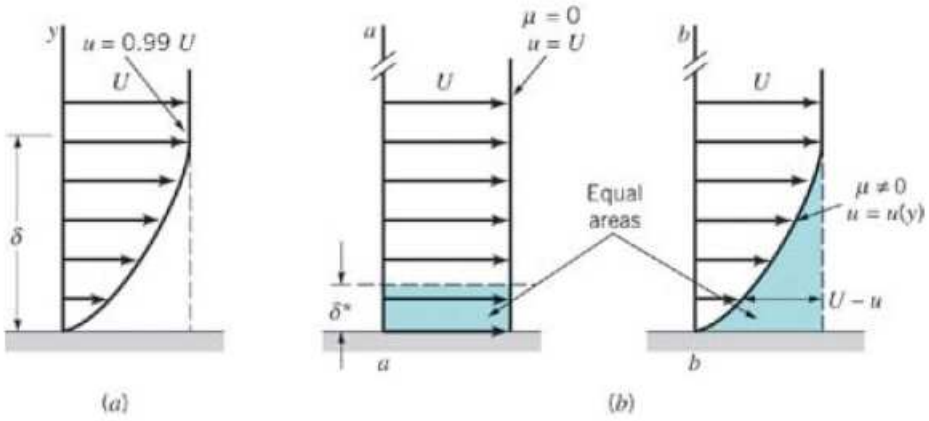

Figure 15: Definition of boundary layer thickness (Ref. [2]).

wall. We can work out the thickness of this layer (which we will call δ^*) by assuming that its mass flux is equal to the amount missing when we compare the real flow and the ideal

$$\rho U \delta^* = \rho \int_0^\infty (U - u) dy \tag{2.15}$$

hence

$$\delta^* = \int_0^\infty \left(1 - \frac{u}{U}\right) dy \tag{2.16}$$

Note that this is an integral definition and so it is also much less sensitive to experimental error than the 99% thickness. We can also do the same for the momentum (we call this thickness θ) and the energy (δ_E) i.e.

$$\theta = \int_0^\infty \frac{(U - u)u}{U^2} dy = \int_0^\infty \left(1 - \frac{u}{U}\right) \frac{u}{U} dy \tag{2.17}$$

and

$$\delta_E = \int_0^\infty \frac{(U^2 - u^2)u}{U^3} dy = \int_0^\infty \left(1 - \left(\frac{u}{U}\right)^2\right) \frac{u}{U} dy \tag{2.18}$$

Note that the momentum thickness and the energy thickness might be more appropriately called the "missing-momentum thickness" and the "missing-energy thickness" since larger values imply that there is more of the quantity missing relative to the inviscid flow. Since there is force acting on the fluid opposite to the flow (the skin-friction drag) then we might expect the momentum thickness to increase since momentum must be lost due to this external force

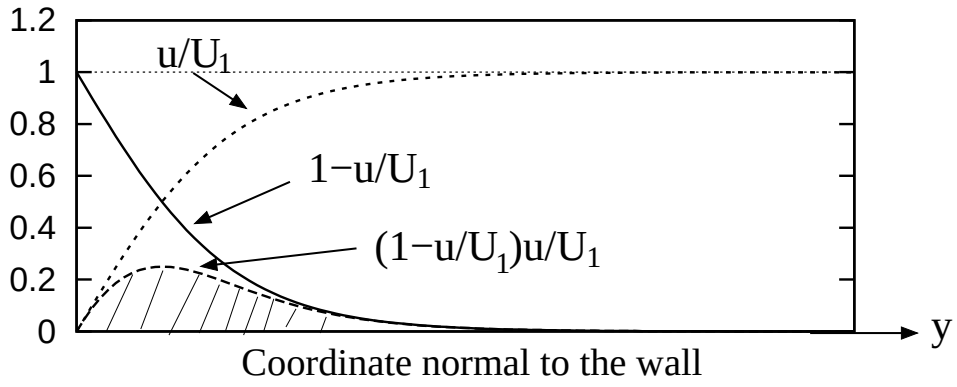

Figure 16: Momentum and displacement thicknesses.

(similarly energy is usually lost in the streamwise direction and so this thickness will usually increase). Note that, in the case of flows with pressure-gradients, there are additional forces acting which can also change these "thicknesses" and they are not always acting in the same direction as the skin-friction (just think about this for later in the lectures).

2.3 Shape factors

Another useful non-dimensional way of looking at boundary layer profiles is to consider the ratios of these lengths. The most common parameter used is simply the ratio of the displacement thickness to the momentum thickness and is called the shape-factor (or form-factor), H. The evaluation of δ^* and θ is illustrated graphically in Fig. 16. Clearly, δ^* is always the greater of the two, hence

$$H = \frac{\delta^*}{\theta} > 1. \tag{2.19}$$

Transition from laminar to turbulent flows is easiest to perceive by a study of the velocity profile in the boundary layer. As seen from Fig. 17(a), transition is shown prominently by a sudden increase in the boundary-layer thickness, $\delta\sqrt{\frac{U}{\nu x}}$, remains constant[3] and equal, approximately, 5. At $Re_x > 3.2 \times 10^5$ a sudden increase in the boundary-layer thickness is clearly visible, and an identical phenomenon is observed in the shape factor. Fig. 17(b) shows that the shape factor decreases from $H \approx 2.6$ in the laminar regime to $H \approx 1.4$ in

[3]This is consistent with the scaling that we have found in Eqn. 2.14. The value 5 is in excellent agreement with the exact Blasius solution that we will derive later

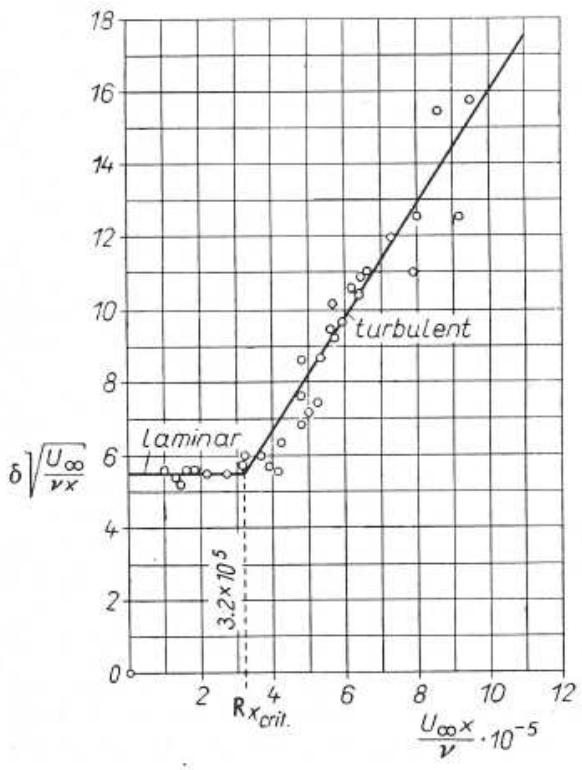

(a)

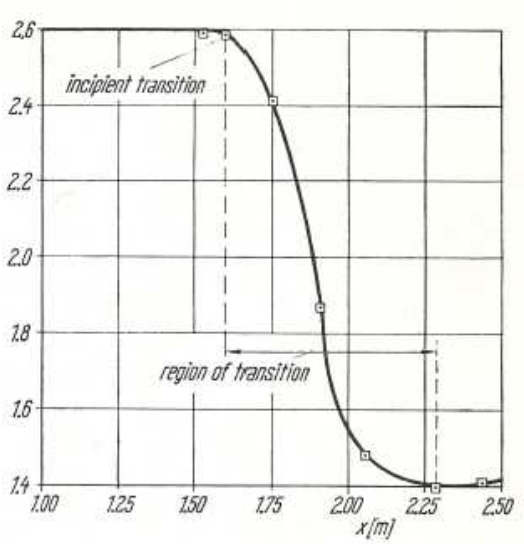

(b)

Figure 17: (a) Boundary layer thickness plotted against the Reynolds number based on the current distance x along a flat plate in parallel flow at zero incidence, (b) change in the shape factor of the boundary layer for a flat plate in the transition region (Ref. [7]).

the turbulent regime. This change in the shape factor in the transition region can be used for the convenient determination of the point of transition, or, rather, the transition region. The shape factor H is also a good indicator of the pressure gradient. The higher the H, the stronger the adverse gradient, and separation occurs approximately at

$$H \approx \begin{cases} 3.5 & \text{laminar} \\ 2.4 & \text{turbulent} \end{cases}$$

Question 1.

An experimentalist has measured the boundary layer velocity profile on a wing and found that a useful curve-fit to the data is given by $u/U = 1 - e^{-5y/\delta}$ where y is the distance from the wall and δ is the 99% thickness of the boundary layer as measured.

a) Find the displacement, momentum and energy thicknesses of the boundary layer at this point in terms of δ.

b) She makes another measurement further downstream. Consider each thickness and state whether it you think will be larger or smaller downstream - giving sensible reasons. Consider how this will depend on where the measurements are taken on the aerofoil.

c) She decides a better curvefit for the flow near the wall is $u/U = 16\eta^{0.926} - 15\eta$, where $\eta = y/\delta$. She realises immediately that there is a difficulty with the behaviour of this function as $y \to \infty$ since it is not bounded. She also realises that the way to fix this is to integrate from 0 to δ, rather than 0 to ∞ since it is a good fit in this range . Work out expressions for the displacement and momentum thickness in this case. Why is this procedure (integrating only up to δ) reasonable? Compare the results with those from part (a) to see the errors involved in this approximation.

Note that this is a very common procedure since it allows for the use of functional forms that are easy to analyse mathematically and only results in very small errors in the computed quantities.

Answers: (a)$\delta/5$, $\delta/10$, $\delta/6$, (b) All increase-faster in APG, (c) 0.193δ, 0.0923δ

Question 2.

In another experiment a researcher decides that a better fit to the velocity profile, in his flow, is one in which the velocity gradient at the edge of the layer ($y = \delta$) is zero and $u/U = 1$ at $y/\delta = 1$. This is often a reasonable approximation since the velocity typically asymptotes to the free-stream value extremely quickly. A suitable fit to the experimental results is $u/U = a_0(y/\delta) - a_1(y/\delta)^2 - a_2(y/\delta)^4$.

a) Apply the boundary conditions in order to relate a_2 and a_1 to a_0. Write down the expression for u/U. Note that the shape of the profile is now determined by only one parameter, a_0 which can be varied to produce different profile shapes - try plotting the function for various values of $0 < a_0 < 2.67$ (this restriction gives physically plausible shapes).

b) Consider the case where $a_0 = 2$. This looks something like a zero pressure-gradient boundary layer (actually the shape is not a great fit to known solutions but that doesn't matter here). Find the displacement thickness and the momentum thickness in terms of δ. Find the shape-factor.

c) Consider the case where $a_0 = 0$. Find the displacement thickness and the momentum thickness in terms of δ. Find the shape-factor. What physical situation does this profile represent (consider the shear stress at the wall)?

Answers: (a) $a_0\eta - (3a_0/2 - 2)\eta^2 - (1 - a_0/2)\eta^4$, (b)$\delta^* = \delta/3$, $\theta = 2\delta/15$, $H = 5/2$, (c) $\delta^* = 8\delta/15$, $\theta = 8\delta/63$, $H = 63/15 = 4.2$, this is a separating (or separated) profile since the wall shear-stress is zero.

2.4 Two-dimensional flow

Consider first the flow around a thin streamlined body, for example a thin aerofoil. Away from the body the Euler equations apply and for steady flow the solution of Laplace's equation will give good results (and may be sufficient in many cases). In the region close to the surface a boundary layer exists and we need to include the viscous terms. If the curvature of the surface is small then we can neglect it and just use the full two-dimensional equations as given above in x and y. Now if the boundary layer is thin we can calculate the velocity *on* the wall streamline, $U(x)$ using Euler and assume it is the same as the velocity at the outer edge of the boundary layer.

Hence the boundary conditions for the solution of the equations are

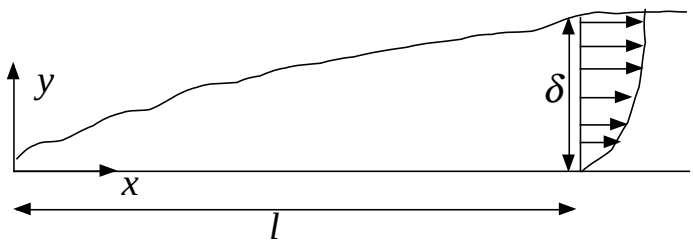

Figure 18: Schematic diagram of the boundary layer. The basic boundary layer theory: A boundary layer is very thin in compare with the scale of the body.

$$y = 0 \quad u = v = 0$$

$$y = \infty \quad u = U(x) \tag{2.20}$$

and in the free stream we know from Euler

$$U\frac{\partial U}{\partial x} = -\frac{1}{\rho}\frac{\partial p}{\partial x} \tag{2.21}$$

(cf. Bernoulli $\frac{1}{2}U^2 + p/\rho = constant$).

So now we have set up the boundary conditions we need to see if we can simplify the equations any further. In order to do this we first consider Prandtl's ORDER OF MAGNITUDE argument which may be used to simplify the full Navier-Stokes equations to a more manageable form in the case where the boundary layer is thin.

3 The boundary layer equations

3.1 Order of Magnitude argument

The essential part of this argument is to recognize that boundary layers are (in general) thin in comparison to their length of development (except perhaps right at the start of the body). Hence δ/l is small, where δ is the thickness of the boundary layer and l is the length over which it develops (see figure 18).

Now we will examine the order of magnitude of all of the terms in the two-dimensional Navier-Stokes equation in the region close to the boundary. By order of magnitude we mean

the size of the terms, which we will represent by $O()$, i.e. this means "is of the order of magnitude of". This sort of argument is often called a *scaling argument*. In essence what we are doing is looking at how the various terms in the equation change when we change the primary flow variables (such as the mean velocity, the size of the object we are studying, the viscosity of the fluid). To say that one variable *scales* with another quantity simply means that we expect it to increase proportionally when we increase that variable. To take an example, the skin friction drag on a body is proportional to its surface area so we might say that the skin friction drag *scales* with the surface area. This approach is very useful to a scientist or engineer since in this way we can determine which terms of an equation are likely to be important under certain conditions and then simplify the equation (by dropping those terms that are likely to be insignificant). It should be noted that we do this all the time, often almost unconsciously, when, for example we ignore relativistic effects in the equations of motion of a body, or neglect quantum effects. We expect these terms to be very small in the situations we encounter most of the time. These are extreme examples (where the extra terms that would appear in the equations are extremely small) but in other situations it is not as obvious which terms we can neglect. The order-of-magnitude analysis provides a formal procedure (in the less obvious cases) by which we can simplify the equations. Now we return to the two-dimensional Navier-Stokes equations and examine the order of magnitude of the terms so we can consider in what circumstances we can neglect some. In particular we are interested in the situation of a boundary layer developing on a wall. Starting from left to right in the equations we find,

$$\begin{aligned} U(x) &= O(U_\infty) \\ \frac{\partial u}{\partial x} &= O\left(\frac{U_\infty}{l}\right) \\ \frac{\partial u}{\partial y} &= O\left(\frac{U_\infty}{\delta}\right) \end{aligned} \tag{3.22}$$

Now near the surface the slope of the streamlines must be $O(\delta/l)$ and therefore

$$\begin{aligned} \frac{v}{U_\infty} &= O\left(\frac{\delta}{l}\right) \\ v &= O\left(\frac{U_\infty \delta}{l}\right) \end{aligned} \tag{3.23}$$

(or we can get the same result using the continuity equation), show this. Also the second order terms are

$$\frac{\partial^2 u}{\partial x^2} = O\left(\frac{U_\infty}{l^2}\right)$$
$$\frac{\partial^2 u}{\partial y^2} = O\left(\frac{U_\infty}{\delta^2}\right) \tag{3.24}$$

and the order of the other terms can be found by similar means.

Substituting these into the momentum equations gives

$$O\left(\frac{U_\infty^2}{l}\right) + O\left(\frac{U_\infty^2}{l}\right) = O\left(-\frac{1}{\rho}\frac{\partial p}{\partial x}\right) + O\left(\nu\left(\frac{U_\infty}{l^2} + \frac{U_\infty}{\delta^2}\right)\right)$$
$$O\left(\frac{U_\infty^2 \delta}{l^2}\right) + O\left(\frac{U_\infty^2 \delta}{l^2}\right) = O\left(-\frac{1}{\rho}\frac{\partial p}{\partial y}\right) + O\left(\nu\left(\frac{U_\infty \delta}{l^3} + \frac{U_\infty}{l\delta}\right)\right) \tag{3.25}$$

Now in order to non-dimensionalise things we divide through by U_∞^2/l This leads to

$$O(1) + O(1) = O\left(-\frac{\partial(p/\rho U_\infty^2)}{\partial(x/l)}\right) + O\left(\frac{1}{\frac{U_\infty l}{\nu}}\right) + O\left(\frac{1}{\frac{U_\infty l}{\nu}}\left(\frac{l}{\delta}\right)^2\right)$$
$$\underbrace{O\left(\frac{\delta}{l}\right) + O\left(\frac{\delta}{l}\right)}_{\text{INERTIA FORCES}} = \underbrace{O\left(-\frac{1}{\rho}\frac{\partial(p/\rho U_\infty^2)}{\partial(y/\delta)}\frac{l}{\delta}\right)}_{\text{PRESSURE GRADIENT FORCES}} + \underbrace{O\left(\frac{\delta}{l}\frac{1}{\frac{U_\infty l}{\nu}}\right) + O\left(\frac{l}{\delta}\frac{1}{\frac{U_\infty l}{\nu}}\right)}_{\text{VISCOUS STRESS FORCES}} \tag{3.26}$$

Now, following Prandtl, we will examine what happens when $U_\infty l/\nu \to \infty$. Consider the first of the two momentum equations, bearing in mind that according to the boundary layer hypothesis $\delta << l$ and hence $(l/\delta)^2 \to \infty$. The term in $1/Re$ goes to zero and the question is what happens to the term

$$\frac{1}{Re}\left(\frac{l}{\delta}\right)^2 \tag{3.27}$$

as $Re \to \infty$??

Prandtl considered three cases:

CASE (a)

$$\frac{1}{Re}\left(\frac{l}{\delta}\right)^2 >> O(1) \tag{3.28}$$

This leads to a balance between the pressure gradient forces and the viscous forces. This sort of balance occurs in low Reynolds number flows (Stokes flows) where the inertia is small. HOWEVER, we are considering the case where $Re \to \infty$. One possible case where this might occur is in the fully developed flow in a parallel pipe or duct. BUT there is a problem with this. Since the inertia terms have dropped out, then Reynolds number cannot be a ratio of inertia to viscous forces so we have a paradox. This case doesn't make sense.

CASE (b)

$$\frac{1}{Re}\left(\frac{l}{\delta}\right)^2 << O(1) \tag{3.29}$$

Here we have a balance between pressure gradient forces and inertia forces. This case is O.K. but it simply represents the Euler equations. It suggests that viscous forces are not important, but we know that they must be in a boundary layer. So this solution is not useful for our purposes. This is where the classical theorists went wrong. They assumed that their inviscid solutions (eg. potential flow) should become more accurate at higher Reynolds number and perhaps exact in the infinite Reynolds number limit. Experiments showed that this was not the case at all (bodies did not seem to approach a situation where they had zero drag, for example)

CASE (c)

$$\frac{1}{Re}\left(\frac{l}{\delta}\right)^2 = O(1) \tag{3.30}$$

In this case inertia, pressure gradient and viscous forces are ALL equally important together. Consideration of this case led to the breakthrough of Prandtl. He recognised that, even in flows at extremely high Reynolds numbers there would be a region near the wall where the velocity dropped to zero and hence, in this region, the local Reynolds number of the flow would be low and so viscous forces could not be neglected. So, regardless of the external

Reynolds number (eg. for a cylinder $U_\infty D/\nu$, there is some region close to the surface, however small, where viscosity is important.

Rearranging the previous equation leads to

$$\frac{\delta}{l} = O\left(\frac{1}{\sqrt{Re}}\right). \tag{3.31}$$

Note that this tells us how the boundary layer thickness varies with distance along a plate (how it grows). Substituting x, the distance from the leading edge for the length l and multiplying across we find

$$\delta = O\left(\sqrt{\frac{\nu x}{U_\infty}}\right). \tag{3.32}$$

Since it is always of this order then we can say that the boundary layer thickness scales in this way - we will find the same result from an exact solution of the boundary layer equations later on. Note also that (3.31) justifies our original assumption that δ/l is small - at least at reasonable Reynolds numbers. Note also that this Reynolds number is based on distance along the plate so we would expect this assumption to break down very near the leading edge where l is small and hence so is $Re = U_\infty l/\nu$.

We can substitute this back into our momentum equations to examine the consequences.

$$\begin{aligned} O(1) + O(1) &= O\left(-\frac{\partial(p/\rho U_\infty^2)}{\partial(x/l)}\right) + O\left(\frac{1}{Re}\right) + O(1) \\ O\left(\frac{1}{\sqrt{Re}}\right) + O\left(\frac{1}{\sqrt{Re}}\right) &= O\left(\frac{\partial(p/\rho U_\infty^2)}{\partial(y/\delta)}\frac{l}{\delta}\right) + O\left(\frac{1}{Re^{3/2}}\right) + O\left(\frac{1}{\sqrt{Re}}\right) \end{aligned} \tag{3.33}$$

Now all the terms in inverse powers of Re go to zero as $Re \to \infty$ and hence $\partial p/\partial y = 0$. We can now simplify the equations to

$$\begin{aligned} u\frac{\partial u}{\partial x} + v\frac{\partial u}{\partial y} &= -\frac{1}{\rho}\frac{\partial p}{\partial x} + \nu\frac{\partial^2 u}{\partial y^2} \\ 0 &= -\frac{\partial p}{\partial y} \end{aligned} \tag{3.34}$$

The second equation suggests that $p \neq f(y)$ and hence $p = p(x)$[4]so to summarize and include this we finally have

$$\begin{aligned} u\frac{\partial u}{\partial x} + v\frac{\partial u}{\partial y} &= -\frac{1}{\rho}\frac{dp}{dx} + \nu\frac{\partial^2 u}{\partial y^2} \\ \frac{\partial u}{\partial x} + \frac{\partial v}{\partial y} &= 0 \end{aligned} \tag{3.35}$$

These equations are known as PRANDTL'S BOUNDARY LAYER EQUATIONS and they become asymptotically correct as $Re \to \infty$. To solve them we need boundary conditions and these are

$$\begin{aligned} y = 0 \quad &, \quad u = v = 0 \\ y = \infty \quad &, \quad u = U(x) \\ U\frac{dU}{dx} &= -\frac{1}{\rho}\frac{dp}{dx} \end{aligned} \tag{3.36}$$

These equations can be solved numerically or by series expansion for various cases and in this course we will consider some exact solutions for laminar boundary layers.

[4]This is useful when we consider using the potential flow solution for the outer flow to determine the pressure along the wall in order to calculate the boundary layer. Since the pressure does not vary through the boundary layer then we can use the pressure-gradient at the wall from the potential flow as the pressure-gradient in the boundary layer equations

Digression: the elementary differential equation with a 'boundary layer' revisited Consider again Eqn. (1.9):

$$\epsilon u'' + u' = 1; \quad u(0) = 0, \quad u(1) = 2 \ ,$$

where ϵ denotes a small positive constant. The exact solution is easily shown to be

$$u = y + \frac{1 - e^{-y/\epsilon}}{1 - e^{-1/\epsilon}} \ .$$

By neglecting the term $\epsilon u''$ on the basis that ϵ is small, we have obtained the 'outer' solution

$$u_o(y) = y + 1 \ .$$

From Fig. 7, we observe that although this first order solution is an excellent approximation in the outer region, it is very different from the exact solution near $y = 0$, no matter how small ϵ is. Here an 'inner' solution, or boundary layer, is needed near $y = 0$, in order to satisfy the boundary condition there. We may recognize variations of u in this boundary layer to be much more rapid than those elsewhere by an order of magnitude argument. Suppose that the length scale of the inner region is δ ($\delta << 1$), then near $y = 0$,

$$u' = O\left(\frac{1}{\delta}\right), \quad u'' = O\left(\frac{1}{\delta^2}\right) \ . \tag{3.37}$$

The only sensible length scale is $\delta \sim \epsilon$ and the first two terms in Eqn. (1.9) are of order $O(1/\epsilon)$ and the right hand side is of $O(1)$. With this scaling the previously negligible second derivative regains its importance so that to a first approximation the inner solution u_i satisfies:

$$\epsilon u'' + u' = 0 \tag{3.38}$$

This is equivalent of the boundary layer Eqn. (9.153), in our simple example. On making the inner solution satisfy the boundary condition $u(0) = 0$ we obtain

$$u_i = A\left(1 - e^{-y/\epsilon}\right)$$

and the matching condition

$$\lim_{y\to\infty} u_i = \lim_{y\to 0} u_o$$

determines that $A = 1$. Thus

$$u = \begin{cases} y+1 & \text{if } y > \epsilon, \\ 1 - e^{-y/\epsilon} & \text{if } y < \epsilon \end{cases}$$

in keeping with our deduction from the exact solution (1.10). These are plotted together in the Fig. 7(b) for $\epsilon = 0.05$. Each is seen to be an excellent approximation in its respective region, although clearly they do not merge to form a complete approximation to the problem.

We may use the inner and outer solution to form a composite function that should be a good approximation over the entire region. A pragmatic approach is suggested in van Dyke 1964: Sum the two solutions and subtract the terms common to both, which would otherwise be counted twice. Thus $u \approx [u_{inner} + u_{outer} - \text{commonterms}]$. In the simple first-order solutions of the above equation, we see that the only common term is 1, which we subtract from the sum and thus obtain the approximation

$$u_{\text{composite}} = 1 - e^{-y/\epsilon} + y \ .$$

This composite estimate is within ± 1 percent of the exact solution, Eqn. (1.10), for all $\epsilon \leq 0.1$. It is plotted in the figure (b) for $\epsilon = 0.05$ (represented by black circles) and is nearly coincident with the exact solution.

Van Dyke generalizes the previous simple first-order procedure into a method of matching inner and outer expansion of any order. We are not going to pursue it in the course.

3.2 Comments on the boundary layer equations

There are many things to notice about this simplified set of equations.

1. The continuity equation is unaffected.

2. The term $\partial^2 u/\partial x^2$ in the x-momentum equation has been neglected.

3. The pressure gradient in the y direction is nearly zero, then, the transverse pressure gradient is negligible in a boundary layer.

$$\frac{\partial p}{\partial y} \approx 0, \qquad p = p(x) \quad \text{only}$$

This splendid observation is due to Prandtl (1904), showing that pressure is a known variable in boundary-layer analysis, with $p(x)$ assumed to be impressed upon the boundary layer from outside by an inviscid outer flow analysis. That is, the freestream outside the boundary layer, $U = U(x)$, where x is the coordinate parallel to the wall, is related to $p(x)$ by Bernoulli's theorem for incompressible flow. For steady flow, for example,

$$\frac{dp}{dx} = -\rho U \frac{dU}{dx} \tag{3.39}$$

so that specifying $p(x)$ is equivalent to specifying $U(x)$

4. Perhaps most interesting, we note that all second derivatives with respect to x have been lost in the boundary layer approximation. This has two consequences: (1) the equations are now parabolic instead of elliptic, so that x is now a marching variable and numerical solutions are relatively easier; and (2) we have lost certain boundary conditions, notably those on v and x. The variable v has only one derivative left, $\partial v/\partial y$, with $\partial v/\partial x$ and the two second derivatives having been discarded. We now need only one condition on v at one y position. The obvious condition is to retain is no slip: $v = 0$ at $y = 0$. We need not specify v at the outer edge of the layer. We have lost one condition on u by discarding $\partial^2 u/\partial x^2$; therefore we disavow all knowledges of u at one x position, the best choice being the exit plan, on which we set no boundary condition for u. The solution will yield the correct values of u at the exit without our specifying them.

To sum up, the boundary layer equations are far simpler than their parents, the Navier-Stokes equations.

Question 3.

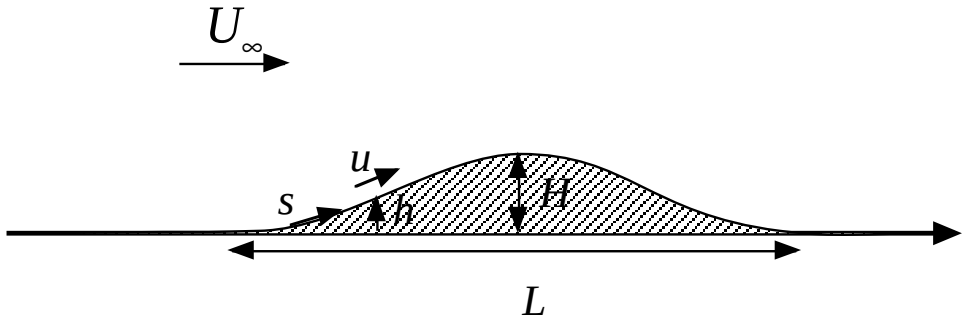

Let us consider the order of magnitude argument for a much simpler equation. Suppose we are examining the flow over a hill on the floor of a wind-tunnel. We are interested in the pressure gradient along the surface of the hill and decide to use Bernoulli's equation in its differentiated form. There is a potential energy term in the equation and we can write Bernoulli as

$$p + \frac{1}{2}\rho u^2 + \rho g h = \text{constant}. \tag{3.40}$$

Since we are interested in the pressure gradient then we take the derivative with respect to s, the distance along the surface (say, just to be careful, outside the boundary layer). This gives

$$\frac{\partial p}{\partial s} + u\frac{\partial u}{\partial s} + \rho g \frac{\partial h}{\partial s} = 0, \tag{3.41}$$

or

$$-\frac{\partial p}{\partial s} = \rho u \frac{\partial u}{\partial s} + \rho g \frac{\partial h}{\partial s}, \tag{3.42}$$

which is, of course the Euler equation. Now the question is "Is it safe to neglect the gravity term?" - if we can the problem becomes much simpler. We might also be interested in whether we can do that in the real case we are modelling which might be a large hill in a field. We will consider the case where the hill is long and low so H/L is quite small ($H/L << 1$), and hence $\frac{\partial}{\partial s} \approx \frac{\partial}{\partial x}$. The simplest way to decide on the importance of the terms is to estimate their size, or their order of magnitude.

Perform an order of magnitude analysis of the equation and hence find under what conditions the contribution of the gravity term to the pressure-gradient may be neglected.

Answer: It depends on the non-dimensional number gH/U_∞^2, if this is small we can neglect the gravity term. Note that this number is a variation on the Froude number.

Fundamentals of Aerodynamics
John Anderson (McGraw−Hill, 2016)

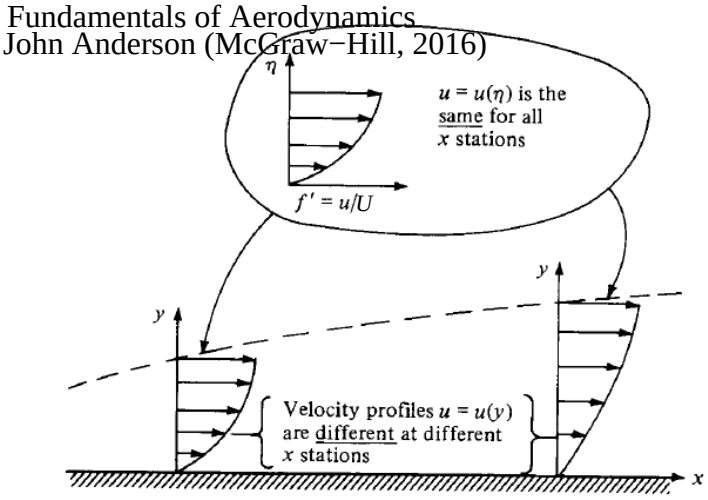

Falkner-Skan solution: $U = Ax^m$, $A > 0$.

$$f''' + ff'' + \beta(1 - f'^2) = 0, \quad \beta = \frac{2m}{m+1}$$

4 Similarity solutions

In this section some special exact solutions of the boundary layer equations will be considered in which the shape of the profiles are invariant as the flow develops. When the flow has no characteristic length scale, we may expect that the velocity distributions across the boundary layer for different values of x will be similar. By this we mean that the distribution for one value of x can be obtained from that for another value of x by a simple change of scale of the y coordinates, the scaling being determined by the corresponding x-coordinates. As illustrated in the following figure, the variation of u normal to the wall will change as the flow progress downstream. However, when plotted versus η, $u = u(\eta)$ (here $\eta = y/g(x)$), is the same for all x positions.

This condition of similarity can be expressed in the form

$$\frac{u}{U(x)} = h(\eta), \quad \eta = y/g(x)$$

where h and g are functions of η and x, respectively, and η is non-dimensional.

This implies that the boundary layer equations, which are partial differential equations in the two independent variables x and y, may be transformed into an ordinary differential equation in terms of η, the solution of which should give the function $h(\eta)$. Mathematically similarity solutions offer obvious and welcome simplifications.

How to find similarity solutions the method usually consists of the following steps:

- Guess the similarity form of the solution (crucial step)

$$u(x,y) = U(x)h(\eta) \quad \text{or} \quad \psi(x,y) = U(x)g(x)f(\eta), \quad \text{where} \quad \eta = y/g(x)$$

- Calculate the expressions for v, $\partial u/\partial x$, $\partial u/\partial y$, and $\partial^2 u/\partial y^2$ in terms g and f (Many times of the chain rule).
- Substitute these expressions into the PDE (Boundary Layer Equations).
- Determine $g(x)$ by setting the coefficients (which may be a function of $g(x)$) in the ODE of $f(\eta)$ as constants (Moment of truth).
- Solve the similarity ODE for $f(\eta)$ with appropriate boundary conditions.

4.1 The boundary layer on a flat plate

On inviscid theory a uniform stream approaching a flat plate at zero angle of attack is unaffected by the presence of the plate, so $U(x)$ is a constant. The boundary layer equations then reduce to

$$u\frac{\partial u}{\partial x} + v\frac{\partial u}{\partial y} = \nu\frac{\partial^2 u}{\partial y^2}\ , \tag{4.43}$$

$$\frac{\partial u}{\partial x} + \frac{\partial v}{\partial y} = 0\ . \tag{4.44}$$

We seek a similarity solution in which u is some function of the single variable

$$\eta = y/g(x), \quad \text{you may guess that} \quad g(x) \sim \sqrt{\nu t} = \sqrt{\nu\frac{x}{U}}\ . \tag{4.45}$$

This implies that the velocity profile at any distance x from the leading edge will be just a 'stretched out' version of the velocity profile at any other distance x; this is a natural assumption if, as we shall suppose, the plate is semi-infinite, from $x = 0$ to $x = \infty$. We here take the similarity method of the previous lecture a little further by not attempting to guess the function $g(x)$ in advance; we show instead how it can be left to emerge in a rational way as the calculation proceeds.

We first satisfy Eqn. (4.44) by introducing a stream function $\psi(x, y)$ such that

$$u = \partial\psi/\partial y \ , \quad v = -\partial\psi/\partial x \ .$$

If we write $u = Uh(\eta)$ we may integrate to obtain

$$\psi = \int_0^y u dy + k(x) = \int_0^y Uh(\eta) dy + k(x) = Ug(x) \int_0^\eta h(s) ds + k(x)$$

But we want the plate itself to be a streamline, so that $\psi = 0$, say, at $\eta = 0$; so $k = 0$. It is more convenient to write ψ in the form

$$\psi = Ug(x)f(\eta), \text{ with } f(0) = 0 \ , \ \eta = y/g(x), \ \frac{\partial\eta}{\partial x} = -\frac{\eta g'}{g}, \ \frac{\partial\eta}{\partial y} = \frac{1}{g}$$

whence

$$u = Uf'(\eta), \ \frac{\partial u}{\partial x} = Uf''\frac{\partial\eta}{\partial x} = -Uf''\frac{\eta g'}{g}, \ \frac{\partial u}{\partial y} = Uf''\frac{\partial\eta}{\partial y} = U\frac{f''}{g} \tag{4.46}$$

$$\frac{\partial^2 u}{\partial y^2} = U\frac{f'''}{g^2}, \quad v = -\frac{\partial\psi}{\partial x} = U(\eta f' - f)g' \ . \tag{4.47}$$

Here, of course, f' denotes $f'(\eta)$, but g' denotes $g'(x)$. On substituting for u and v in Eqn. (4.43), we obtain

$$Uf'\left(-Uf''\frac{\eta g'}{g}\right) + U(\eta f' - f)g'U\frac{f''}{g} = \nu U\frac{f'''}{g^2} \ \Rightarrow \ f''' + \frac{Ugg'}{\nu}ff'' = 0 \ .$$

Our aim is, of course, to obtain an ordinary differential equation for f as a function of η. We must therefore choose gg'—which would otherwise be a function of x—to be a constant. Clearly the choice of ν/U for this constant is convenient in that it rids the equation of all parameters of the problem, and integrating $gg' = \nu/U$ gives

$$\frac{1}{2}g^2 = \frac{\nu x}{U} + d \ .$$

where d is an arbitrary constant. Now, if g vanishes for some value of x, certain flow quantities such as

$$\partial u/\partial y = Uf''/g$$

become singular. We clearly expect some such behaviour at the leading edge, if only because on $y = 0$ the velocity suddenly changes from U in $x < 0$ to zero in $x > 0$. We therefore choose $d = 0$ to ensure that such behaviour occurs at the leading edge. Thus $g = (2\nu x/U)^{\frac{1}{2}}$ and, to sum up, we have found that

$$\psi = (2\nu x U)^{\frac{1}{2}} f(\eta), \quad \text{where} \quad \eta = \frac{y}{(2\nu x/U)^{\frac{1}{2}}} \ . \tag{4.48}$$

and

$$f''' + f f'' = 0 \ . \tag{4.49}$$

This equation must be supplemented by the boundary conditions

$$f(0) = f'(0) = 0, \quad f'(\infty) = 1 \ . \tag{4.50}$$

The first these stems from Eqn. (4.47), and the second from Eqn. (4.46), and the third from the fact that u must tend to U, the mainstream value, as we leave the boundary layer (cf. Eqn. (3.36)).

The Blasius equation has never yielded to exact analytical solution. Blasius himself (1908) gave matching inner and outer series solutions. Many other methods of attack are chronicled in the text by Rosenhead [9]. With the advent of the personal computer, it is now a simple matter to solve Eqns. (4.49) and (4.50) using the Runge-Kutta method.

The problem is to find the correct value $f''(0)$ which will make f' approach 1.0 as η approaches infinity. By a simple asymptotic analysis, we find that "infinity" is approximately $\eta = 10$, and we can run off a few solutions for various $f''(0)$, all of which behave beautifully. From these guesses, we can interpolate to find the value $f''(0)$ which makes $f'(\infty) \approx 1.0$. The accepted value, correct to six significant figures, is

$$f''(0) = 0.469600... \tag{4.51}$$

The velocity profile $f' = u/U$ of the Blasius's solution is shown in Fig. 19, where it is compared with the experiments of Liepmann. The ratio u/U is 0.99 at $\eta \approx 3.5$. Thus we have a value of the 99 percent boundary-layer thickness

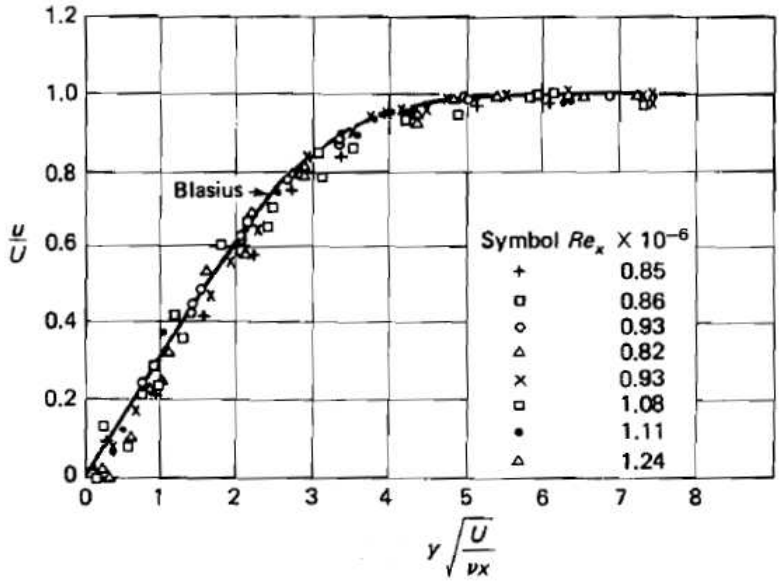

Figure 19: The Blasius solution for the flat-plate boundary layer and comparison of $f' = u/U$ with experiments by Liepmann. Ref. [5].

$$\delta_{99\%} \approx 3.5 \left(\frac{2\nu x}{U}\right)^{\frac{1}{2}} \quad \text{or} \quad \frac{\delta_{99\%}}{x} \approx \frac{5.0}{\sqrt{Re_x}}$$

As the boundary layer thickness the horizontal stress on the plate

---

$$\tau_{\text{wall}} = \mu \left(\frac{\partial u}{\partial y} + \frac{\partial v}{\partial x}\right)_{y=0} = \mu \frac{\partial u}{\partial y}_{y=0} = \mu U \left(\frac{U}{2\nu x}\right)^{\frac{1}{2}} f''(0)$$

---

decreases with x.

Application of the theory to a finite flat plate of length L . It is natural to hope that the above similarity solution will hold reasonably well for a finite plate of length L, even if behaviour of a different kind must be expected near and beyond the trailing edge. Taking into account the top and the bottom of the plate, we obtain for the drag

---

$$D = 2 \int_0^L \tau_{\text{wall}} dx = 2\sqrt{2} f''(0) \rho U^2 L Re_L^{-\frac{1}{2}} , \qquad (4.52)$$

---

where $Re_L = UL/\nu$. Thus D is proportional to $L^{\frac{1}{2}}$, rather than L, because the velocity gradient decreases with x, corresponding to the thickening of the boundary layer. The drag is proportional to $\nu^{\frac{1}{2}}$, and vanishes as $\nu \to 0$. The numerical value of $f''(0) = 0.4696$.

The agreement between boundary layer theory and experiment is very good, both in respect of the expression (4.52) for the drag and in respect of the details of the velocity profile (see Fig. 19). This agreement does break down, however, if the Reynolds number is very high, for the boundary layer then becomes unstable and turbulent flow ensues. The critical value of Re at which this happens can be anywhere between about 10^5 and 3×10^6, depending on the level of turbulence in the oncoming stream and the roughness of the plate surface.

4.2 Inviscid flow past wedges and corners

The outer boundary condition for velocity in the boundary layer theory is often calculated with the inviscid flow theory. In order to find interesting solutions to the boundary equation, we first investigate plane inviscid flow of interest. Corner flow is a flow pattern that cannot be conveniently produced by superimposing sources, sinks, and vortices. It has a strikingly simple complex representation in polar coordinates:

$$f(z) = Bz^n = Br^n \cos n\theta + iBr^n \sin n\theta$$

where B and n are constants.

It follows from the complex function theory that for this flow pattern

$$\phi = Br^n \cos n\theta, \psi = Br^n \sin n\theta, u_r = Bnr^{n-1} \cos n\theta, u_\theta = -Bnr^{n-1} \sin n\theta. \quad (4.53)$$

Streamlines from Eqn. (4.53) are plotted in Fig. 20 for five different values of n. The flow is seen to represent a stream turning through an angle $\alpha = \pi/n$. Patterns in Fig. 20d and e are not realistic on the downstream side of the corner, where separation will occur due to the adverse pressure gradient and sudden change of direction. In general, separation always occurs downstream of salient, or protruding corners, except in creeping flows at low Reynolds number $Re < 1$.

If we expand the plot of Fig. 20a to c to double size, we can represent stagnation flow toward a corner of angle $2\alpha = 2\pi/n$. This is done in Fig. 21 for $n = 3$, 2, and 3/2. These are very realistic flows; although they slip at the wall, they can be patched to boundary-layer theories very successfully.

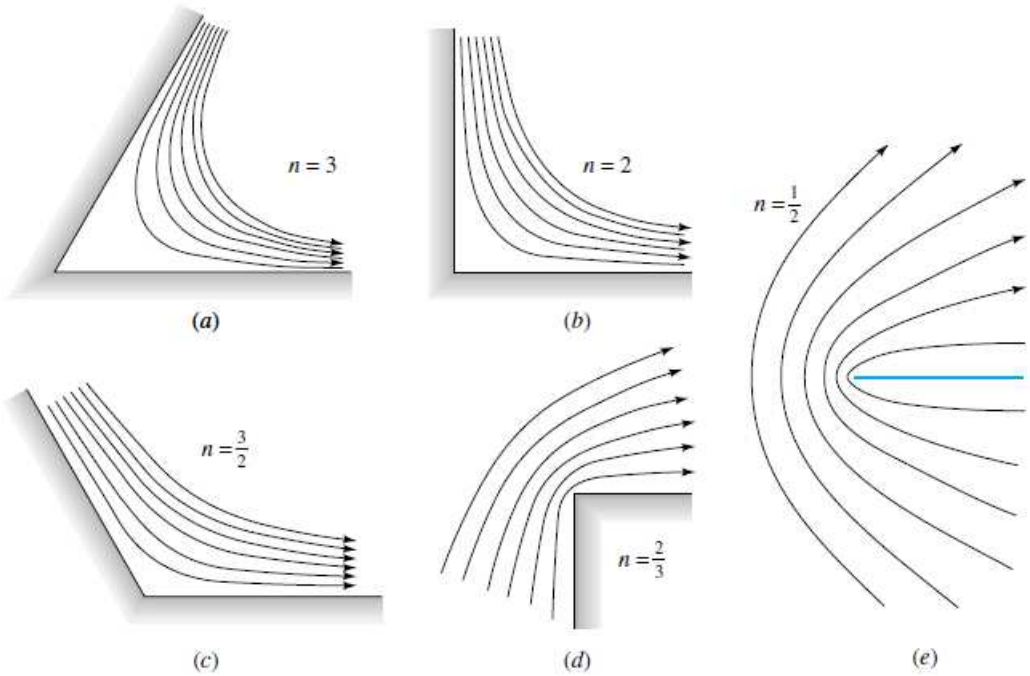

Figure 20: Streamlines for corner flow, Eqn. (4.53) for corner angle α of (a) 60°, (b) 90°, (c) 120°, (d) 270°, and (e) 360°. Ref. [3].

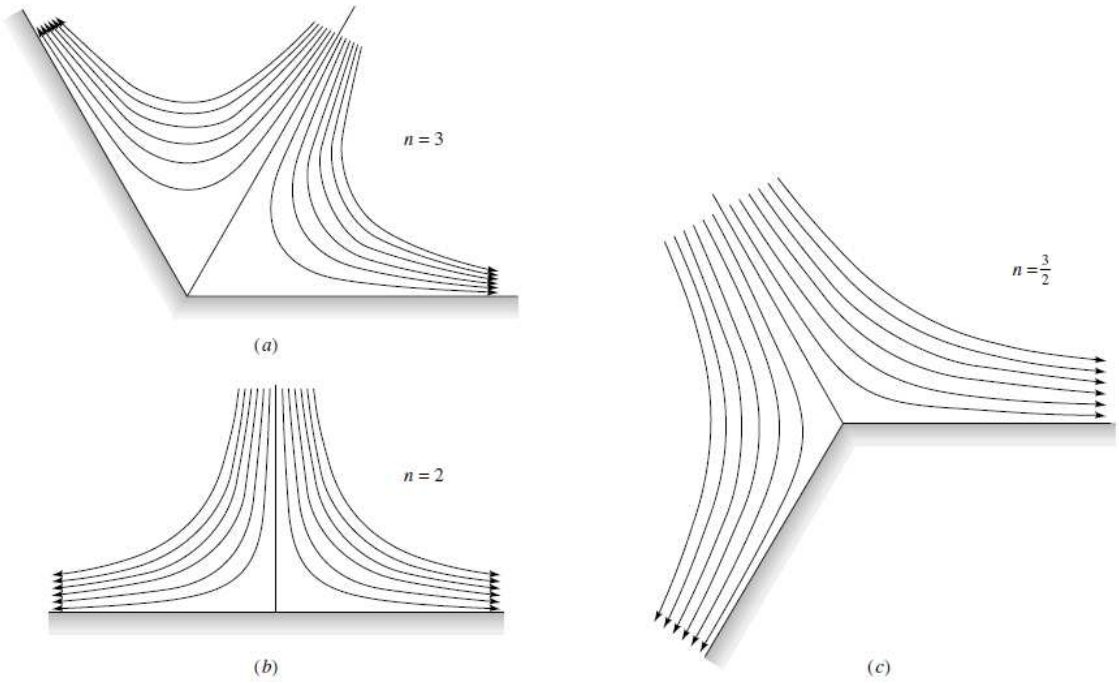

Figure 21: Streamlines for stagnation flow from Eqn. (8.49) for corner angle 2α of (a) 120°, (b) 180°, and(c) 240°. Ref. [3].

4.3 The Falkner-Skan Wedge Flows

The most famous family of boundary-layer similarity solutions was discovered by Falkner and Skan (1931) and later calculated numerically by Hartree (1937). Rather than merely "anticipating" the solution, let us search for similarity.

To begin with, we consider a general situation where the free-stream velocity is a function of x position, $U = U(x)$. We look for a general similarity solution with x dependence (in contrast to the Blasius solution),

---

$$\psi(x,y) = F(x)f(\eta), \quad \eta = y/g(x), \quad \frac{\partial \eta}{\partial x} = -\frac{yg'}{g^2} = -\frac{\eta g'}{g}, \quad \frac{\partial \eta}{\partial y} = \frac{1}{g}$$

---

to the boundary layer equations, where ψ denotes the stream function. By the definition of stream function (we use the chain rule),

---

$$u(x,y) = \frac{\partial \psi}{\partial y} = F(x)f'(\eta)/g(x) \to U(x), \quad \text{as } y \to \infty \ .$$

Therefore

$$F(x) = cU(x)g(x), \quad c = 1/f'(\infty)$$

We take $c = 1$,

$$\psi = U(x)g(x)f(\eta), \quad u = U(x)f'(\eta),$$
$$v = -\frac{\partial \psi}{\partial x} = -(U'g + Ug')f + Uyg'f'/g \ .$$

We need the following derivatives

$$\frac{\partial u}{\partial x} = U'f' - Uyg'f''/g^2,$$

$$\frac{\partial u}{\partial y} = Uf''/g$$

$$\frac{\partial^2 u}{\partial y^2} = Uf'''/g^2$$

Substitutions in the boundary layer equation,

$$Uf'(U'f' - \underline{Uyg'f''/g^2}) + (\underline{Uyg'f'/g} - U'gf - Ug'f)Uf''/g = UU' + \nu Uf'''/g^2 \ ,$$

$$UU'f'^2 - (UU' + U^2g'/g)ff'' = UU' + \nu Uf'''/g^2 \ ,$$

Hence

$$f'^2 - \underbrace{\left(1 + \frac{Ug'}{U'g}\right)}_{x\text{'s dependence}} ff'' = 1 + \underbrace{\frac{\nu}{g^2U'}}_{x\text{'s dependence}} f''' \ , \tag{4.54}$$

Similarity is achieved if each of the two coefficients in this relation is such that all x's disappear, leaving only constant. From Eqn. (4.54), this implies that

$$\frac{Ug'}{U'g} = \text{const}, \quad g^2U' = \text{const} \ .$$

From the first equality,

$$(\ln U)' = C_1(\ln g)', \quad U = C_2g^{C_1}$$

Substituting into the second equality, we deduce

$$U'U^{C_3} = C_4$$

Finally,

if $C_3 = -1$, we obtain $(\ln U)' = C_4 \Rightarrow U(x) \sim e^{\alpha x}$
If $C_3 \neq -1$, we obtain

$$(U^{C_3+1})' = C_4(C_3 + 1) \Rightarrow U(x) \sim (x - x_0)^m$$

In the case,

$$U(x) = Ax^m, \quad A > 0,$$

since $g^2U' = \text{const}$,

$$g = \text{const} \times (U')^{-1/2} \sim x^{(1-m)/2}$$

Choosing

$$g(x) = \left[\frac{2\nu}{(m+1)Ax^{m-1}}\right]^{\frac{1}{2}} = \left[\frac{2\nu x}{(m+1)U(x)}\right]^{\frac{1}{2}}, \text{so } \left(1 + \frac{Ug'}{U'g}\right) = \frac{\nu}{g^2U'} = \frac{m+1}{2m},$$

leads to

$$f''' + ff'' + \beta(1 - f'^2) = 0, \quad \beta = \frac{2m}{m+1}\ . \tag{4.55}$$

The boundary conditions are exactly the same as for the flat plate:

$$f(0) = f'(0) = 0, \quad f'(\infty) = 1 \tag{4.56}$$

The parameter β is a measure of the pressure gradient dp/dx. If β is positive, the pressure gradient is negative or favorable, and negative β denotes an unfavorable positive pressure gradient. Naturally, $\beta = 0$ denotes the flat plate.

Inviscid flow past wedges and corners The Falkner and Skan solution illustrates both favorable and adverse pressure gradients and is a realistic engineering flow pattern. The power-law freestream, $U = Ax^m$, is the exact solution to inviscid flow pas a wedge or a corner shape. As shown in the previous subsection (we take $n = m + 1$), an exact solution is

$$\psi(r, \theta) = \text{const} \times \ r^{m+1} \sin[(m+1)\theta], \tag{4.57}$$

This formula has certain radial streamlines that can be interpreted as the "wall" of a wedge or a corner, as in Fig. 22, depending upon the value of $\beta = 2m/(m+1)$. The velocity along these walls has the form $U = Ax^m$ and represents the freestream driving the boundary layer on the wall, with $x = 0$ at the tip of the wedge. We may list the following cases:

1. $-2 \le \beta \le 0$, $-\frac{1}{2} \le m \le 0$: flow around an expansion corner of turning angle $\beta\pi/2$.
2. $\beta = 0$, $m = 0$: the flat plate.
3. $0 \le \beta \le 2$, $0 \le m \le \infty$: flow against a wedge of half-angle $\beta\pi/2$.
4. $\beta = 1$, $m = 1$: the stagnation point (180° wedge).

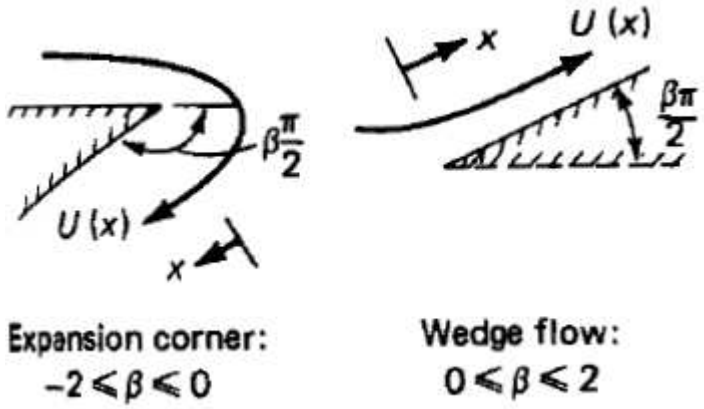

Figure 22: Some examples of Falkner-Skan potential flows. Ref. [5].

These are similar flows, i.e., for a given β the velocity profiles all look alike when scaled by $U(x)$ and $\delta(x)$. They may also be used, with modest success, to predict the behavior of nonsimilar flows.

Eqn. (4.55) can be solved on a digital-computer using the Runge-Kutta method. We select β and try to find the proper value for $f''(0)$ that makes $f'(\infty)$ asymptotically approach unity.

Although we could easily attack Eqn. (4.55) with our personal computers, in fact, the Falkner-Skan solutions have been well tabulated and charted. The most important results are plotted in Fig.23, spanning the range from the stagnation point $\beta = m = 1$ down through the flat-plate flow $\beta = m = 0$ to the separation point $\beta = -0.19884$, $m = -0.09043$. Fig.23 (a) shows the velocity profiles $u/U = f'$, which grow thicker as β decreases and, for $\beta < 0$, become S-shaped and separate ($\tau_w = 0$ for $\beta = -0.19884$. Separation corresponds to an expansion angle in Fig.22 of only $18°$.

Fig.23 (b) shows the shear-stress profiles $f''(\eta)$. Note that shear, in accelerated (favorable) flows, falls away from the wall value but instead rises from the wall in decelerated (adverse) flows. This is a consequence of the momentum-equation condition $\partial\tau/\partial y|_{\text{wall}} = dp/dx$ and is true also in turbulent boundary layers.

4.4 The boundary layer as vorticity

Now that we have solved the boundary layer equations for some cases we can go on to look at the flows in a slightly different manner. The vorticity in a two-dimensional flow is given by

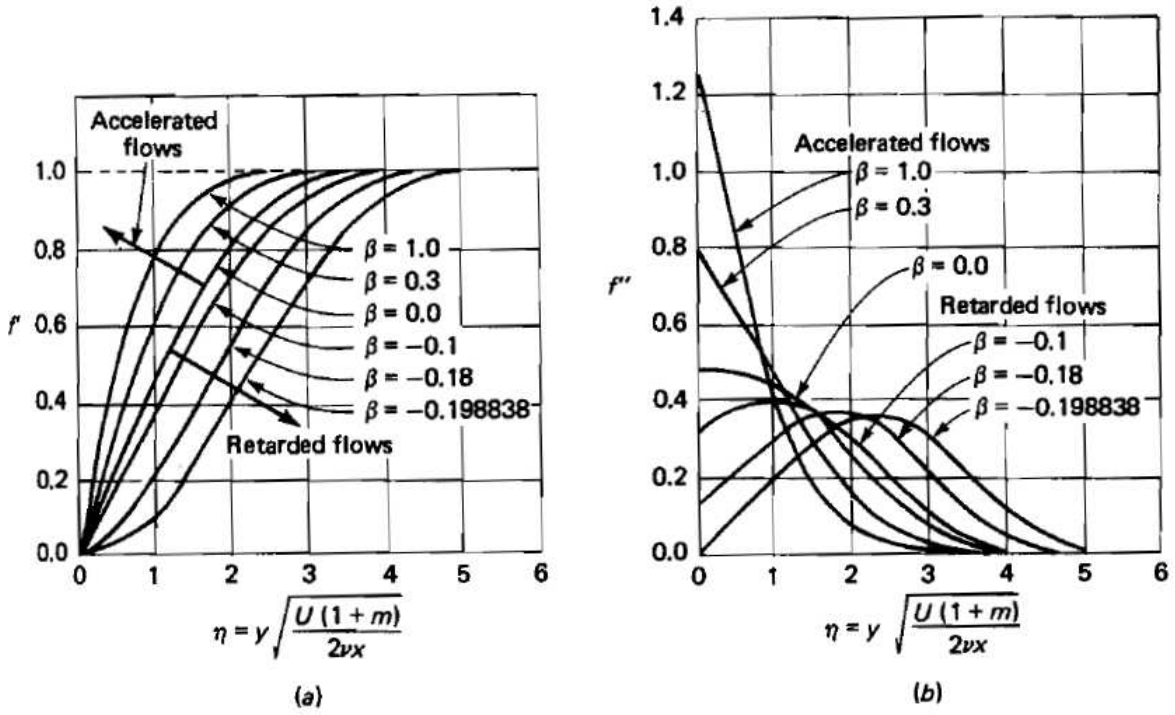

Figure 23: (a) Velocity profiles and (b) shear-stress profiles for Falkner-Skan equation. Ref. [5].

$$\omega = \frac{\partial v}{\partial x} - \frac{\partial u}{\partial y}. \tag{4.58}$$

The boundary layer approximation suggests that the first term is very small relative to the second and so we will ignore it. If we now examine the Blasius solution we can differentiate the velocity profile to find the vorticity. Simple inspection of the profile suggests what this will look like but it is plotted in Fig. 24.

We see that the boundary layer is simply a layer of vorticity near the wall (it dies off rather rapidly at large distances from the wall). So an alternative way of looking at a boundary layer is as a layer of vorticity. To examine how this evolves (in this laminar case) we can use the vorticity equation which is, in 2D[5],

$$\frac{D\omega}{Dt} = \nu \left(\frac{\partial^2 \omega}{\partial x^2} + \frac{\partial^2 \omega}{\partial y^2} \right). \tag{4.59}$$

[5]bear in mind that the equation in three dimensions has vortex stretching and tilting terms not present here

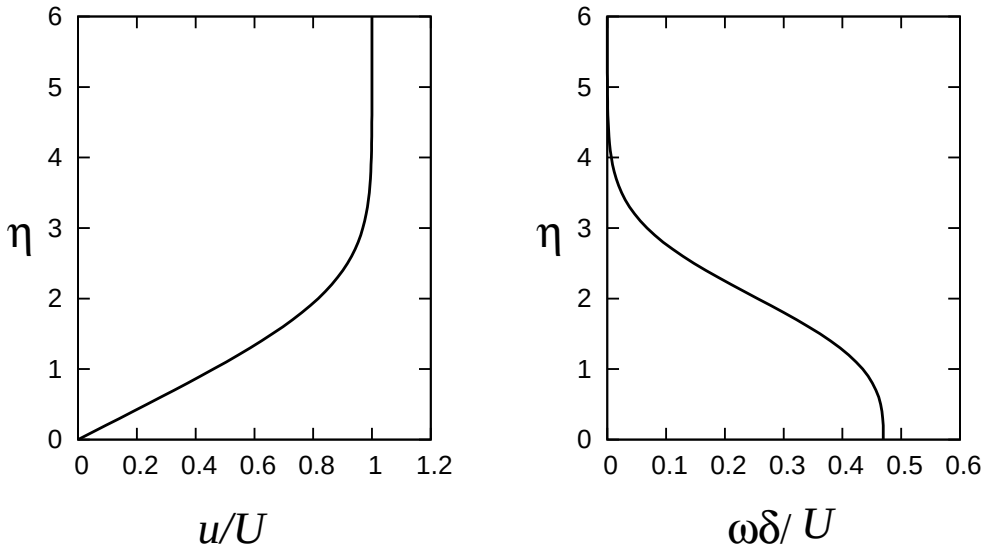

Figure 24: The Blasius velocity profile (left) and vorticity distribution (right).

The first term on the right is very small under the boundary layer approximation and we can consider the material derivative on the left as being the rate of change with time when moving with the fluid - in this case we can just consider it a normal derivative, hence

$$\frac{\partial \omega}{\partial t} = \nu \frac{\partial^2 \omega}{\partial y^2}. \tag{4.60}$$

The solution to this equation is a Gaussian vorticity profile of the form

$$\omega = \omega_o e^{-y^2/4\nu t}. \tag{4.61}$$

(see the examples question in which you can derive this). A measure of the thickness of the layer is $\delta_{vort} = \sqrt{4\nu t}$ (which is the standard deviation of the Gaussian). Finally we ask how we relate time in the moving frame to our fixed frame - moving at a velocity U in a time, t, we cover a distance of $x = Ut$ metres and hence we can relate the time of the moving observer to the distance along the plate $t = x/U$. So then the thickness of this layer should grow with distance as $\delta_{vort} = \sqrt{4\nu x/U}$ - which is exactly the form of growth rate we worked out for the Blasius layer using the similarity solution. Note that the actual shape of the Blasius vorticity profile is not quite Gaussian due to the terms we have neglected. Nevertheless it is a reasonable approximation for our purposes. This approach clearly illustrates the boundary

layer as a convection/diffusion problem - convection along the wall due to the flow and diffusion out by the gradients.

What is the effect of Reynolds number then on the boundary layer thickness? If we slow down the flow (for example) then for a given distance the layer has a longer time to diffuse and hence we expect thicker boundary layers at low Reynolds number. Similarly if we increase the viscosity then the vorticity diffuses more quickly and we find the same result.

This conceptual model can be extended to give a qualitative idea of the effect of pressure-gradients. We are not going to pursue it here.

Question 4.

As we noted above the boundary layer can be considered to be a layer of vorticity near the wall. In this question we consider a layer of vorticity in an otherwise still fluid (apart from the velocity induced by the vortex layer) - away from any boundary. We can use the *similarity* method above to work out how the layer develops (we have already discussed the solution in the notes but here we will derive it as an exercise in finding similarity solutions). Consider a thin layer of vorticity in an otherwise irrotational flow. We consider that it extends to infinity in the positive and negative x-directions. In this case it is indeed very long and thin and so the boundary layer approximation applies (exactly) since if it is uniform along its length there are no gradients in that direction (they are not just small as they are for the Blasius solution). In this case the solution is governed by the vorticity equation of this form

$$\frac{\partial \omega}{\partial t} = \nu \frac{\partial^2 \omega}{\partial y^2}. \tag{4.62}$$

Now we look for a similarity solution where the shape of the vorticity profile remains the same with time but it spreads out and the peak vorticity drops in some fashion i.e.

$$\omega = \omega_o f(y/\delta) = \omega_o f(\eta), \tag{4.63}$$

where δ is some measure of the thickness of the layer and ω_o is, say the peak vorticity at the centre of the layer. We have introduced $\eta = y/\delta$ just to simplify the notation. Note that this is an unsteady problem and hence ω_o and δ are both functions of time. Note also that since they are single values they are not functions of position, y. Now you can substitute this function into the equation and find an ODE for the function $f(y/\delta)$. Note as a hint that since f depends on δ then $\partial f/\partial t$ is not zero - you must use the chain rule eg. $\partial f/\partial t$ $=(\partial f/\partial \eta)(d\eta/dt=(\partial f/\partial \eta)(d\eta/d\delta)(d\delta/dt)$ etc.

a) Find the ODE for the function f

b) Find the function f either by solving the ODE (not too hard) or by guessing the solution and showing it satisfies the ODE.

c) Find expressions for the variation of δ and ω_o with time, t

Answers: (a) $f'' = \dfrac{\delta^2}{\nu\omega_o}\dfrac{d\omega_o}{dt} f - \dfrac{\delta}{\nu}\dfrac{d\delta}{dt}\eta f'$, (b) $f(\eta) = e^{-\eta^2}$, (c) $\delta = \sqrt{4\nu t}$, $\omega_o \propto 1/\sqrt{t}$.

5 The Momentum Integral Equation

Now we will look at the integral constraints of the boundary layer as a whole. In other words we ignore the details of the velocity profiles and instead integrate them up and see

what we can say about the general growth of the boundary layer based on the fact that the rate-of-change of momentum must be equal to the sum of the external forces. This should say something about, for example, how the (missing) momentum thickness changes along a plate. There are two, equivalent approaches from slightly different perspectives - one proceeding from the boundary layer equations and the other from a straightforward control volume approach. We will study the second approach.

5.1 The control volume approach

In order to find the momentum integral equation we consider forces on a small control volume which is part of the boundary layer. The rate of change of momentum of this control volume must be balanced by the forces on the control volume (i.e. the wall stress and the pressure gradient forces).

Consider a control volume MASS FLOW BALANCE Mass flow in through AE into control

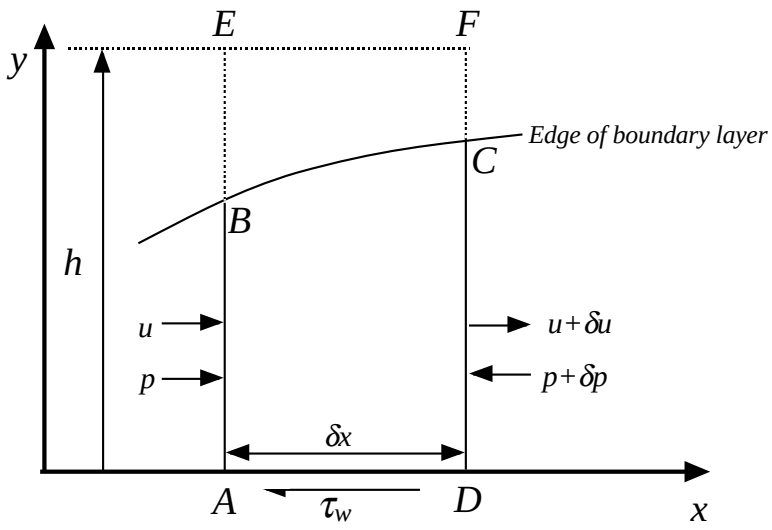

Figure 25: Control volume for derivation of momentum equation

volume AEFD is

$$\rho \int_0^h u dy \tag{5.64}$$

Mass flow out of volume through DF is

$$\rho \int_0^h u dy + \frac{d}{dx}\left[\rho \int_0^h u dy\right] .dx + O((dx)^2) \tag{5.65}$$

So the net mass flow across DF and AE, OUT OF the control volume AEFD is

$$\frac{d}{dx}\left[\rho \int_0^h u dy\right] .dx + O((dx)^2) \tag{5.66}$$

So now we can calculate the mass-flow through the top, i.e. EF If V_h is the average velocity over EF then the rate of mass flow through EF is

$$\rho V_h dx \tag{5.67}$$

and therefore, by continuity, (continuity of mass requires that there be no net rate of change of mass inside AEFD and hence)

$$\rho V_h = -\frac{d}{dx}\left[\rho \int_0^h u dy\right] + O(dx) \tag{5.68}$$

So now we know the mass-flow through the sides of the control volume. We can now work out the momentum flux.

MOMENTUM BALANCE We can work out the net flux of x-momentum through the control volume and balance this with the x-direction forces acting on the control volume.

$$(\dot{M}_x)_{DF} - (\dot{M}_x)_{AE} = \frac{d}{dx}\left[\int_0^h \rho u^2 dy\right] dx + O((dx)^2) \tag{5.69}$$

$$(\dot{M}_x)_{EF} = \rho V_h U dx = -U\frac{d}{dx}\left[\rho \int_0^h u dy\right] dx + O((dx)^2) \tag{5.70}$$

Forces

Pressure force in x-direction on AEFD is $-h.dp$

$$Pressure\ force = -h\frac{dp}{dx}dx + O((dx)^2) \tag{5.71}$$

Skin friction force is $-\tau_o.dx$, τ_o is the mean frictional stress over the length AD.

Hence balancing the net forces with the net efflux of momentum

$$\frac{d}{dx}\left[\int_0^h \rho u^2 dy\right] dx - U\frac{d}{dx}\left[\rho \int_0^h u dy\right] dx = -h\left(\frac{dp}{dx}\right) dx - \tau_o dx + O((dx)^2) \tag{5.72}$$

Now we divide through by dx and then let $dx \to 0$ and hence the term $O((dx)^2) \to 0$ and the equation becomes

$$\frac{d}{dx}\left[\int_0^h \rho u^2 dy\right] - U\frac{d}{dx}\left[\rho \int_0^h u dy\right] = -h\left(\frac{dp}{dx}\right) - \tau_o \tag{5.73}$$

This is the momentum integral equation but is is most usefully expressed in terms of the momentum and displacement thicknesses.

Now it only remains to rearrange this so we can express things in terms of δ^* and θ where as stated earlier

$$\delta^* = \int_0^\infty (1 - \frac{u}{U}) dy \tag{5.74}$$

and

$$\theta = \int_0^\infty \frac{u}{U}(1 - \frac{u}{U}) dy \tag{5.75}$$

Because

$$-U\frac{d}{dx}\left[\rho \int_0^h u dy\right] = -\frac{d}{dx}\left[\rho U \int_0^h u dy\right] + \frac{dU}{dx}\left[\int_0^h \rho u dy\right],$$

we get

$$\frac{d}{dx}\left[\int_0^h \rho u(u-U) dy\right] + \frac{dU}{dx}\left[\int_0^h \rho u dy\right] = h\rho U\frac{dU}{dx} - \tau_o \tag{5.76}$$

and rearranging this

$$\frac{d}{dx}\left[\int_0^h \rho u(U-u) dy\right] + \frac{dU}{dx}\left[\int_0^h \rho (U-u) dy\right] = \tau_o \tag{5.77}$$

which leads to

$$\rho U^2\frac{d\theta}{dx} + 2\rho U\theta\frac{dU}{dx} + \rho U H\theta\frac{dU}{dx} = \tau_o \tag{5.78}$$

if we let $h \to \infty$. Finally we get the von Kármán momentum integral equation

$$\frac{d\theta}{dx} + \frac{H+2}{U}\theta\frac{dU}{dx} = \frac{\tau_o}{\rho U^2} = \frac{C_f'}{2} \tag{5.79}$$

Some points to note are that

- This equation is valid for both laminar and turbulent flow
- It forms a good basis for approximate methods for solving boundary layer problems
- It also always serves as a good check on both calculations and experimental data
- When the pressure gradient is zero, the equation is reduced to

$$\frac{d\theta}{dx} = \frac{\tau_{\text{wall}}}{\rho U^2} = \frac{C_f'}{2} \tag{5.80}$$

Example: An incompressible flow at high Reynolds number past a flat plate is sketched in Fig. 26. The sharp edge of the plate is at $(x, y) = (0, 0)$. The fluid exerts a drag force on the plate due to the no-slip condition. The velocity distribution $u(y)$ at any particular downstream position x shows a smooth drop-off to zero at the wall. Assume that the flow is steady and the freestream outside the boundary layer is $u = U = \text{constant}$.

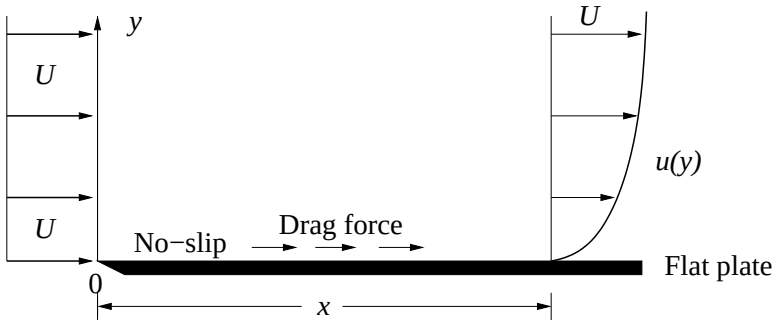

Figure 26: Flow past a flat-plate.

The beauty of Kármán's idea is that we can guess a reasonable form for $u(y)$ and get reasonable estimates of the drag and wall shear, because integration tends to wash out the positive and negative deviations of the assumed profile.

Let us therefore try a simple expression for $u(y)$ at the position in Fig.26. We will satisfy three physical conditions for the profile:

No slip condition at the wall: $u(0) = 0,$

Smooth merging with the stream:

$$u(\delta) = U, \qquad \left.\frac{\partial u}{\partial y}\right|_{y=\delta} = 0$$

We can satisfy these conditions for laminar flow with a second-order polynomial

$$u \approx U\left(\frac{2y}{\delta} - \frac{y^2}{\delta^2}\right)$$

Now insert this approximation into Eqns. (2.16) and (2.17) to estimate

$$\delta^* \approx \int_0^\infty \left(1 - \frac{2y}{\delta} + \frac{y^2}{\delta^2}\right) dy \approx \frac{\delta}{3}, \quad \theta \approx \frac{2\delta}{15}, \quad H \approx \frac{5}{2} \qquad (5.81)$$

This is not enough. We must relate wall shear to the assumed shape $u(y)$, which we do, following Kármán (1921), by differentiating the profile relation,

$$\tau_w = \mu \frac{\partial u}{\partial y}|_{y=0} \approx \frac{2\mu U}{\delta} \qquad (5.82)$$

Substituting Eqns. (5.81) and (5.82) into the momentum integral equation (5.79), and noting that $dU/dx = 0$, we obtain

$$\frac{d}{dx}\left(\frac{2\delta}{15}\right) \approx \frac{d\theta}{dx} = \frac{C_f'}{2} \approx \frac{\mu U}{\frac{1}{2}\rho U^2 \delta}$$

or

$$\delta d\delta \approx \frac{15\mu dx}{\rho U}$$

Integrate, assume that the boundary layer begins at the leading edge, $\delta(0) = 0$. The result is

$$\delta^2 \approx \frac{30\mu x}{\rho U}$$

or

$$\frac{\delta}{x} \approx \frac{5.5}{\sqrt{Re_x}}$$

where $Re_x = \rho U x/\mu$. This is only 10 percent higher than the exact solution for laminar flat-plate flow given by Blasius (1908).

By substituting δ into Eqns. (5.81) and (5.82), we obtain the additional flat-plate estimates

$$\frac{\delta^*}{x} \approx \frac{1.83}{\sqrt{Re_x}}$$

$$\frac{\theta}{x} = C_f' \approx \frac{0.73}{\sqrt{Re_x}}$$

which are also within 10 percent of the exact solutions. Finally, by integration of $C_f'(x)$, we obtain the drag coefficient:

$$C_D \approx \frac{1.46}{\sqrt{Re_L}} = 2C_f'(L)$$

As Kármán (1921) pointed out, these results are quite easily obtained compared to a full-blown attack on the continuity and momentum partial differential equations.

All of the previous integral momentum estimates for the flat-plate flow are collected in the following table and compared with the exact solution due to Blasius (1908). The error is 10 percent, which is typical of integral theories. The advantage is that, by integrating across the boundary layer in the y direction, we are left only with an ordinary differential equation to solve in the x direction for parameters such as $\delta(x)$.

parameters	u from the current study	Exact from Blasius	Error, %
$\frac{\theta}{x}\sqrt{Re_x}$	0.73	0.664	+ 10
$\frac{\delta^*}{x}\sqrt{Re_x}$	1.83	1.721	+ 6
$\frac{\delta_{99\%}}{x}\sqrt{Re_x}$	5.5	5.0	+ 10
$C'_f\sqrt{Re_x}$	0.73	0.664	+ 10
$C_D\sqrt{Re_L}$	1.46	1.328	+ 10

Question 5.

A boundary layer develops with zero pressure-gradient. Its profile is measured at a streamwise location and it is found that a good fit to the function is given by $u/U = 1.54 * (y/\delta) - 0.61 * (y/\delta)^4$ for $0 < y < \delta$ where δ is, say, the 99% thickness which is found in this case to be 10mm. Another measurement is made 20mm downstream and the 99% thickness there is found to be 12mm. The same function also fits the profile well at this point.

Use the momentum integral equation to estimate the value of the skin-friction coefficient (C'_f) at this location. Comment on the likely accuracy of this estimate.

Answer: $C'_f = 0.0257$

Question 6.

Uniform suction at the plate is sometimes used to control boundary layers - in some cases to maintain laminar flow and in others to reduce the thickness of the boundary layer. Consider the flow of a boundary layer over a porous surface through which flow is sucked such that the velocity normal to the plate is uniform and equal to $-V_o$.

We will assume that there is no streamwise pressure-gradient in order to simplify the problem. Derive the momentum integral equation for this flow. Note that the boundary layer equations are unchanged but the boundary condition at the wall is now different. In this case the continuity equation may be written as

$$v = -\int_0^y \frac{\partial u}{\partial x} dy - V_o \tag{5.83}$$

which ensures that at the wall the vertical velocity component is equal to the wall suction velocity. Note that if we differentiate both sides with respect to y we get back the usual continuity equation since V_o is constant everywhere.

You can proceed either by integrating the boundary layer equations or by applying a control volume analysis. If you are keen do the problem using both methods.

Answer: $d\theta/dx + V_o/U_1 = C'_f/2$

Question 7.

The boundary layer equations apply to any long thin flow - that is any flow in which gradients across the flow are much larger than those along the flow. There was no explicit mention of a wall in the derivation (the wall enters through the application of boundary conditions when solving the equations). As a result it is possible to apply them to other flows. Consider the 2D laminar wake behind a body (eg. an aerofoil) as shown. The wake must have some deficit in velocity since some momentum is lost from the fluid due to the drag of the body.

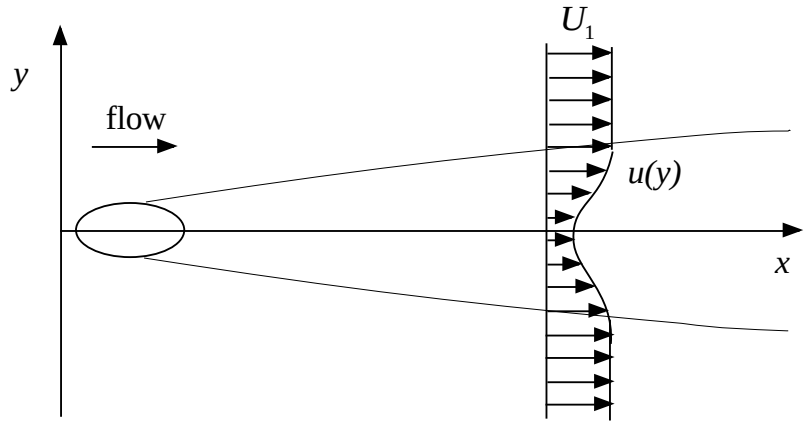

The equations are exactly the same as for the 2D boundary layer as given in (9.153). The definition of the momentum thickness is the same here as for the boundary layer except that the integration is from $y = -\infty$ and $y = +\infty$.

a) Derive the integral momentum equation in this case by integrating the boundary layer equation with respect to y between these limits and hence find an expression for $d\theta/dx$. Note that you can follow the basic procedure in the notes above. The end result is rather simple and quite different from that for the boundary layer.

b)Could you have predicted this result without doing any analysis - if so what is the reasoning?

c) Repeat the process using the control volume method (the *ab initio* approach).

Answers: (a) $d\theta/dx = 0$, (b) Yes

Question 8.

A two dimensional laminar jet issues from a slot into a still fluid. At some point downstream the centreline velocity is U_o and the width of the jet is δ (this might be measured by the point at which the velocity drops to half U_o for example). Assume that a similarity solution of the form

$$u(x,y) = U_o f\left(\frac{y}{\delta}\right) \tag{5.84}$$

is applicable.

a) Find the ODE for the velocity profile in this case. Note that the boundary layer equations hold for this flow.

b) Find the condition on the variation of U_o and δ such that the shape of the profile is invariant with streamwise distance.

c) Using the result from (b) and the momentum integral equation (which is the same as for the laminar wake in question 7) find the functional variation of U_o and δ with x. (Note there is no streamwise pressure-gradient in this problem).

Answers: (a) $f'' = a(f^2 - I_1 f') - bI_1 f'$, where $a = (\delta^2/\nu)\ dU_o/dx$, $b = (U_o\delta/\nu)\ d\delta/dx$, $I_1 = \int_0^\eta f\, d\eta$ (b) $a =$ constant, (c) $U_o \propto 1/x^{1/3}$, $\delta \propto x^{2/3}$

Question 9.

Consider the laminar wake from question 7. Assume a self-similar distribution of the velocity given by

$$u(x,y) = U_1 - U_o(x) f(\eta), \tag{5.85}$$

where $\eta = y/\delta$.

It can be shown that for the zero pressure-gradient case (in which we are interested) a similarity solution can only apply in the limit where $U_1/U_o \to \infty$. Since the wake spreads and the deficit velocity drops off then this corresponds to a long way downstream. Consider this case. (Note you cannot just say $U = U_1$ since this corresponds to no wake at all).

a) Find the ODE for the velocity profile $f(\eta)$(do not solve it) - retain only the largest terms in the limit.

b) Find the variation of the thickness δ with x by assuming similarity applies.

c) Use the momentum integral equation (derived earlier) with the result from (b) to find the variation of U_o with x.

Answers: (a) $f'' + a\eta f' - bf = 0$ where $a = (\delta U_1/\nu)\ d\delta/dx$, $b = (\delta U_1/\nu)(\delta/U_o)\ dU_o/dx$, (b)$\delta \propto \sqrt{x}$, (c)$U_o \propto 1/\sqrt{x}$

6 Boundary layer separation

The flat-plate analysis of the previous sections should give us a good feeling for the behavior of laminar boundary layers, except for one important effect: flow separation. Separation like that in Fig. 9b is caused by excessive momentum loss near the wall in a boundary layer trying to move downstream against increasing pressure, $dp/dx > 0$, which is called an adverse pressure gradient. The opposite case of decreasing pressure, $dp/dx < 0$, is called a favorable gradient, where flow separation can never occur. In a typical immersed-body flow, e.g., Fig. 9, the favorable gradient is on the front of the body and the adverse gradient is in the rear.

6.1 Geometric argument

We can explain flow separation with a geometric argument about the second derivative of velocity u at the wall. From the momentum equation at the wall, where $u = v = 0$, we obtain

$$\frac{\partial \tau}{\partial y}\Big|_{\text{wall}} = \mu \frac{\partial^2 u}{\partial y^2} = \frac{dp}{dx}$$

or

$$\frac{\partial^2 u}{\partial y^2} = \frac{1}{\mu}\frac{dp}{dx} \tag{6.86}$$

for either laminar or turbulent flow. We note that the second derivative of velocity must be negative at the outer layer ($y = \delta$) to merge smoothly with the mainstream flow $U(x)$. Fig. 27 illustrates the general case. In a favorable pressure gradient, $\partial^2 u/\partial y^2(0) < 0$ (Fig. 27a), the velocity profile is very rounded, there is no point of inflection ($\partial^2 u/\partial y^2 = 0$), there can be no separation. In a zero pressure gradient (Fig. 27b), e.g., flat-plate flow, the point of inflection is at the wall itself. There can be no separation.

In an adverse gradient (Fig. 27c to e), the second derivative of velocity is positive at the wall; yet it must be negative at the outer layer ($y = \delta$) to merge smoothly with the mainstream flow $U(x)$. It follows that the second derivative must pass through zero somewhere in between, and any boundary-layer profile in an adverse gradient must exhibit a characteristic S shape. The point of inflection (PI) occurs in the boundary layer, its distance from the wall increasing with the strength of the adverse gradient. For a weak gradient (Fig. 27c) the flow does not actually separate. At a moderate gradient, a critical condition (Fig. 27d) is reached where the wall shear is exactly zero ($\partial u/\partial y = 0$). This is defined as the separation point ($\tau_w = 0$), because any stronger gradient will actually cause backflow at the wall (Fig. 27e):

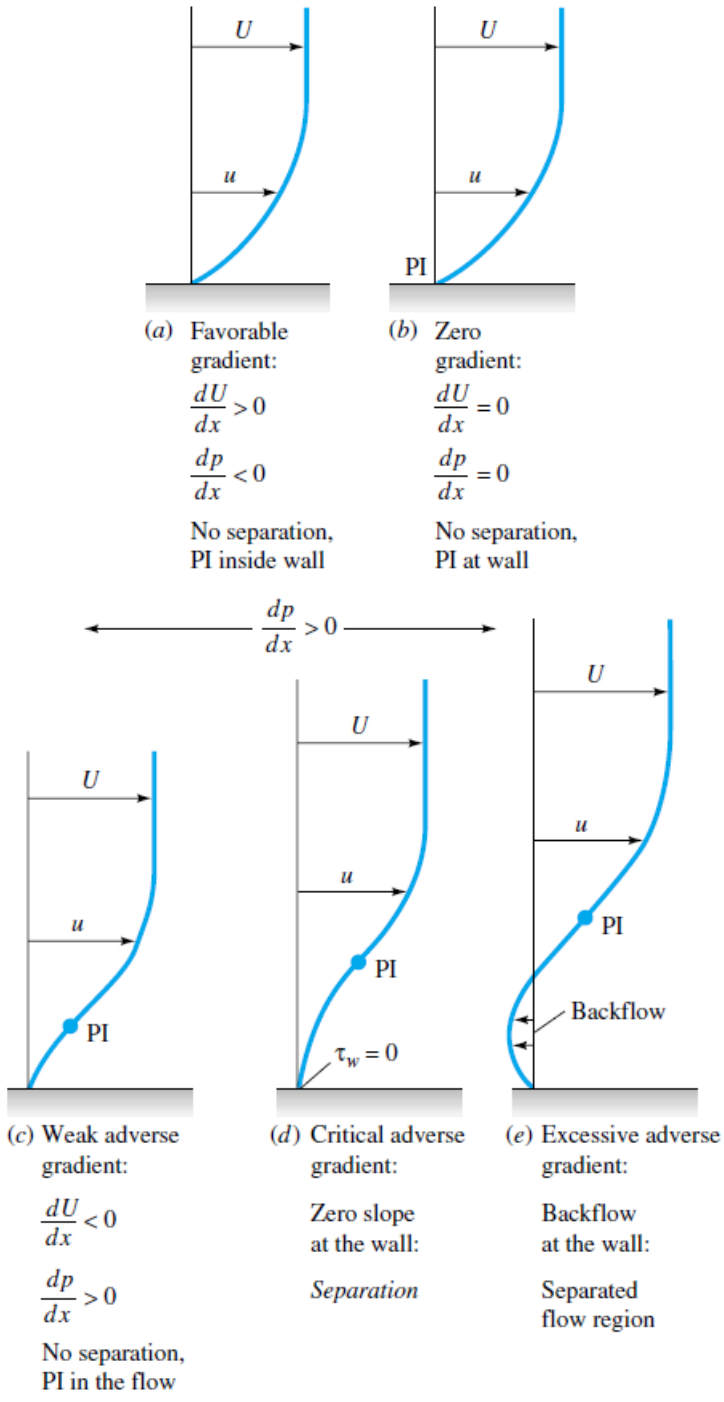

Figure 27: Effect of pressure gradient on boundary layer profiles; PI = point of inflection. Ref. [3].

the boundary layer thickens greatly, and the main flow breaks away, or separates, from the wall (Fig. 9b).

The flow profiles of Fig. 27 usually occur in sequence as the boundary layer progresses along the wall of a body. For example, in Fig. 9b, a favorable gradient occurs on the front of the cylinder, zero pressure gradient occurs just upstream of the shoulder, and an adverse gradient occurs successively as we move around the rear of the cylinder.

At present boundary-layer theory can compute only up to the separation point, after which it is invalid. New techniques are currently being developed for analyzing the strong interaction effects caused by separated flows.

Von Kármán's general two-dimensional boundary-layer integral equation (5.79) is valid for both laminar and turbulent boundary layers. We can integrate Eqn. (5.79) to determine the momentum thickness $\theta(x)$ for a given $U(x)$ if we correlate C_f' and the shape factor H with the momentum thickness. This has been done by examining typical velocity profiles of laminar and turbulent boundary-layer flows for various pressure gradients. Some examples are given in Fig. 28, showing that the shape factor H is a good indicator of the pressure gradient. The higher the H, the stronger the adverse gradient, and separation occurs approximately at

$$H \approx \begin{cases} 3.5 & \text{laminar} \\ 2.4 & \text{turbulent} \end{cases}$$

The laminar profiles (Fig. 28a) clearly exhibit the S shape and a point of inflection with an adverse gradient. But in the turbulent profiles (Fig. 28b) the points of inflection are typically buried deep within the thin viscous sublayer, which can hardly be seen on the scale of the figure.

There are scores of turbulent theories on flow separation in the literature, but they are all complicated algebraically and will be omitted here. The reader is referred to advanced texts [5, 7]. For laminar flow, a simple and effective method was developed by Thwaites.

6.2 Thwaites Method

(see Duncan, Thom and Young pp.273–278)

In the general case of an arbitrary pressure-gradient we can no longer assume that the velocity profile remains self-similar - the shape may change as the flow develops. If we are only interested in the integral properties of the boundary layer (eg. how thick it is, the value of the skin-friction etc.) then we might instead make the next simplest assumption that is that the shape is no longer invariant but can be expressed in terms of one extra parameter

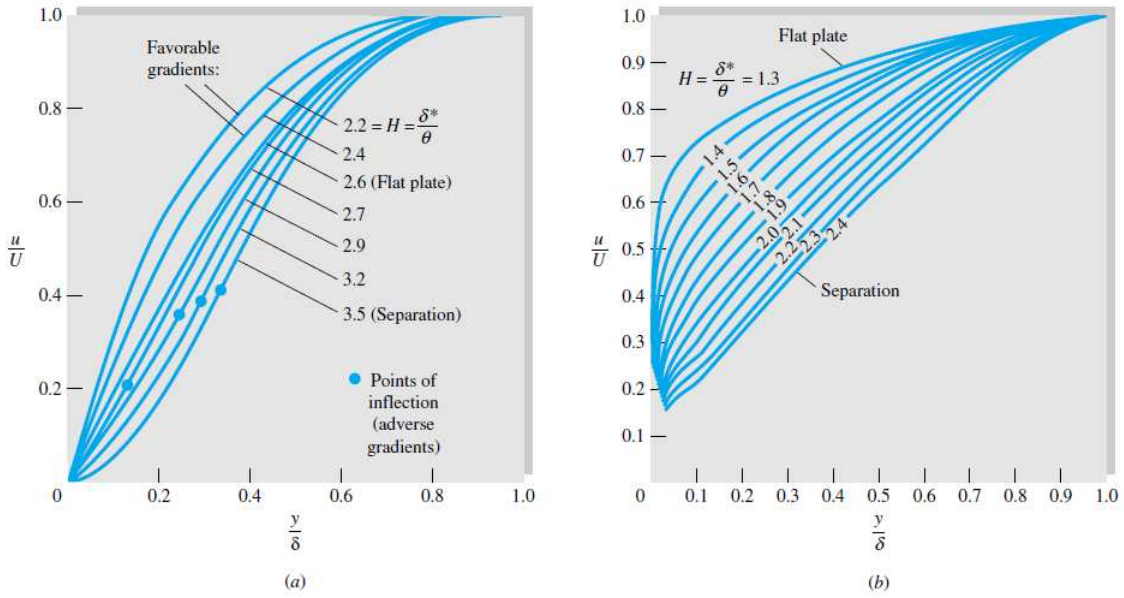

Figure 28: Velocity profiles with pressure gradient: (a) laminar flow; (b) turbulent flow with adverse gradients. The axes are exchanged compared to usual presentation. Ref. [3].

- hence by giving a value to this parameter we determine the shape. This type of method is classed as an integral method, since the aim is to solve the momentum integral equation

$$\frac{d\theta}{dx} + \frac{H+2}{U}\theta\frac{dU}{dx} = \frac{\tau_w}{\rho U^2} = \frac{C_f'}{2}$$

for the variation of the integral parameters of the flow as it develops. Recall that the momentum integral equation relates three basic parameters (the momentum thickness, θ, the shape parameter, H, and the skin friction coefficient C_f') hence we need three equations in total: the momentum integral equation provides one.

In Thwaites method he defined a parameter, m, related to the shape of the profile as

$$m = \frac{\theta^2}{U}\left(\frac{\partial^2 u}{\partial y^2}\right)_w \qquad (6.87)$$

where the subscript w means at the wall ($y = 0$). This is directly related to the applied pressure-gradient since at the wall

$$\nu \left(\frac{\partial^2 u}{\partial y^2} \right)_w = \frac{1}{\rho} \frac{dp}{dx} = -U \frac{dU}{dx}. \tag{6.88}$$

so we can also write m as,

$$m = -\frac{\theta^2}{\nu} \frac{dU}{dx}. \tag{6.89}$$

He also defined a non-dimensional skin-friction parameter as

$$l = \frac{\theta}{U} \left(\frac{\partial u}{\partial y} \right)_w \tag{6.90}$$

which is the thing that we might wish to find. So the situation is that we have a form parameter, m which in some way uniquely determines the shape of the velocity profile and a skin-friction parameter, l that is related to the skin-friction and must be a function only of m since the skin friction depends only on the shape of the profile and the profile is uniquely determined, in some fashion, by m. Note also that the shape-factor H that appears in the momentum-integral equation must also just be a function of m since it is determined by the shape of the profile. Now if we use the momentum-integral equation we can find an equation that relates l to m and H and the growth of the momentum thickness. If we knew l as a function of m and H as a function of m then we could simply integrate the equation and find how the momentum thickness and skin-friction vary with x for any pressure-gradient. The way Thwaites proceeded originally takes the momentum integral equation and using the above definitions with a little manipulation derives this equation

$$U \frac{d}{dx}(\theta^2) = 2\nu[m(H+2) + l] = \nu L(m), \tag{6.91}$$

where the $L(m) = 2[m(H+2) + l]$ which is, of course only a function of m. So we now find we have an equation with an expression for the change of momentum thickness on the left (actually of θ^2 - but we can find the growth rate from this) and on the right something that is a function only of m. So if we can find the function on the RHS we can then go on to predict the growth of the boundary layer. To find this function Thwaites took the results for various exact similarity solutions and plotted $L(m)$ versus the value of m - he found that

a good fit was given by $L(m) = 0.45 + 6m$ - although there was some scatter especially for adverse pressure gradients (the reason for the scatter is that, in reality, the profiles cannot be expressed simply in terms of one parameter, m - but it's not a bad approximation to the truth). With this (or any other) relationship that gives L in terms of m then the momentum integral equation simplifies and , in the case of this fit, we find

$$U\frac{d}{dx}(\theta^2) - 0.45\nu + 6\frac{dU}{dx}\theta^2 = 0 \tag{6.92}$$

which can be rearranged

$$\frac{d}{dx}(U^6\theta^2) = 0.45\nu U^5 \tag{6.93}$$

and solved

$$\theta^2(x_1) = \theta_0^2\left(\frac{U(0)}{U(x_1)}\right)^6 + \frac{0.45\nu}{(U^6)_{x_1}}\int_0^{x_1} U^5 dx \tag{6.94}$$

where the particular quantities are evaluated at some point along the flow where $x = x_1$ and θ_0 is the momentum thickness at $x = 0$ (usually taken to be zero). Separation ($C_f' = 0$) was found to occur at a particular value of m:

$$\text{Separation :} \qquad m = 0.09\ . \tag{6.95}$$

Finally, Thwaites correlated values of the dimensionless shear stress $\tau_w\theta/(\mu U)$ with m, and his graphed result can be curve-fitted as follows:

$$S(m) = \frac{\tau_w\theta}{\mu U} \approx (0.09 - m)^{0.62} \tag{6.96}$$

This parameter is related to the skin friction by the identity

$$S \equiv \frac{1}{2}C_f' Re_\theta, \quad Re_\theta = \frac{U\theta}{\mu}. \tag{6.97}$$

Equations (6.94) to (6.96) constitute a complete theory for the laminar boundary layer with variable $U(x)$, with an accuracy of ± 10 percent compared with exact digital-computer solutions of the laminar-boundary-layer equations (9.153). Complete details of Thwaites' and other laminar theories are given in [5].

Question 10.
(a) Deduce Eqn. (6.91) from the momentum integral equation.
(b) Deduce Eqn. (6.94) from (a) with $L(m) = 0.45 + 6m$.

Question 11.
In 1938 Howarth proposed a linearly decelerating external-velocity distribution

$$U(x) = U_0 \left(1 - \frac{x}{L}\right)$$

as a theoretical model for laminar-boundary-layer study. (a) Use Thwaites' method to compute the separation point x_{sep} for $\theta_0 = 0$, and compare with the exact digital-computer solution $x_{sep}/L = 0.119863$ given by H. Wipperman in 1966. Note that the separation condition is given by Eqn. (6.95). (b) Also compute the value of $C'_f = 2\tau_w/(\rho U^2)$ at $x/L = 0.1$.
Answers: (a) $x_{sep}/L = 0.123$. (b) $C'_f = 0.77/Re_L^{1/2}$, $Re_L = UL/\nu$.

7 Turbulent boundary layer flow

The analytical results in the previous sections are restricted to laminar boundary layer flows along a flat plate. They agree quite well with experimental results up to the point where the boundary layer flow becomes turbulent, which will occur for any free-stream velocity and any fluid provided the plate is long enough. This is true because the parameter that governs the transition to turbulent flow is the Reynolds number—in this case the Reynolds number based on the distance from the leading edge of the plate, $Re_x = Ux/\nu$.

7.1 Transition from laminar to turbulent flow

The value of the Reynolds number at the transition location is a rather complex function of various parameters involved, including the roughness of the surface, the curvature of the surface (for example, a flat plate or a sphere), and some measure of the disturbances (turbulence intensity) in the flow outside the boundary layer. On a flat plate with a sharp leading edge in the typical airstream, the transition takes place at a distance x from the

Figure 29: An arrowhead form turbulent spot and the transition from laminar to turbulent boundary layer flow on a flat plate. Flow from left to right. Ref. [5].

leading edge given by $Re_{xcr} = 2 \times 10^5$ to 3×10^6. Unless otherwise stated, we will use $Re_{xcr} = 5 \times 10^5$.

The actual transition from laminar to turbulent boundary layer flow may occur over a region of the plate, not a specific single location. This occurs, in part, because of the spottiness of the transition. Typically, the transition begins at random locations on the plate in the vicinity of $Re = Re_{xcr}$. These spots grow rapidly as they convected downstream until the entire width of the plate is covered with turbulent flow. Fig. 29 illustrates this transition process.

The overall picture of the transition process in quite (low turbulence intensity) boundary-layer flow past a smooth surface consists of the following processes as one moves downstream:

1. Stable laminar flow near the leading edge.
2. Unstable two-dimensional Tollmien-Schlichting waves (see Fig. 31).
3. Development of three-dimensional unstable waves and hairpin eddies.
4. Vortex breakdown at region of high localized shear.
5. Formation of turbulent spots at locally intense fluctuations.
6. Coalescence of spots into fully turbulent flow.

These phenomena are sketched as an idealized flat-plate flow in Fig. 30, which also illustrate the contamination effect of the lateral edges of the plate.

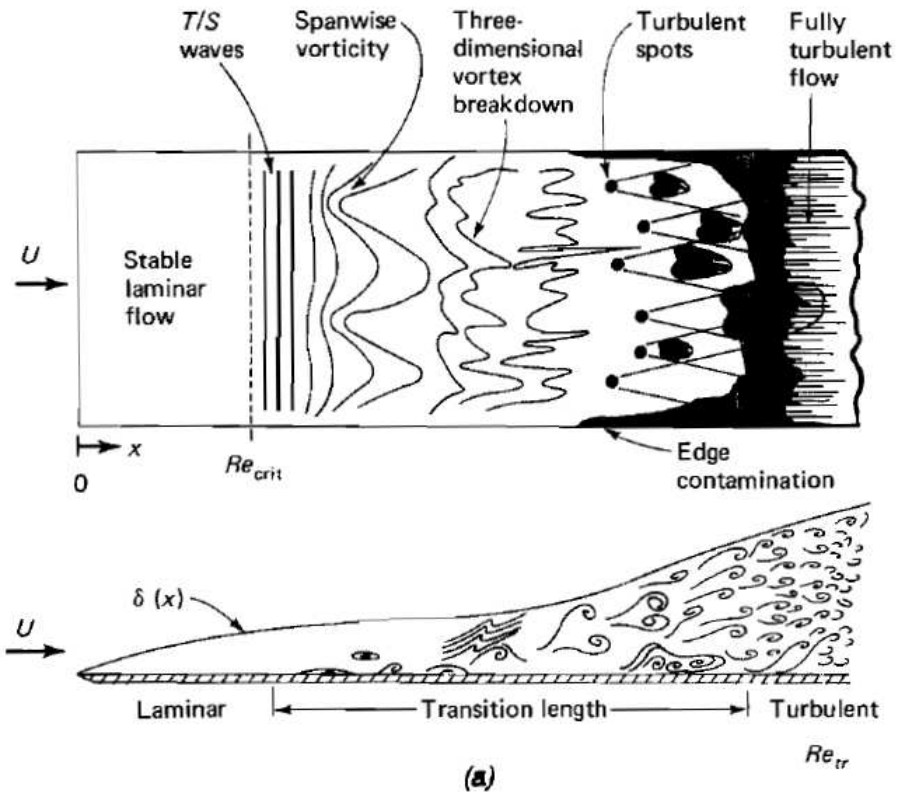

Figure 30: Idealized sketch of transition zone in the boundary layer on a flat plate at zero incident. Ref. [5].

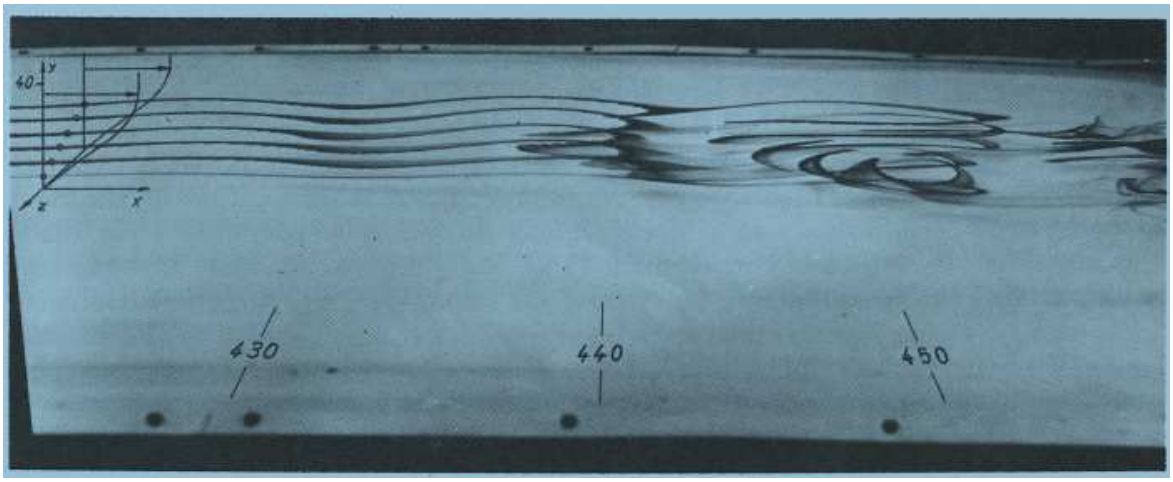

Figure 31: Illustrating the instability of two-dimensional Tollmien-Schlichting waves in the laminar boundary layer Aalong a plane wall. Disturbance was created artificially by an oscillating strip. The rolling up of streak lines downstream is a consequence of the instability of the perturbation waves. The figure denotes distances in cm. Ref. [7].

The complex process of transition from laminar to turbulent flow involves the instability of the flow field. Small disturbances imposed on the boundary layer flow (i.e., from a vibration of the plate, a roughness of the surface, or a "wiggle" in the flow past the plate) will either grow (instability) or decay (stability), depending on where the disturbance is introduced into the flow. If these disturbances occur at a location with $Re < Re_{xcr}$ they will die out, and the boundary layer will return to laminar flow at that location. Disturbances imposed at a location $Re > Re_{xcr}$ will grow and transform the boundary layer flow downstream of this location into turbulence. The study of the initiation, growth, and the structure of the turbulence burst or spots is an active area of fluid mechanics research.

Transition from laminar to turbulent flow also involves a noticeable change in the shape of the boundary layer velocity profile. Typical profiles obtained in the neighborhood of the transition location are indicated in Fig. 32. The turbulent profiles are flatter, have a larger velocity gradient at the wall, and produce a larger boundary layer thickness than do the laminar profiles.

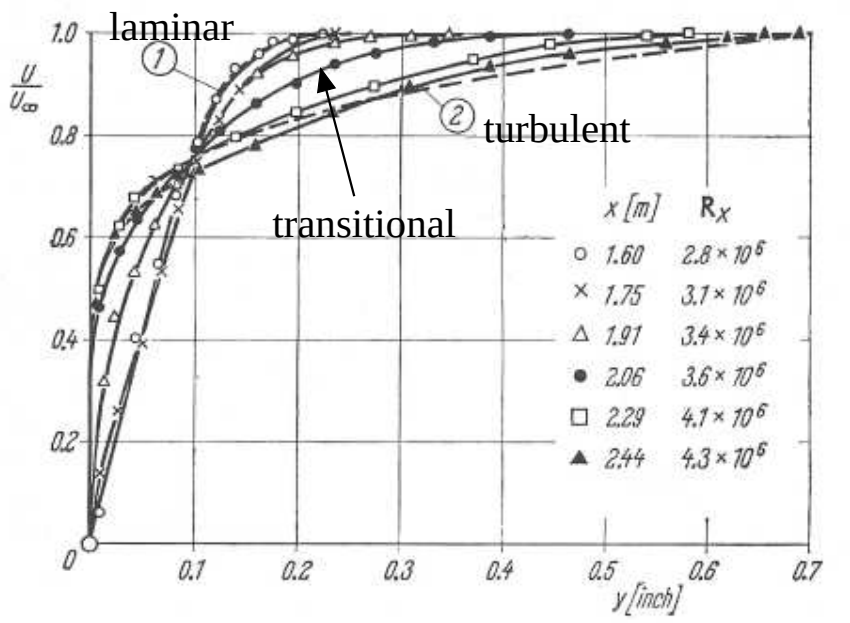

Figure 32: Typical boundary layer profiles on a flat plate for laminar, transitional, and turbulent flows. The axes are exchanged compared to usual presentation. Ref. [7].

Question 12.
A fluid flows steadily past a flat plate with a velocity of $U = 3$ m/s. At approximately what location will the boundary layer become turbulent, and how thick is the boundary layer at that point if the fluid is (a) water at 15°C, (b) standard air, r (c) glycerin at 20°C? Here the kinematic viscosity ν of the three fluids are 1.12×10^{-6} m^2/s, 1.46×10^{-5} m^2/s and 1.19×10^{-3} m^2/s. Assume $Re_{xcr} = 5 \times 10^5$.
Answer: (a) $x_{cr} = 0.187$ m, $\delta_{cr} = 1.32 \times 10^{-3}$ m. (b) $x_{cr} = 2.43$ m, $\delta_{cr} = 0.017$ m. (c) $x_{cr} = 198.3$ m, $\delta_{cr} = 1.40$ m.

7.2 Turbulent boundary layer flow

We have discussed some common characteristics of turbulent flows in subsection 1.4, namely disorder, efficient mixing and three-dimensional vortex line stretching. The structure of turbulent boundary layer flow is very complex, random, and irregular. It shares many of the characteristics described for turbulent pipe flow (which we will study later). In particular, the velocity at any given location in the flow is unsteady in a random fashion. The flow can be thought of as a jumbled mix of intertwined eddies (or swirls) of different sizes (diameters and

angular velocities). Fig. 12 shows a visualization of a turbulent boundary layer on a flat plate (side view). The various fluid quantities involved (i.e., mass, momentum, energy) are convected downstream in the free-stream direction as in a laminar boundary layer. For turbulent flow they are also convected across the boundary layer (in the direction perpendicular to the plate) by the random transport of finite-sized fluid particles associated with the turbulent eddies. There is considerable mixing involved with these finite-sized eddies—considerably more than is associated with the mixing found in laminar flow where it is confined to the molecular scale. Although there is very little net transfer of mass across the boundary layer—the largest flowrate by far is still parallel to the plate.

There is, however, a considerable net transfer of x component of momentum perpendicular to the plate because of the random motion of the particles. Fluid particles moving toward the plate (in the negative y direction) have some of their excess momentum (they come from areas of higher velocity) removed by the plate. Conversely, particles moving away from the plate (in the positive y direction) gain momentum from the fluid (they come from areas of lower velocity). The net result is that the plate acts as a momentum sink, continually extracting momentum from the fluid. For laminar flows, such cross-stream transfer of these properties takes place solely on the molecular scale. For turbulent flow the randomness is associated with fluid particle mixing. Consequently, the shear force for turbulent boundary layer flow is considerably greater than it is for laminar boundary layer.

It is possible to solve the Prandtl boundary layer equations for laminar flow past a flat plate to obtain the Blasius solution and Falkner-Skan solution (which is "exact" within the framework of the assumptions involved in the boundary layer equations). Since there is no precise expression for the shear stress in turbulent flow, "exact" solutions are not available for turbulent flow. Approximate turbulent boundary layer results can also be obtained by use of the momentum integral equation, which is valid for either laminar or turbulent flow. What is needed for the use of this equation are reasonable approximations to the velocity profile $u = Ug(\eta)$, where $\eta = y/\delta$ and u is the time-average velocity, and a functional relationship describing the wall shear stress. For laminar flow the wall stress was used as $\tau_w = \mu(\partial u/\partial y)_{y=0}$. In theory, such a technique should work for turbulent boundary layers also. However, the details of the velocity gradient at the wall are not well understood for turbulent flow. Thus, it is necessary to use some empirical relationship for the wall stress.

This is illustrated in the following question.

Question 13.
Consider turbulent flow of an incompressible fluid past a flat plate. The boundary layer velocity profile is assumed to be $u/U = (y/\delta)^{1/7}$ for $\eta = y/\delta \leq 1$ and $u = U$ for $\eta > 1$. This is a reasonable approximation of experimentally observed profiles, except very near the plate where this formula gives $\partial u/\partial y = \infty$ at $y = 0$. Assume also that the shear stress agrees with the experimentally determined formula:

$$\tau_{\rm w} = 0.0225\rho U^2 \left(\frac{\nu}{U\delta}\right)^{1/4} .$$

Determine the boundary layer thicknesses δ, δ^*, θ and the wall shear stress τ_w, as a function of x.
Answer: $\delta/x = 0.370/Re_x^{1/5}$, $\delta^*/x = 0.0463/Re_x^{1/5}$, $\theta/x = 0.036/Re_x^{1/5}$, $\tau_w = 0.0288\rho U^2/Re_x^{1/5}$.

8 Turbulence Modeling

We consider incompressible Navier-Stokes equations

$$\begin{aligned} \text{Continuity}: \quad & \frac{\partial u}{\partial x} + \frac{\partial v}{\partial y} + \frac{\partial w}{\partial z} = 0 \\ \text{Momentum}: \quad & \rho\frac{D\mathbf{V}}{Dt} = -\nabla p + \mu\nabla^2\mathbf{V} \end{aligned} \tag{8.98}$$

subject to no slip at the walls and known inlet and exit conditions. Both laminar and turbulent flows satisfy Eqs. (8.98). For laminar flow, where there are no random fluctuations, we can go right to the attack and solve them for a variety of geometries.

8.1 Reynolds's time-averaging concept

For turbulent flow, because of the fluctuations, every velocity and pressure term in Eqs. (8.98) is a rapidly varying random function of time and space. At present our mathematics cannot handle such instantaneous fluctuating variables. No single pair of random functions $\mathbf{V}(x, y, z, t)$ and $p(x, y, z, t)$ is known to be a solution to Eqs. (8.98). Moreover, our attention as engineers is toward the average or mean values of velocity, pressure, shear stress, etc., in a high-Reynolds-number (turbulent) flow. This approach led Osborne Reynolds in 1895 to rewrite Eqs. (8.98) in terms of mean or time-averaged turbulent variables. Instead of asking "what is the instantaneous value of the velocity at some point in the flow" we might instead

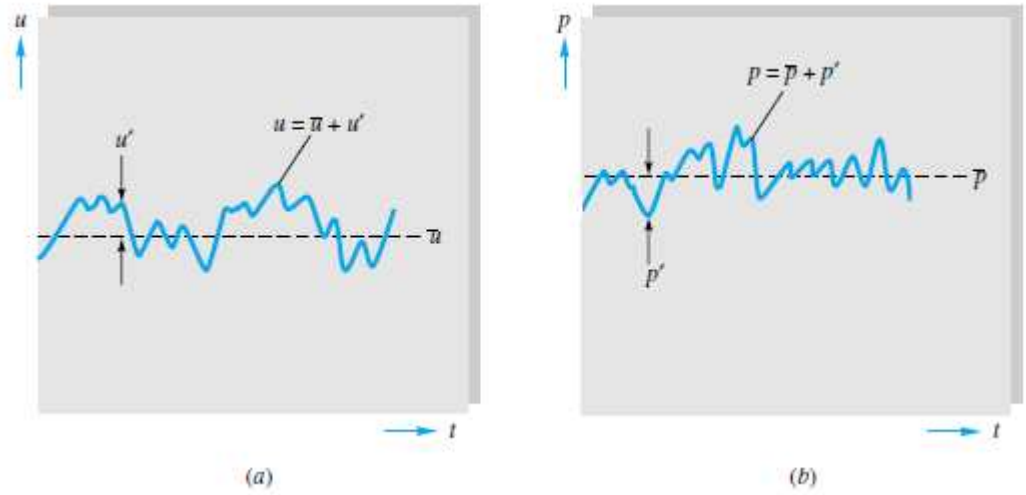

Figure 33: Definition of mean and fluctuating turbulent variables: (a) velocity; (b) pressure. Ref. [3].

ask "what is the time-average value of the velocity at that point". To proceed in this manner we consider splitting the variables into mean and fluctuating parts. We can do this since, in our flows of interest the turbulence is a random, STATIONARY process (its mean values are independent of time) and hence we can break up the velocity components into a mean value and a fluctuating component. The time mean $\overline{u}$ of a turbulent function $u(x, y, z, t)$ is defined by

$$\overline{u} = \frac{1}{T}\int_0^T u dt \tag{8.99}$$

where T is an averaging period taken to be longer than any significant period of the fluctuations themselves. The mean values of turbulent velocity and pressure are illustrated in Fig. 33. For turbulent gas and water flows, an averaging period $T \approx 5$ s is usually quite adequate.

The fluctuation u' is defined as the deviation of u from its average value

$$u' = u - \overline{u} \tag{8.100}$$

also shown in Fig. 33. It follows by definition that a fluctuation has zero mean value

$$\overline{u'} = \frac{1}{T}\int_0^T (u - \overline{u}) dt = \overline{u} - \overline{u} = 0 \tag{8.101}$$

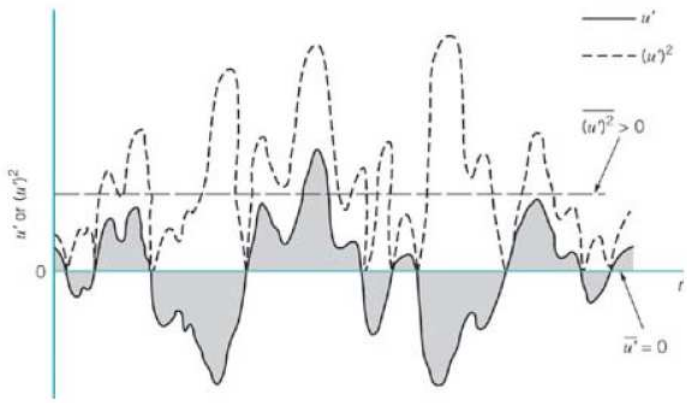

Figure 34: Average of the fluctuations and average of the square of the fluctuations. Ref. [2].

However, as indicated in Fig. 34, the mean square of a fluctuation is not zero and is a measure of the intensity of the turbulence

$$\overline{(u')^2} = \frac{1}{T}\int_0^T (u')^2 dt \neq 0 \tag{8.102}$$

Nor in general are the mean fluctuation products such as $\overline{u'v'}$ and $\overline{u'p'}$ zero in a typical turbulent flow.

Reynolds idea was to split each property into mean plus fluctuating variables

$$u = \overline{u} + u', \quad v = \overline{v} + v', \quad w = \overline{w} + w', \quad p = \overline{p} + p' \tag{8.103}$$

We must observe the following rules:

$$\overline{\frac{\partial u}{\partial x}} = \frac{\partial \overline{u}}{\partial x}$$
$$\overline{u + v} = \overline{u} + \overline{v}$$
$$\overline{\overline{u}.\overline{v}} = \overline{u}.\overline{\overline{v}} = \overline{u}.\overline{v}$$
$$\overline{\overline{u}u'} = \overline{u}.\overline{u'} = 0$$

But it is important to note that while $\overline{u'} = 0$ and $\overline{v'} = 0$ but $\overline{u'v'}$ is not in general zero (this can occur if u' and v' are 90° out of phase).

Substitute these into Eqs. (8.98), and take the time mean of each equation. The continuity relation reduces to

$$\frac{\partial \overline{u}}{\partial x} + \frac{\partial \overline{v}}{\partial y} + \frac{\partial \overline{w}}{\partial z} = 0 \tag{8.104}$$

which is no different from a laminar continuity relation.

Question 14.
Show that

$$\overline{u\frac{\partial u}{\partial x}+v\frac{\partial u}{\partial y}+w\frac{\partial u}{\partial z}}=\bar{u}\frac{\partial \bar{u}}{\partial x}+\bar{v}\frac{\partial \bar{u}}{\partial y}+\bar{w}\frac{\partial \bar{u}}{\partial z}+\frac{\partial \overline{u'^2}}{\partial x}+\frac{\partial \overline{u'v'}}{\partial y}+\frac{\partial \overline{u'w'}}{\partial z}$$

However, each component of the momentum equation of (8.98), after time averaging, will contain mean values plus three mean products, or correlations, of fluctuating velocities. The most important of these is the momentum relation in the mainstream, or x, direction, which takes the form

$$\rho\frac{D\bar{u}}{Dt}=\rho\left(\bar{u}\frac{\partial \bar{u}}{\partial x}+\bar{v}\frac{\partial \bar{u}}{\partial y}+\bar{w}\frac{\partial \bar{u}}{\partial z}\right)=-\frac{\partial \bar{p}}{\partial x}+\frac{\partial}{\partial x}\left(\mu\frac{\partial \overline{u}}{\partial x}-\rho\overline{u'^2}\right)$$
$$+\frac{\partial}{\partial y}\left(\mu\frac{\partial \overline{u}}{\partial y}-\rho\overline{u'v'}\right)+\frac{\partial}{\partial z}\left(\mu\frac{\partial \overline{u}}{\partial z}-\rho\overline{u'w'}\right) \qquad (8.105)$$

The three correlation terms $-\rho\overline{u'^2}$, $-\rho\overline{u'v'}$ and $-\rho\overline{u'w'}$ are called turbulent stresses because they have the same dimensions and occur right alongside the newtonian (laminar) stress terms $\mu(\partial\bar{u}/\partial x)$, etc. Actually, they are convective acceleration terms (which is why the density appears), not stresses, but they have the mathematical effect of stress and are so termed almost universally in the literature.

The turbulent stresses are unknown a priori and must be related by experiment to geometry and flow conditions. Fortunately, in duct and boundary-layer flow, the stress $-\rho\overline{u'v'}$ associated with direction y normal to the wall is dominant, and we can approximate with excellent accuracy a simpler streamwise momentum equation

$$\rho\frac{D\bar{u}}{Dt}\approx-\frac{\partial \bar{p}}{\partial x}+\frac{\partial \tau}{\partial y} \qquad (8.106)$$

where

$$\tau=\mu\frac{\partial \bar{u}}{\partial y}-\rho\overline{u'v'}=\tau_{\text{lam}}+\tau_{\text{turb}} \qquad (8.107)$$

Fig. 35 shows the distribution of τ_{lam} and τ_{turb} from typical measurements across a turbulent-shear layer near a wall. Laminar shear is dominant near the wall (the wall layer), and turbulent shear dominates in the outer layer. There is an intermediate region, called the overlap layer, where both laminar and turbulent shear are important. These three regions are labeled in Fig. 35.

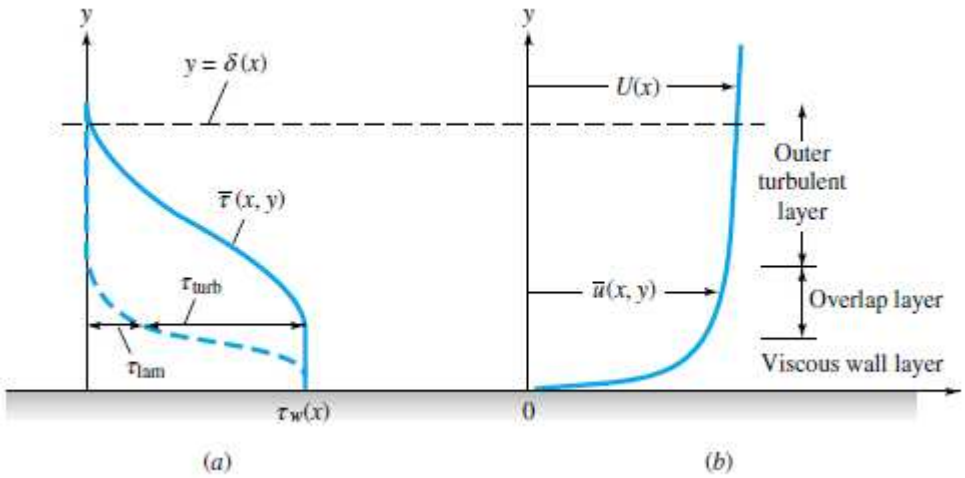

Figure 35: Typical velocity and shear stress distributions in turbulent flow near a wall: (a) shear; (b) velocity. Ref. [3].

In the outer layer τ_{turb} is two or three orders of magnitude greater than τ_{lam}, and vice versa in the wall layer. These experimental facts enable us to use a crude but very effective model for the velocity distribution $\bar{u}(y)$ across a turbulent wall layer.

8.2 The logarithmic overlap law of wall flows

We have seen in Fig. 35 that there are three regions in turbulent flow near a wall:

1. Wall layer: Viscous shear dominates.
2. Outer layer: Turbulent shear dominates.
3. Overlap layer: Both types of shear are important.

From now on let us agree to drop the overbar from velocity $\bar{u}$. Let τ_w be the wall shear stress, and let δ and U represent the thickness and velocity at the edge of the outer layer, $y = \delta$.

Using the physical arguments we have just discussed and some others we can do some dimensional analysis in order to work out something about the shape of the mean velocity profile.

Before making any assumptions we might look at the things on which the velocity profile might depend. Just consider all the relevant independent (or imposed) variables that affect the flow

$$u = f_1(y, \tau_w, \rho, \nu, \delta, U), \tag{8.108}$$

where f_1 is some unknown function. Dimensional analysis would then lead us to four non-dimensional groups - which is not that helpful for our purposes. Now in order to simplify it we look at the different regions discussed above and see what variables we can throw away.

Before starting, to simplify things note that the quantity $\sqrt{\tau_w/\rho}$ has the dimensions of a velocity and since we are interested in velocities we can use this in place of τ_w. The "velocity" produced is known as the friction velocity and here we will give it the symbol u^* hence $u^* = \sqrt{\tau_w/\rho}$. In this way we also remove direct effects of the density since it only enters in modifying the kinematic viscosity and the friction velocity[6].

Now consider a region quite close to the wall. If we are far enough away from the outer edge then we might guess that the local flow does not know anything directly about the free-stream velocity or the boundary layer thickness (except in so far as they affect the shear stresses etc.). In this case we can write

$$u = f(y, u^*, \nu) \tag{8.109}$$

By dimensional analysis, this is equivalent to

$$u^+ = \frac{u}{u^*} = F\left(\frac{y u^*}{\nu}\right) \tag{8.110}$$

Equation (8.110) is called the law of the wall.

We have seen from Fig. 35 that the viscosity is important only very close to the wall. With increasing y it ceases to play a role long before parameters other than those in (8.110) have an influence. One can then say the mean velocity gradient depends only on u^* and y,

$$\frac{\partial u}{\partial y} = f(u^*, y) \tag{8.111}$$

although one cannot say the same for u because it is separated from its origin by a region in which ν is important. Dimensional analysis applied to (8.111) gives

$$\frac{\partial u}{\partial y} = \frac{1}{\kappa}\frac{u^*}{y} \tag{8.112}$$

where κ is a universal constant (the Kármán constant) of turbulent wall flows. Integration of (8.112) gives that the overlap-layer velocity varies logarithmically with y:

[6] u^* depends on the flow as whole, but once it is specified, the structure of the wall region is specified.

$$\frac{u}{u^*} = \frac{1}{\kappa} \ln\left(\frac{y u^*}{\nu}\right) + B \quad \text{overlap layer} \tag{8.113}$$

Over the full range of turbulent smooth wall flows, the dimensionless constants κ and B are found to have the approximate values $\kappa \approx 0.41$ and $B \approx 5.0$. Equation (8.113) is called the logarithmic-overlap layer. Thus by dimensional reasoning and physical insight we infer that a plot of u versus $\ln y$ in a turbulent-shear layer will show a curved wall region, a curved outer region, and a straight-line logarithmic overlap. Fig. 35 shows that this is exactly the case. The wall law is unique and follows the linear viscous relation

$$u^+ = \frac{u}{u^*} = \frac{y u^*}{\nu} = y^+ \tag{8.114}$$

from the wall to about $y^+ = 5$ thereafter curving over to merge with the logarithmic law at about $y^+ = 30$.

Believe it or not, Fig. 36, which is nothing more than a shrewd correlation of velocity profiles, is the basis for most existing theory of turbulent-shear flows. Notice that we have not solved any equations at all but have merely expressed the streamwise velocity in a neat form. The logarithmic law (8.113), instead of just being a short overlapping link, actually approximates nearly the entire velocity profile, except for the outer law when the pressure is increasing strongly downstream (as in a diffuser). The inner-wall law typically extends over less than 2 percent of the profile and can be neglected. Thus we can use Eqn. (8.113) as an excellent approximation to solve nearly every turbulent-flow problem presented in this and the next section. Many additional applications are given in Refs. [5] and [7].

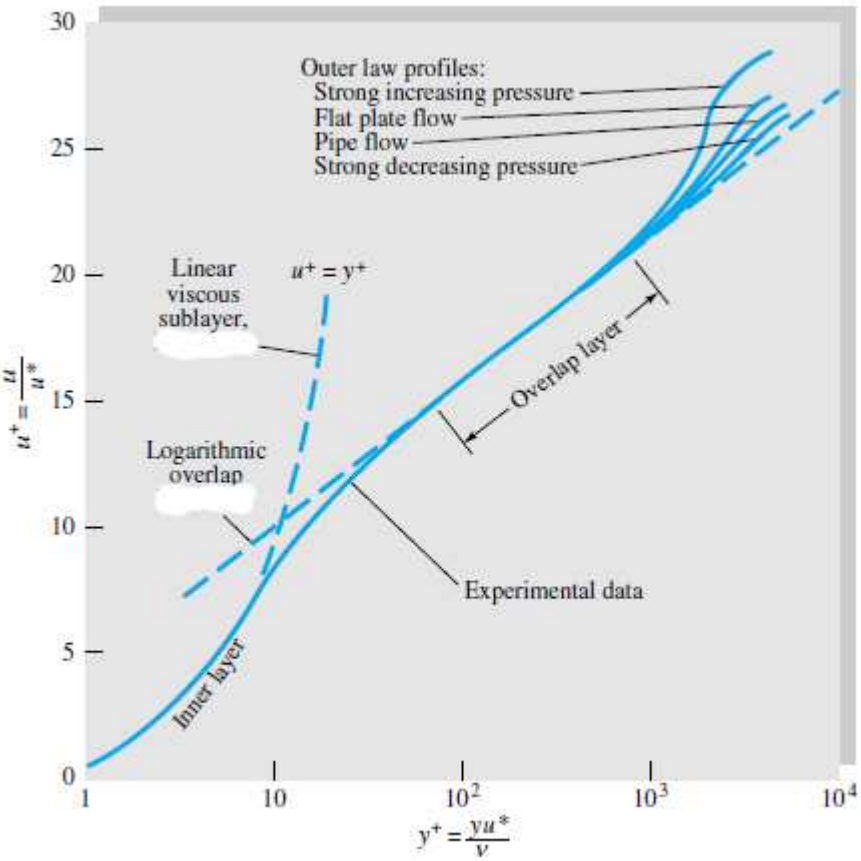

Figure 36: Experimental verification of the inner, outer, and overlap layer laws relating velocity profiles in turbulent wall flow. Ref. [3].

Question 15.
By analogy with laminar shear, $\tau = \mu du/dy$, T. V. Boussinesq in 1877 postulated that turbulent shear could also be related to the mean-velocity gradient $\tau_{\text{turb}} = \epsilon du/dy$ where ϵ is called the eddy viscosity and is much larger than μ. If the logarithmic-overlap law, Eqn. (8.113), is valid with $\tau_{\text{turb}} \approx \tau_{\text{w}}$, show that $\epsilon \approx \kappa \rho u^* y$.

Question 16.
Theodore von Karman in 1930 theorized that turbulent shear could be represented by $\tau_{\text{turb}} = \epsilon du/dy$ where $\epsilon = \rho \kappa^2 y^2 |du/dy|$ is called the mixing-length eddy viscosity and $\kappa \approx 0.41$ is Karmans dimensionless mixing-length constant. Assuming that $\tau_{\text{turb}} \approx \tau_{\text{w}}$ near the wall, show that this expression can be integrated to yield the logarithmic-overlap law, Eqn. (8.113).

9 Viscous pipe flow

The basic piping problem is this: Given the pipe geometry, plus the desired flow rate and fluid properties, what pressure drop is needed to drive the flow? It may be stated in alternate form: Given the pressure drop available from a pump, what flow rate will ensue?

Any fluid flowing in a pipe had to to enter the pipe at some location. The region of flow near where the fluid enters the pipe is termed the entrance region and is illustrated in Fig. 37. In the entrance region, a nearly inviscid upstream flow converges and enters the pipe. Viscous boundary layers grow downstream, retarding the axial flow $u(r, x)$ at the wall and thereby accelerating the center-core flow to maintain the incompressible continuity requirement

$$Q = \int u dA = \text{const} \tag{9.115}$$

At a finite distance from the entrance, the boundary layers merge and the inviscid core disappears. The pipe flow is then entirely viscous, and the axial velocity adjusts slightly further until at $x = L_e$ it no longer changes with x and is said to be fully developed, $u \approx u(r)$ only. Downstream of $x = L_e$ the velocity profile is constant, the wall shear is constant, and the pressure drops linearly with x, for either laminar or turbulent flow. All these details are shown in Fig. 37. Dimensional analysis shows that the Reynolds number is the only parameter affecting entrance length. We assume that L_e is a function of the pipe diameter d, the

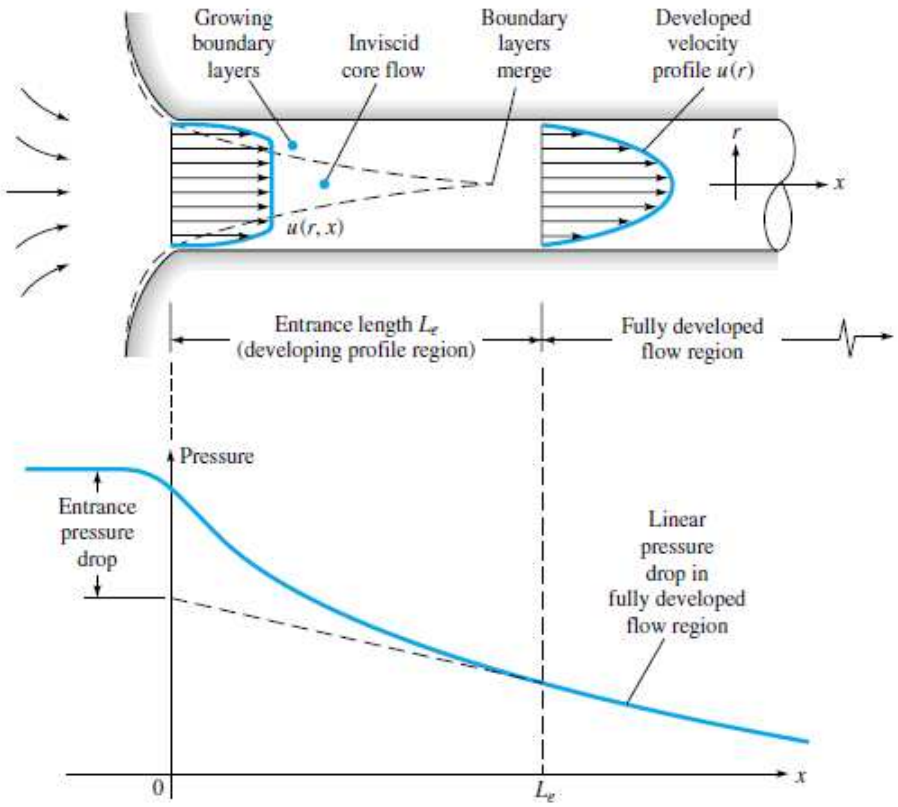

Figure 37: Developing velocity profiles and pressure changes in the entrance of a duct flow. Ref. [3].

average velocity of the fluid in the pipe, V, the fluid density ρ and viscosity μ:

$$L_e = f(d, V, \rho, \mu) \qquad V = Q/A$$

Since there are five variables that can be written in terms of the three reference dimensions MLT, the above equation can be written in dimensionless form in terms of 2 dimensionless groups. One such representation is

$$\frac{L_e}{d} = g\left(\frac{\rho V d}{\mu}\right) = g(Re) \tag{9.116}$$

where $g(Re)$ is an unknown function of the Reynolds number. For laminar flow, the accepted correlation is

$$\frac{L_e}{d} \approx 0.06 Re \qquad \text{laminar} \tag{9.117}$$

The maximum laminar entrance length, at $Re_{d,crit} = 2300$, is $L_e = 138d$, which is the longest development length possible. In turbulent flow the boundary layers grow faster, and L_e is relatively shorter, according to the approximation for smooth walls

$$\frac{L_e}{d} \approx 4.4 Re^{1/6} \qquad \text{turbulent} \tag{9.118}$$

Some computed turbulent entrance lengths are thus

Re_d	4000	10^4	10^5	10^6	10^7	10^8
L_e/d	18	20	30	44	65	95

Now 95 diameters may seem "long", but typical pipe-flow applications involve an L/d value of 1000 or more, in which case the entrance effect may be neglected and a simple analysis made for fully developed flow. This is possible for both laminar and turbulent flows, including rough walls and noncircular cross sections.

9.1 Fully developed laminar flow

The flow in long, straight, constant diameter sections of a pipe become fully developed. Although this is true whether the flow is laminar or turbulent, the details of the velocity

profile (and other flow properties) are quite different for these two types of flow. Knowledge of the velocity profile can lead directly to other useful information such as pressure drop, head loss, flowrate, and the like. If the flow is not fully developed, a theoretical analysis becomes much more complex and is outside the scope of this course. If the flow is turbulent, a rigorous theoretical analysis is as yet not possible.

Although most of flows are turbulent rather than laminar, and many pipes are not long enough to allow the attainment of fully developed flow, a theoretical treatment and fully understanding of fully developed laminar is of considerable importance. First, it represents one of the few theoretical viscous analyses that can be carried out "exactly" (within the framework of quite general assumption) without using other ad hoc assumptions or approximations. An understanding of the method of analysis and the results obtained provides a foundation from which to carry out more complicated analyses. Second, there are many practical situations involving the use of fully developed laminar pipe flow.

There are numerous ways to derive important results pertaining to fully developed laminar flow. Three alternatives include: (1) from $\mathbf{F} = m\mathbf{a}$ applied directly to to fluid element, (2) from dimensional analysis methods, and (3) from the Navier-Stokes equations of motion. We will use the second approach in this course. The third approach is reported in the appendix A at the end of the lecturenotes.

9.2 Hagen-Poiseuille flow

Probably the best known exact solution to the Navier-Stokes equations is for steady, incompressible, laminar flow through a straight circular pipe with constant cross section. This type of flow is commonly called Hagen-Poiseuille flow, or simply Poiseuille flow.

Consider the flow through a horizontal circular pipe of radius R as in shown in Fig. 38a. Because of the cylindrical geometry it is convenient to use cylindrical coordinates. We assume that the flow is parallel to the walls so that $v_r = 0$ and $v_\theta = 0$, and from the continuity equation $\partial v_z/\partial z = 0$. Also, for steady, axisymmetric flow, v_z and p are not functions of t or θ, so the velocity v_z is only a function of the radial position within the pipe—that is, $v_z = v_z(r)$. The Navier-Stokes equations for axisymmetrical flows in the cylindrical coordinates read

$$\frac{1}{r}\frac{\partial}{\partial r}(rv_r) + \frac{\partial v_z}{\partial z} = 0 \ ,$$

$$\rho\left(\frac{\partial v_r}{\partial t} + v_r\frac{\partial v_r}{\partial r} + v_z\frac{\partial v_r}{\partial z}\right) = -\frac{\partial p}{\partial r} + \mu\left[\frac{1}{r}\frac{\partial}{\partial r}\left(r\frac{\partial v_r}{\partial r}\right) + \frac{\partial^2 v_r}{\partial z^2} - \frac{v_r}{r^2}\right] \ ,$$

$$\rho\left(\frac{\partial v_z}{\partial t} + v_r\frac{\partial v_z}{\partial r} + v_z\frac{\partial v_z}{\partial z}\right) = -\frac{\partial p}{\partial z} + \mu\left[\frac{1}{r}\frac{\partial}{\partial r}\left(r\frac{\partial v_z}{\partial r}\right) + \frac{\partial^2 v_z}{\partial z^2}\right] \ .$$

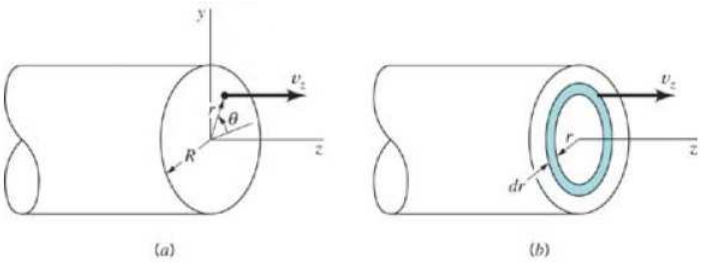

Figure 38: The viscous flow in a horizontal, circular pipe: (a) coordinate system and notation used in analysis; (b) flow through differential annular ring. Ref. [2].

Under the above conditions, they reduce to

$$0 = -\frac{\partial p}{\partial r} \tag{9.119}$$

$$0 = -\frac{\partial p}{\partial z} + \mu\left[\frac{1}{r}\frac{\partial}{\partial r}\left(r\frac{\partial v_z}{\partial r}\right)\right] \tag{9.120}$$

The pressure is not a function of r or θ.

The equation of motion in the z direction can be written in the form

$$\frac{1}{r}\frac{\partial}{\partial r}\left(r\frac{\partial v_z}{\partial r}\right) = \frac{1}{\mu}\frac{\partial p}{\partial z}$$

and integrated (using the fact that $\partial p/\partial z =$ constant) to give

$$r\frac{\partial v_z}{\partial r} = \frac{1}{2\mu}\left(\frac{\partial p}{\partial z}\right) r^2 + c_1$$

Integrating again we obtained

$$v_z = \frac{1}{4\mu}\left(\frac{\partial p}{\partial z}\right) r^2 + c_1 \ln r + c_1 \tag{9.121}$$

The shape of the velocity profile depends on the values of the two constants c_1 and c_2.

Since we wish v_z to be finite at the center of the pipe ($r = 0$), it follows that $c_1 = 0$. At the wall ($r = R$) the velocity must be zero so that

$$c_2 = -\frac{1}{4\mu}\left(\frac{\partial p}{\partial z}\right) R^2$$

and the velocity distribution becomes

$$v_z = \frac{1}{4\mu}\left(\frac{\partial p}{\partial z}\right)(r^2 - R^2) \tag{9.122}$$

Thus, at any cross section the velocity distribution is parabolic.

To obtain a relationship between the volume rate of flow, Q, passing through the pipe and the pressure gradient, we consider the flow through the differential, washer-shaped ring of Fig. 38b. Since v_z is constant on this ring, the volume rate of flow through the differential area $dA = (2\pi r)dr$ is

$$dQ = v_z(2\pi r)dr$$

and therefore

$$Q = 2\pi \int_0^R v_z r dr \tag{9.123}$$

Eqn. (9.122) for v_z can be substituted into Eqn. (9.123) and the resulting equation integrated to yield

$$Q = -\frac{\pi R^4}{8\mu}\left(\frac{\partial p}{\partial z}\right) \tag{9.124}$$

This relationship can be expressed in terms of the pressure drop, Δp, which occurs over a length, L, along the pipe, since

$$\frac{\Delta p}{L} = -\left(\frac{\partial p}{\partial z}\right)$$

and therefore

$$Q = \frac{\pi R^4 \Delta p}{8\mu L} \tag{9.125}$$

For a given pressure drop per unit length, the volume rate of flow is inversely proportional to the viscosity and proportional to the pipe radius to the fourth power. Eqn. (9.125) is commonly called Poiseuille's flow.

In terms of the mean velocity, V, where $V = Q/\pi R^2$, Eqn. (9.125) becomes

$$V = \frac{R^2 \Delta p}{8\mu L} \tag{9.126}$$

The maximum velocity v_{max} occurs at the center of the pipe, where from Eqn. (9.122)

$$v_{max} = -\frac{R^2}{4\mu}\left(\frac{\partial p}{\partial z}\right) = \frac{R^2 \Delta p}{4\mu L} \tag{9.127}$$

so that

$$v_{max} = 2V \tag{9.128}$$

The velocity distribution can be rewritten in terms of v_{max} as

$$\frac{v_z}{v_{max}} = 1 - \left(\frac{r}{R}\right)^2 \tag{9.129}$$

Numerous experiments performed to substantiate the theoretical results show that the theory and experiment are in agreement for the laminar flow of Newtonian fluids in circular pipes. In general, the flow remains laminar for Reynolds numbers, $Re = \rho V(2R)/\mu$, below 2100.

It is usually advantageous to describe a process in terms of dimensionless quantities. Thus, the Darcy friction factor for laminar fully developed pipe flow is simply

$$f = \frac{64}{Re} \tag{9.130}$$

The Navier-Stokes equations in the cylindrical coordinates read

$$\frac{1}{r}\frac{\partial}{\partial r}(rv_r) + \frac{1}{r}\frac{\partial(v_\theta)}{\partial\theta} + \frac{\partial(v_z)}{\partial z} = 0.$$

$$r: \quad \rho\left(\frac{\partial v_r}{\partial t} + v_r\frac{\partial v_r}{\partial r} + \frac{v_\theta}{r}\frac{\partial v_r}{\partial\theta} + v_z\frac{\partial v_r}{\partial z} - \frac{v_\theta^2}{r}\right) = -\frac{\partial p}{\partial r} + \mu\left[\frac{1}{r}\frac{\partial}{\partial r}\left(r\frac{\partial v_r}{\partial r}\right) + \frac{1}{r^2}\frac{\partial^2 v_r}{\partial\theta^2} + \frac{\partial^2 v_r}{\partial z^2} - \frac{v_r}{r^2} - \frac{2}{r^2}\frac{\partial v_\theta}{\partial\theta}\right] + \rho g_r$$

$$\theta: \quad \rho\left(\frac{\partial v_\theta}{\partial t} + v_r\frac{\partial v_\theta}{\partial r} + \frac{v_\theta}{r}\frac{\partial v_\theta}{\partial\theta} + v_z\frac{\partial v_\theta}{\partial z} + \frac{v_r v_\theta}{r}\right) = -\frac{1}{r}\frac{\partial p}{\partial\theta} + \mu\left[\frac{1}{r}\frac{\partial}{\partial r}\left(r\frac{\partial v_\theta}{\partial r}\right) + \frac{1}{r^2}\frac{\partial^2 v_\theta}{\partial\theta^2} + \frac{\partial^2 v_\theta}{\partial z^2} + \frac{2}{r^2}\frac{\partial v_r}{\partial\theta} - \frac{v_\theta}{r^2}\right] + \rho g_\theta$$

$$z: \quad \rho\left(\frac{\partial v_z}{\partial t} + v_r\frac{\partial v_z}{\partial r} + \frac{v_\theta}{r}\frac{\partial v_z}{\partial\theta} + v_z\frac{\partial v_z}{\partial z}\right) = -\frac{\partial p}{\partial z} + \mu\left[\frac{1}{r}\frac{\partial}{\partial r}\left(r\frac{\partial v_z}{\partial r}\right) + \frac{1}{r^2}\frac{\partial^2 v_z}{\partial\theta^2} + \frac{\partial^2 v_z}{\partial z^2}\right] + \rho g_z.$$

9.3 From dimensional analysis

Although fully developed laminar pipe flow is simple enough to allow rather straightforward solutions, it may be worthwhile to consider this flow from a dimensional analysis standpoint. Thus, we assume that the pressure drop in a horizontal pipe, Δp, is a function of the average velocity of the fluid in the pipe, V, the length of the pipe, L, the pipe diameter, d, the viscosity of the fluid, μ, as shown by Fig. 39. We have not included the density of the fluid ρ as parameter because for such flows it is not an important parameter (Why?). Thus

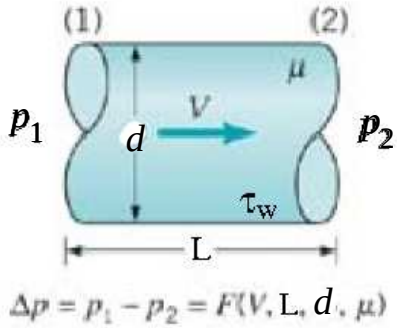

Figure 39: Definition of variables for a fully developed laminar pipe flow. Ref. [2].

$$\Delta p = F(V, L, d, \mu)$$

Five variables can be described in terms of three reference dimensions (M, L, T). According to the results of dimensional analysis, this flow can be described in terms of $5 - 3 = 2$ dimensionless groups. One such representation is

$$\frac{\Delta p}{\mu V/D} = \phi\left(\frac{L}{d}\right) \tag{9.131}$$

where $\phi(L/d)$ is an unknown function of the length to diameter ratio of the pipe.

Although this is as far as dimensional analysis can take us, it seems reasonable to impose a further assumption that the pressure drop is directly proportional to the pipe length. That is, it takes twice the pressure drop to force fluid through a pipe if its length is doubled. The only way that this can be true is if $\phi(L/d) = CL/d$, where C is a constant. Thus, Eqn. (9.131) becomes

$$\frac{D\Delta p}{\mu V} = \frac{CL}{d}$$

which can be rewritten as

$$\Delta p = \frac{C\mu V L}{d^2} \tag{9.132}$$

The value of C must be determined by theory or experiment. For a round pipe, $C = 32$ for laminar flow. For ducts of other cross-sectional shapes, the value of C is different.

It is usually advantageous to described a process in terms of dimensionless quantities. To this end we divide both sides of Eqn. (9.132) by the dynamic pressure, $\rho V^2/2$, to obtain the dimensionless from as

$$\frac{\Delta p}{\frac{1}{2}\rho V^2} = \frac{C\mu LV}{\frac{1}{2}\rho V^2 d^2} = 2C\left(\frac{\mu}{\rho V d}\right)\left(\frac{L}{d}\right)$$

This is often written as

$$\Delta p = f\left(\frac{L}{d}\right)\frac{\rho V^2}{2}$$

where the dimensionless quantity

$$f = \Delta p(d/L)/(\rho V^2/2) \tag{9.133}$$

is termed the Darcy friction factor. Thus the Darcy friction factor for laminar fully developed pipe flow is simply

$$f = \frac{64}{Re_d}, \qquad Re_d = \frac{Vd}{\nu} \tag{9.134}$$

But in pipe flow (either laminar or turbulent), the pressure drop Δp and wall shear stress τ_w are related through

$$\pi\left(\frac{d}{2}\right)^2 \Delta p = (\pi d L)\tau_w \quad \text{or} \quad \Delta p = \frac{4\tau_w L}{d} \tag{9.135}$$

It follows from the momentum equation for the control volume indicated in Fig. 39. By substituting the pressure drop in terms of the wall shear stress (Eqn. 9.135), we obtain an alternate expression, for the friction factor as a dimensionless wall stress

$$f = \frac{8\tau_w}{\rho V^2} \tag{9.136}$$

Knowledge of the friction factor will allow us to obtain a variety of information regarding pipe flow. For turbulent flow the dependence of the friction factor on the Reynolds number is much more complex than that given Eqn. (9.134) for laminar flow. This is discussed in detail in the following subsections.

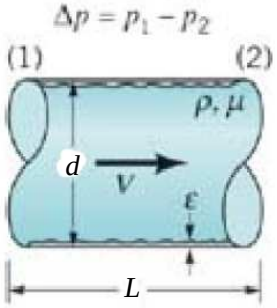

Figure 40: Turbulent pipe flow properties dependent on the fluid density and the pipe roughness. Ref. [2].

9.4 Dimensional analysis of turbulent flow

A dimensional analysis treatment of pipe flow provides the most convenient base from which to consider turbulent, fully developed pipe flow. An introduction to this topic was given in the previous subsection for laminar pipe flow. A fundamental difference between laminar and turbulent flow is that the shear stress for turbulent flow is a function of the density of the fluid, ρ. The pressure drop in a pipe is dependent on the wall shear stress, τ_w. For laminar flow, the shear stress is independent of the density, leaving the viscosity, μ, as the only important fluid property. For turbulent flow, the turbulent stress $\tau_{\text{turb}} = \rho\overline{u'v'}$ is dominant.

Thus, the pressure drop, Δp, for steady, incompressible turbulent flow in a horizontal pipe of diameter d can be written in functional form as

$$\Delta p = F(V, L, d, \epsilon, \mu, \rho) \tag{9.137}$$

where ϵ is a measure of the roughness of the pipe wall. It is clear that Δp should be a function of V, d and L. The dependence of Δp on the fluid properties μ and ρ is expected because of the dependence of τ on these parameters.

Although the pressure drop for laminar flow is found to be independent of the roughness of the pipe, it is necessary to include this parameter when considering turbulent flow. As illustrated in Fig. 41, for turbulent flow there is a relatively thin viscous sublayer formed in the fluid near the pipe. In many instances this layer is very thin; $\delta_s/d \ll 1$, where δ_s is the sublayer thickness. If a typical wall roughness element protrudes sufficiently far into (or even through) this layer, the structure and properties of the viscous sublayer (along with Δp and τ_w) will be different than if the wall were smooth. Thus, for turbulent flow the pressure drop

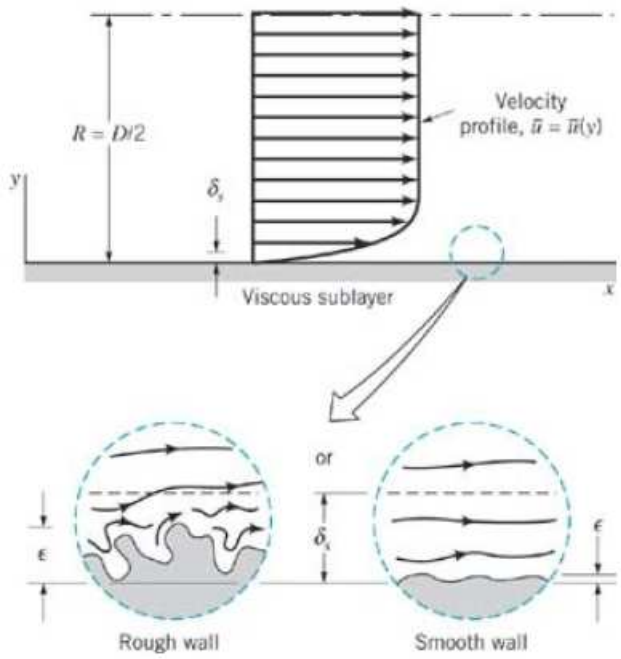

Figure 41: Flow in the viscous sublayer near rough and small walls. Ref. [2].

is expected to be a function of the wall roughness. For laminar flow there is no thin viscous layer—viscous effects are important across the entire pipe. Thus, relatively small roughness elements ($0 \leq \epsilon/d \leq 0.05$) have completely negligible effects on laminar pipe flow.

The list of parameters given in the above equation is apparently a complete one. Since there are seven variables that can be written in terms of the three reference dimensions MLT, the above equation can be written in dimensionless form in terms of 4 dimensionless groups. One such representation is

$$\frac{\Delta p}{\frac{1}{2}\rho V^2} = \tilde{\phi}\left(\frac{\rho V d}{\mu}, \frac{L}{d}, \frac{\epsilon}{d}\right) \tag{9.138}$$

This results differs from that used for laminar flow (see Eqn. 9.131) in two ways. First, we have chosen to make the pressure dimensionless by dividing by the dynamic pressure, $\rho V^2/2$, rather than a characteristic viscous shear stress, $\mu V/D$. This convention was chosen in recognition of the fact that the shear stress for turbulent flow is normally dominated by τ_{turb} which is a stronger function of the density than it is of viscosity. Second, we have introduced two additional dimensionless parameters, the Reynolds number $Re = \rho V d/\mu$, and the relative roughness, ϵ/d, which are not present in the laminar formulation because the two parameters ρ and ϵ are not important in fully developed laminar pipe flow.

As was done for laminar flow, the functional representation can be simplified by imposing the reasonable assumption that the pressure drop should be proportional to the pipe length. (Such a step is not within the realm of dimensional analysis. It is merely a logical assumption supported by the experiments.) The only way that this can be true is if the L/d dependence is factored out as

$$\frac{\Delta p}{\frac{1}{2}\rho V^2} = \frac{L}{d}\phi\left(Re, \frac{\epsilon}{d}\right)$$

As discussed in the previous subsection, the quantity $\Delta p(d/L)/(\rho V^2/2)$ is termed the Darcy friction factor, f. Thus for a horizontal pipe

$$\Delta p = f\left(\frac{L}{d}\right)\frac{\rho V^2}{2}$$

where

$$f = \phi\left(\frac{\rho V d}{\mu}, \frac{\epsilon}{d}\right)$$

For laminar fully developed flow, the value of f is simply $f = 64/Re$, independent of ϵ/d. For turbulent flow, the functional dependence of the friction factor on the Reynolds number and the relative roughness, $f = \phi(Re, \epsilon/d)$, is rather complex one that cannot, as yet, be obtained from a theoretical analysis. The results are obtained from an exhaustive set of experiments and usually presented in terms of a curve-fitting formula or the equivalent graphical form.

9.5 Smooth wall pipe flows

For turbulent pipe flow we need not solve a differential equation but instead proceed with the logarithmic law. Assume that the log-law (8.113) correlates the local mean velocity $u(r)$ all the way across the pipe

$$\frac{u(r)}{u^*} \approx \frac{1}{\kappa}\ln\frac{(R-r)u^*}{\nu} + B \qquad (9.139)$$

where R is the pipe radius and $u^* = \sqrt{\tau_w/\rho}$ is the friction velocity. We have replaced y by $R - r$. Compute the average velocity from this profile

$$V = \frac{Q}{A} = \frac{1}{\pi R^2}\int_0^R u(r)\, 2\pi r dr \approx u^*\left(\frac{1}{\kappa}\ln\frac{Ru*}{\nu} + B - \frac{3}{2\kappa}\right) \qquad (9.140)$$

Introducing $\kappa = 0.41$ and $B = 5.0$, we obtain, numerically,

$$\frac{V}{u^*} \approx 2.44 \ln\left(\frac{Ru*}{\nu}\right) + 1.34 \tag{9.141}$$

This looks only marginally interesting until we realize that V/u^* is directly related to the Darcy friction factor

$$\frac{V}{u^*} = \left(\frac{\rho V^2}{\tau_w}\right)^{1/2} = \left(\frac{8}{f}\right)^{1/2} \tag{9.142}$$

Moreover, the argument of the logarithm in (9.141) is equivalent to

$$\frac{Ru*}{\nu} = \frac{\frac{1}{2}Vd}{\nu}\frac{u^*}{V} = \frac{1}{2}Re_d\left(\frac{f}{8}\right)^{1/2}, \qquad Re_d = \frac{Vd}{\nu}, \qquad d = 2R \tag{9.143}$$

Introducing (9.142) and (9.143) into Eq. (9.141),

$$\frac{1}{f^{1/2}} \approx 0.863 \ln(Re_d f^{1/2}) - 1.02 \tag{9.144}$$

changing to a base-10 logarithm, and rearranging, we obtain

$$\frac{1}{f^{1/2}} \approx 1.99 \log_{10}(Re_d f^{1/2}) - 1.02 \tag{9.145}$$

In other words, by simply computing the mean velocity from the logarithmic-law correlation, we obtain a relation between the friction factor and Reynolds number for turbulent pipe flow. Prandtl derived Eq. (9.145) in 1935 and then adjusted the constants slightly to fit friction data better

$$\frac{1}{f^{1/2}} \approx 2.0 \log_{10}\left(Re_d f^{1/2}\right) - 0.8 = 2.0 \log_{10}\left(\frac{Re_d f^{1/2}}{2.51}\right) \tag{9.146}$$

This is the accepted formula for a smooth-walled pipe. Some numerical values may be listed as follows:

Re_d	4000	10^4	10^5	10^6	10^7	10^8
f	0.0399	0.0309	0.0180	0.0116	0.0081	0.0059

Thus f drops by only a factor of 5 over a 10,000-fold increase in Reynolds number. Equation (9.146) is cumbersome to solve if Re_d is known and f is wanted. There are many alternate approximations in the literature from which f can be computed explicitly from Re_d

$$f = \begin{cases} 0.316\ Re_d^{-1/4} & 4000 < Re_d < 10^5 \\ \left(1.8 \log_{10}\dfrac{Re_d}{6.9}\right)^{-2} & Re_d > 10^5 \end{cases} \tag{9.147}$$

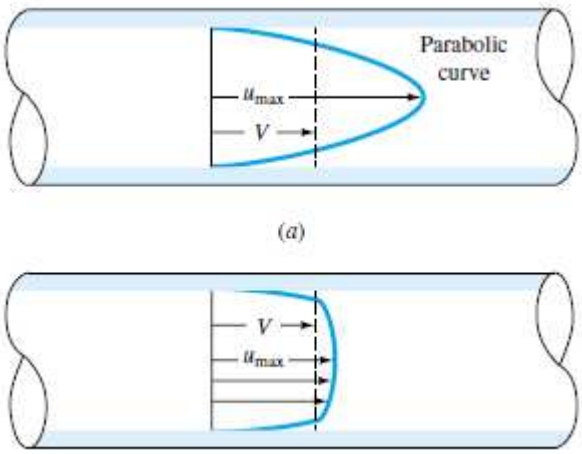

Figure 42: Comparison of laminar and turbulent pipe-flow velocity profiles for the same volume flow: (a) laminar flow; (b) turbulent flow. Ref. [3].

The maximum velocity in turbulent pipe flow is given by Eq. (9.139), evaluated at $r = 0$:

$$\frac{u_{\max}}{u^*} \approx \frac{1}{\kappa} \ln \frac{Ru^*}{\nu} + B \tag{9.148}$$

Combining this with Eq. (9.140) (related to V/u^*), we obtain the formula relating mean velocity to maximum velocity

$$\frac{V}{u_{\max}} \approx (1 + 1.3\sqrt{f})^{-1} \tag{9.149}$$

Some numerical values are

Re_d	4000	10^4	10^5	10^6	10^7	10^8
$V/u_{\max}$	0.794	0.814	0.852	0.877	0.895	0.909

The ratio varies with the Reynolds number and is much larger than the value of 0.5 predicted for all laminar pipe flow. Thus a turbulent velocity profile, as shown in Fig. 42, is very flat in the center and drops off sharply to zero at the wall.

Question 17.

(a) Show Eqn. (9.140):

$$V \approx u^* \left(\frac{1}{\kappa} \ln \frac{Ru*}{\nu} + B - \frac{3}{2\kappa} \right)$$

(b) Show Eqn. (9.149)

$$\frac{V}{u_{\max}} \approx (1 + 1.3\sqrt{f})^{-1}$$

Hint: you may use $\int \ln y dy = y \ln y - y$, $\int y \ln y dy = y^2(\ln y)/2 - y^2/4$.

9.6 Effect of Rough Walls

It was not known until experiments in 1800 by Coulomb that surface roughness has an effect on friction resistance. It turns out that the effect is negligible for laminar pipe flow. But turbulent flow is strongly affected by roughness. In Fig. 35 the linear viscous sublayer only extends out to $y^+ = yu^*/\nu = 5$. Thus, compared with the diameter, the sublayer thickness δ_s is only

$$\frac{\delta_s}{d} = \frac{5\nu/u^*}{d} = \frac{10\sqrt{2}}{Re_d f^{1/2}} \tag{9.150}$$

For example, at $Re_d = 10^5$, $f = 0.0180$, and $\delta_s/d = 0.001$, a wall roughness of about $0.001d$ will break up the sublayer and profoundly change the wall law in Fig. 36.

It is not easy to determine the functional dependence of the friction factor on the Reynolds number and relative roughness. Much of this information is a result of experiment conducted by J. Nikuradse in 1933 and amplified by many others since then. One difficulty lies in the determination of the roughness of the pipe. Nikuradse used artificially roughened pipes produced by using gluing sand gains of known size onto pipe walls to produce pipe with sandpaper-type surfaces. In commercially available pipes the roughness is not as uniform and well defined as in the artificially roughened pipes used by Nikuradse. However, it is possible to obtain a measure of the effective relative roughness of typical pipes and thus to obtain the friction factor. Fig. 43 shows the functional dependence of f on Re and ϵ/d and is called the Moody chart in honor of L.F. Moody, who along with C. F. Colebrook, correlated the original data of Nikuradse in terms of the relative roughness of commercially available pipe material.

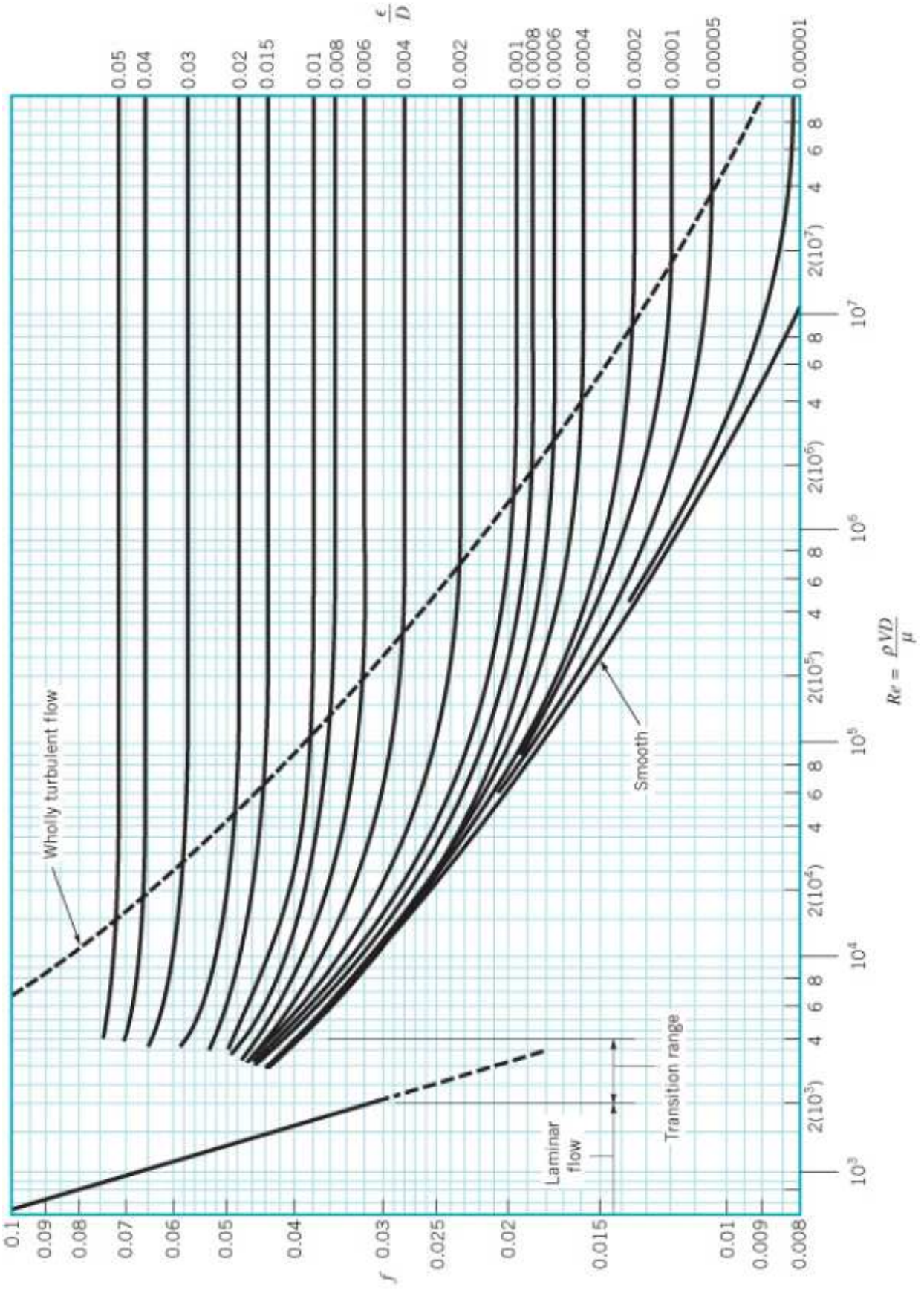

Figure 43: The Moody chart for pipe friction with smooth and rough walls. This chart is identical to Eqn. (9.151) for turbulent flow. Ref. [2].

The following characteristics are observed from the data of Fig. 43. For laminar flow, $f = 64/Re$, which is independent of relative roughness. For turbulent flows with very large Reynolds numbers, $f = \phi(\epsilon/d)$, which, is independent of the Reynolds number. For such flows, commonly termed as completely turbulent flow (or wholly turbulent flow), the laminar sublayer is so thin (its thickness decreases with increasing Re) that the surface roughness completely dominates the character of the flow near the wall. Hence, the pressure drop required is a result of an inertia-dominated turbulent shear stress rather than the viscosity-dominated laminar shear stress normally found in the viscous sublayer. For flow with moderate values of Re, the friction factor is indeed dependent on both Reynolds number and relative roughness—$f = \phi(Re, \epsilon/d)$. The gap in the figure for which no values of f are given (the $2100 < Re < 4000$ range) is a result of the fact that the flow in this transition range may be laminar or turbulent (or an unsteady mix of both) depending on the specific circumstances involved.

Note that the Moody chart covers an extremely wide range in flow parameters. The nonlaminar region covers more than four orders of magnitude in Reynolds number—from $Re = 4 \times 10^3$ to $Re = 10^8$. Because of the large variety in pipes (d), fluids (rho and μ), and velocity (V), such a wide range of Re is needed to accommodate nearly all applications of pipe flow. The Moody chart is universally valid for all steady, fully developed, incompressible pipe flows.

Various investigators have attempted to obtain an analytical expression for $f = \phi(Re, \epsilon/d)$. The following equation from Colebrook is valid for the entire nonlaminar part of the Moody chart

$$\frac{1}{f^{1/2}} = -2.0 \log_{10} \left(\frac{\epsilon/d}{3.7} + \frac{2.51}{Re_d f^{1/2}} \right) \tag{9.151}$$

In fact, the Moody Chart is a graphical representation of this equation, which is an empirical fit of the pipe flow pressure drop data. Eqn. (9.151) is called the Colebrook formula. We note that when $\epsilon = 0$, we recover the result for smooth walls, Eqn. (9.146). Indeed, the Colebrook formula is clever interpolation formula of the smooth wall [Eq. (9.146)] and fully rough (which is not proved in this course) relations. A difficulty with its use is that it is implicit in the dependence of f. That is, for given conditions (Re and ϵ/d), it is not possible to solve for f without some sort of iterative scheme. With the use of modern computers and calculators, such calculations are not difficult. A word of caution is in order concerning the use of the Moody Chart or the equivalent Colebrook formula. Because of various inherent inaccuracies involved (uncertainty in the relative roughness, uncertainty in the experimental data used to

produce the Moody chart, etc), as a rule of thumb, a 10% accuracy is the best expected. It is possible to obtain an equation that adequately approximates the Colebrook/Moody chart relationship but does not require an iterative scheme. For example, the Haaland equation, which is easy to use, is given by

$$\frac{1}{f^{1/2}} \approx -1.8 \log_{10} \left[\left(\frac{\epsilon/d}{3.7} \right)^{1.11} + \frac{6.9}{Re_d} \right] \tag{9.152}$$

where one can solve for f explicitly.

Question 18.
Compute the pressure drop in 60 m of horizontal 15 cm-diameter asphalted cast iron pipe carrying water with a mean velocity of 1.8 m/s. For asphalted cast iron iron $\epsilon = 0.12$ mm. You may use Eqn. (9.152).
Answer: $Re_d = 2.7 \times 10^5$, $f \approx 0.01974$, $\Delta p \approx 12.8$ kPa.

Appendix: Boundary Layer Theory Data Card

Displacement thickness;

$$\delta^* = \int_0^\infty \left(1 - \frac{u}{U}\right) dy$$

Momentum thickness;

$$\theta = \int_0^\infty \frac{(U-u)u}{U^2} dy = \int_0^\infty \left(1 - \frac{u}{U}\right) \frac{u}{U} dy$$

Energy thickness;

$$\delta_E = \int_0^\infty \frac{(U^2-u^2)u}{U^3} dy = \int_0^\infty \left(1 - \left(\frac{u}{U}\right)^2\right) \frac{u}{U} dy$$

$$H = \frac{\delta^*}{\theta}$$

Prandtl's boundary layer equations (laminar flow);

$$\begin{aligned} u\frac{\partial u}{\partial x} + v\frac{\partial u}{\partial y} &= -\frac{1}{\rho}\frac{dp_1}{dx} + \nu\frac{\partial^2 u}{\partial y^2} \\ \frac{\partial u}{\partial x} + \frac{\partial v}{\partial y} &= 0 \end{aligned}$$

von Karman momentum integral equation;

$$\frac{d\theta}{dx} + \frac{H+2}{U}\theta\frac{dU}{dx} = \frac{\tau_w}{\rho U^2} = \frac{C_f'}{2}$$

Boundary layer equations for turbulent flow;

$$\begin{aligned} \overline{u}\frac{\partial \overline{u}}{\partial x} + \overline{v}\frac{\partial \overline{u}}{\partial y} &= \frac{-1}{\rho}\frac{d\overline{p}}{dx} - \frac{\partial \overline{u'v'}}{\partial y} + \nu\frac{\partial^2 \overline{u}}{\partial y^2} \\ \frac{\partial \overline{u}}{\partial x} + \frac{\partial \overline{v}}{\partial y} &= 0 \end{aligned}$$

References

[1] Vennard J.K. and Street R. *Elementary Fluid Mechanics*. John Wiley & Sons, 1982.

[2] Munson B. R., Okiishi T. H., Huebsch W., and Rothmayer A. P. *Fluid Mechanics*. John Wiley & Son, 2013.

[3] Frank M. White. *Fluid Mechanics*. McGraw-Hill, 2004.

[4] D.J. Acheson. *Elementary fluid dynamics*. Oxford : Clarendon, 1990.

[5] Frank M. White. *Viscous Fluid Flow*. McGraw-Hill, 2006.

[6] Cebeci T. and Cousteix J. *Modeling and Computation of Boundary-Layer Flows*. Springer, 2005.

[7] H. Schlichting. *Boundary Layer Theory*. McGraw-Hill, 1979.

[8] Schetz J. C. *Boundary Layer Analysis*. Prentice Hall, 1992.

[9] Rosenhead L. *Laminar Boundary Layers*. Oxford Univ. Press, London, 1963.

[10] Van Dyke. *Album of Fluid Motion*. Parabolic Pr, 1982.

[11] Nakayama Y. (ed.). *Visualized Flow*. Pergamon, Oxford, 1988.

[12] Homsy et al. *Multimedia Fluid Mechanics DVD-ROM*. Cambridge Univ. Press, 2008.